Pós-Graduação
ZOOLOGIA
MPEG/UFPA

MUSEU PARAENSE EMÍLIO GOELDI

UNIVERSIDADE FEDERAL DO PARÁ

PROGRAMA DE PÓS-GRADUAÇÃO EM ZOOLOGIA

CURSO DE DOUTORADO EM ZOOLOGIA

DIVERSIFICAÇÃO MORFOLÓGICA E MOLECULAR EM LAGARTOS DACTYLOIDAE SUL-AMERICANOS

ANNELISE BATISTA D'ANGIOLELLA

Belém - PA

2015

ANNELISE BATISTA D'ANGIOLELLA

DIVERSIFICAÇÃO MORFOLOGICA E MOLECULAR EM LAGARTOS DACTYLOIDAE SUL-AMERICANOS

Tese apresenta ao Programa de Pós-Graduação em Zoologia do convênio Universidade Federal do Pará e Museu Paraense Emílio Goeldi, para obtenção do título de doutora em zoologia.

Orientadora: Dra. Tereza Cristina Ávila Pires

Co-Orientadora: Dra. Ana Carolina Carnaval

Belém - PA

2015

"É capaz quem pensa que é capaz."

Agradecimento

"Dedico essa tese a minha mãe Lygia Maria, meu pai Antonio D'Angiolella (*in memorian*) e aos meus irmãos Eduardo e Gustavo, pelo constante e incansável apoio."

Sumário

LISTA DE FIGURAS

Capítulo 1 - POPULATION STRUCTURE AND DIVERSIFICATION OF THE MAINLAND FOREST ANOLE *NOROPS FUSCOAURATUS* (SQUAMATA: DACTYLOIDAE)

Capítulo 3 - HEMIPENIAL MORPHOLOGY AND DIVERSITY IN BRAZILIAN ANOLES (SQUAMATA: DACTYLOIDAE)

1. Introdução Geral

A compreensão dos padrões de distribuição da diversidade biológica, tem sido um tema amplamente discutido em estudos ecológicos e biogeográficos nas últimas décadas (Gaston, 2000; Ricklefs, 2004; Diniz-Filho et al. 2009). Nesse contexto, a região neotropical sul-americana destaca-se pela sua alta diversidade, distribuída nos mais diversos biomas (Morrone, 2004; Turchetto-Zolet et al. 2013). Estudos recentes demonstram que as alterações climáticas e geomorfológicas apoiam um cenário de mudanças complexas na paisagem do continente, influenciando na distribuição espacial dos táxons, riqueza de espécies, endemismos, diversidade genética e padrões biogeográficos observados (Nores 2004; Rull, 2008; Antonelli et al, 2009; Carnaval et al, 2009; Hoorn et al, 2010; Thomé et al. 2010; Werneck et al, 2012; Ribas et al 2012; Turchetto-Zolet et al. 2013; Rull, 2011, 2013).

A conformação atual da América do Sul foi grandemente influenciada pelo soerguimento dos Andes, processo iniciado há aproximadamente 65 Ma, causando alterações climáticas e hidrográficas no continente (Hoorn et al. 1995; Van der Hammen & Hooghiemstra, 2000). Uma das principais consequências da elevação dos Andes foi a alteração do padrão de drenagem continental, levando à formação da bacia amazônica como a conhecemos atualmente (Hoorn et al 2010). Embora haja discordâncias sobre quando o Rio Amazonas começou a correr para o leste, a partir dos Andes, diferentes dados indicam que este já havia atingido seu fluxo atual a partir do Plioceno inferior (Figueredo et al. 2009; Latrubesse et al. 2010). Ainda que em menor escala, contudo, movimentos tectônicos continuaram a ocorrer na região, produzindo alterações ao menos locais, até o início do Holoceno (Rosseti et al. 2005; Rosseti & Valeriano, 2007).

Oscilações climáticas também tiveram profunda influência na dinâmica da biodiversidade, alterando a paisagem da América do Sul (Colinvaux & De Oliveira, 2001; Rull, 2007; Cheng et al. 2013). Períodos glaciais e interglaciais no Quaternário provocaram alterações vegetacionais, ora promovendo a expansão de áreas florestadas, ora de savanas (Hafer 1969, 2008; Vanzolini & Williams, 1970; Van der Hammen & Hooghiemstra, 2000). Durante a fase final do Plioceno (aproximadamente entre 3 e 2,5 milhões de ano atrás), um forte resfriamento deu origem ao que seria a primeira era glacial do Pleistoceno, período marcado por uma série de oscilações climáticas (Van der Hammen & Hooghiemstra, 2000; Werneck, 2011). Um estudo envolvendo a dinâmica

5

climática da região nordeste do Brasil durante o Quaternário tardio, aponta para a predominância, de vegetação semi-árida de Caatinga nesse período, com alguns curtos intervalos mais úmidos, especialmente em torno de 40.000, 33.000 e 24,000 ^{14}C anos AP e entre 15.500 e 11.800 ^{14}C anos AP (Behling et al. 2000). Neste último período foi detectada a expansão de florestas de altitude, de galeria e alagadas, permitindo o intercâmbio biótico entre a Amazônia e a Floresta Atlântica (De Oliveira et al. 1999; Behling et al*.,* 2000, Mayle & Beerling, 2004; Mayle et al., 2004; Werneck, 2011). Os brejos de altitude, enclaves naturais de florestas úmidas, parecem ser o que restou dessa conexão entre Amazônia e Floresta Atlântica, em meio à vegetação de Caatinga, no nordeste do Brasil (de Oliveira et al., 1999; Werneck, 2011).

Avanços nas técnicas de sequenciamento de DNA e a crescente disponibilidade e acessibilidade a esses dados, tem contribuído para o aumento no número de estudos evolutivos que busquem compreender o papel de eventos geomorfológicos e climáticos na produção dos mais diversos padrões de diversificação biótica observados na região tropical (Moritz et al. 2000; Emerson et al. 2001; Rull, 2007). Meta-analises recentes baseadas em filogenias datadas retratam um cenário complexo, com diversos eventos atuando de forma simultânea nas mais diversas escalas temporais e espaciais (Rull, 2008; Turchetto-Zolet et al., 2013). A crescente utilização de técnicas moleculares em estudos filogenéticos e filogeográficos também tem se mostrado uma excelente ferramenta na identificação de espécies crípticas (Geurgas & Rodrigues, 2010; Gamble et al., 2012; Prado et al., 2012; Werneck et al., 2012; Domingos et al., 2014; Gehara et al., 2014), trazendo à tona uma diversidade da herpetofauna até então subestimada. Considerando que uma única espécie pode apresentar estruturação geográfica de suas populações, buscar entender como tais populações se relacionam e quais os principais processos que atuaram e/ou influenciaram moldando a sua história evolutiva auxilia não só na compreensão da história da região, como numa melhor definição de políticas para sua conservação.

Um dos focos do presente estudo é o lagarto *Norops fuscoauratus*, pertencente à família Dactyloidae (Towsend et al, 2011; Nicholson et al, 2012), de habito semi-arborícola, pequeno porte (comprimento rostro-cloacal máximo de 54 mm), encontrado em áreas de floresta primária e secundária (Avila-Pires, 1995). A espécie também está presente nos brejos de altitude do Nordeste brasileiro, fragmentos de floresta úmida localizados entre 600-1100 metros de altitude que abrigam espécies de áreas florestais

incapazes de sobreviver nas condições áridas/semiáridas do ambiente de Caatinga que cercam esses fragmentos (Borges-Nojosa & Caramaschi, 2003; Loebmann & Haddad, 2010).

Os lagartos pertencentes à família Dactyloidae caracterizam-se principalmente pela presença de duas estruturas características: apêndice gular e lamelas subdigitais (Losos, 2009). As lamelas geralmente variam em tamanho e em quantidade e tal variação parece estar relacionada ao habito da espécie, se terrestre ou arborícola (Nicholson et al. 2006). Já o apêndice gular ou papo é composto por uma extensão de pele situada na região do pescoço ligada ao músculo ceratobranquial, podendo estar presente tanto em fêmeas quanto em machos (Nicholson et al. 2007). O papo é utilizado para comunicação intra e interespecífica em várias situações incluindo interações agonísticas e corte. Por ser uma estrutura altamente diversa, apresentando variação quanto ao padrão de cor, forma e tamanho, o apêndice gular tem sido o foco de diversos estudos que busquem quantificar a diversidade morfológica dessa estrutura e compreender os fatores que influenciam na sua evolução dentro e entre espécies (Nicholson et al. 2007; Vanhooydonk et al. 2009; Glor & Laport, 2012; Ng et al, 2013, Macedonia et al. 2014). Além disso, variações no tamanho e cor do papo são frequentemente utilizadas como caracteres diagnósticos de espécies e portanto, consideradas como importantesrt no processo de especiação e divergência populacional (Losos & Schneider, 2009). Dessa forma, muitas descrições e caracterizações de espécies de Dactyloidae se baseiam, ao menos em parte, nos padrões de coloração e tamanho do papo (Avila-Pires, 1995; D'Angiolella et al, 2011; Köhler, 2011).

Uma outra estrutura de grande importância na taxonomia e sistemática de Squamata em geral, é o hemipenis, o órgão copulatório masculino. Hemipenes são estruturas pareadas e tubulares que variam em relação a ornamentação, forma e tamanho (Dowling & Savage, 1960). A morfologia hemipeniana tem se mostrado como uma excelente ferramenta capaz de auxiliar na identificação de espécies e contribuir para elucidar relações filogenéticas (Dowling & Savage 1960, Böhme 1991, Ziegler & Böhme 1997, Keogh, 1999; Köhler et al. 2012). Muitos estudos reportam a importância da morfologia hemipeniana na identificação de espécies crípticas, principalmente em situações onde a morfologia externa é conservativa e com alto nível de paralelismos (Keogh, 1999, Nunes et al, 2012; Köhler et al., 2012). Além disso, por estarem diretamente envolvidos no processo reprodutivo, alterações na morfologia hemipeniana

podem representar um mecanismo físico de isolamento reprodutivo (Arnold, 1986, Köhler & Sunyer 2008, Köhler 2009; Nunes et al., 2012).

Com relação a *N. fuscoauratus,* somente os machos possuem apêndice gular que se estende até quase o meio-corpo, e apresentam uma ampla variação de coloração, com papos em tons de cinza, verde, amarelo, vermelho e bicolores (Avila-Pires, 1995). A morfologia externa da espécie foi estudada por Avila-Pires (1995), que analisou espécimes provenientes de diversas localidades na Amazônia e, a despeito da grande variação na coloração do papo, não reportou grandes variações morfológicas, embora tenha destacado a importância de amostras provenientes da Floresta Atlântica serem incluídas em uma análise futura. Glor et al. (2001) encontraram uma baixa diversidade genética em *N. fuscoauratus* quando a compararam com outras espécies de *Norops* e *Dactyloa* ocorrentes na Amazônia. Os autores estimaram uma idade mínima para a espécie de 3 Ma, e sugeriram que *N. fuscoauratus* seria uma colonizadora recente da América do Sul. No entanto, as bases evolutivas das variações de coloração e conservatismo morfológico em *N. fuscoauratus* ainda não foram investigadas por meio de amostragens geográficas densas e baseadas em marcadores moleculares independentes.

Nesse sentido, o presente trabalho se propõe a examinar *N. fuscoauratus* buscando compreender a sua história populacional e diversificação dessa espécie amplamente distribuída ao longo de áreas florestadas disjuntas da América do Sul. Busca-se também verificar se a grande variação na coloração do papo desta espécie pode estar relacionada a variação em outros caracteres morfológicos, hemipenianos e genéticos, e/ou ser influenciada por variáveis ambientais.

Dessa forma, a presente tese encontra-se estruturada em três capítulos, onde nos dois primeiros me proponho responder as seguintes questões:

1) Qual a estrutura populacional e como se deu a diversificação de *Norops fuscoauratus* na América do Sul?

2) As diferentes cores do papo encontradas em *Norops fuscoauratus* representam grupos distintos entre si capazes de serem associados a caracteres genéticos, morfológicos e hemipenianos?

Além disso, diante da falta de informações acerca da morfologia hemipeniana em relação as espécies sul-americanas, no terceiro capitulo busco minimizar essa lacuna de conhecimento e apresento dados sobre a diversidade dos hemipenes das espécies de Dactyloidae (*Norops* e *Dactyloa*) que ocorrem no Brasil, fornecendo descrições dessa importante estrutura utilizada na taxonomia e sistemática de Squamata, relacionando a sua variação com as atuais propostas filogenéticas disponíveis na literatura.

Sendo assim, no primeiro capitulo utilizei um gene mitocondrial e quatro genes nucleares para estimar as relações filogenéticas e o tempo de divergência entre as populações de *Norops fuscoauratus;* realizei uma analise de agrupamento bayesiano para identificar a possível existência de clusters espaciais de indivíduos; estimei os parâmetros demográficos e a estrutura filogeográfica do marcador mitocondrial ao longo da distribuição da espécie e por fim, busquei quantificar a contribuição relativa do clima e da distancia geográfica na estrutura genética de *N. fuscoauratus* através de uma análise de partição de variância.

Para responder a pergunta do segundo capitulo, busquei quantificar a variação na coloração do papo agrupando as cores em classes abrangentes que me permitissem abarcar a maior parte do gradiente de coloração observado. Caracteres morfométricos, merísticos, hemipenianos e genéticos de indivíduos de *N. fuscoauratus* que apresentavam informação de coloração do papo foram então coletados e analisados. Utilizei as variáveis bioclimáticas da base de dados do Worlclim para verificar a influência das mesmas na coloração do papo de *N. fuscoauratus*.

Por fim, no terceiro capítulo, faço a compilação das hipóteses filogenéticas existentes que incluem as espécies de *Norops* e *Dactyloa* que ocorrem no Brasil, buscando observar se existe congruência entre os caracteres hemipenianos observados e as relações filogenéticas propostas.

Os nossos resultados mostram que apesar de ser uma espécie amplamente distribuída, com alto grau de variação na coloração do apêndice gular, *N. fuscoauratus* apresenta, em geral, baixa diferenciação geográfica e baixa diversidade genética. A diversificação da espécie parece ter ocorrido há aproximadamente 2.2 Ma, datando portanto do início do período Pleistocênico. As análises populacionais e a análise demográfica coalescente multilocus apontam para um cenário geral de expansão populacional, apoiando a proposta

de Glor et al. (2001) de que *N. fuscoauratus* é uma espécie colonizadora recente da América do Sul.

Além disso, as diferentes cores do papo presentes em *N. fuscoauratus* não parecem estar relacionadas a variações genéticas, morfológicas e hemipenianas, com os grupos de coloração do papo não correspondendo a espécies crípticas, ou sequer a um indicio de diferenciação dentro da espécie. Contudo, a variação na coloração do papo parece responder a fatores climáticos como alterações nas taxas de precipitação e temperatura, embora essa relação evidenciada tenha sido baixa, de acordo com o coeficiente de determinação.

Com relação a variação hemipeniana nas espécies de *Norops* e *Dactyloa* ocorrentes no Brasil, os resultados mostram que caracteres hemipenianos são, em geral, filogeneticamente informativos, com os hemipenis apresentando um certo grau de similaridade, mas diferindo entre si em com relação a forma e ornamentação. Em certos casos, estruturas similares estiveram presentes em espécies filogeneticamente distantes dentro do mesmo gênero.

Dessa forma, o presente estudo demonstra que, nem sempre espécies amplamente distribuídas representam espécies crípticas ou unidades evolutivas independentes. Além disso, evidenciamos que variações na coloração do papo, uma estrutura amplamente utilizada na taxonomia e sistemática de Dactyloidae, podem simplesmente refletir um polimorfismo mantido dentro da população, sem que hajam correlatos com outros caracteres morfológicos, genéticos e hemipenianos que indiquem algum sinal adaptativo.

2. Referências

Avila-Pires, T.C.S (1995). Lizards of Brazilian Amazonia (Reptilia: Squamata). *Zoologische verhandelingen*, *299*(1), 1-706.

Antonelli, A., Nylander, J. A., Persson, C., & Sanmartín, I. (2009). Tracing the impact of the Andean uplift on Neotropical plant evolution. *Proceedings of the National Academy of Sciences*, *106*(24), 9749-9754.

Arnold E.N. (1986). Why copulatory organs provide so many useful taxonomic characters: the origin and maintenance of hemipenial differences in lacertid lizards (Reptilia: Lacertidae). *Biological Journal of the Linnean Society 29*:263–281.

Behling, H., Arz, H. W., Pätzold, J., & Wefer, G. (2000). Late Quaternary vegetational and climate dynamics in northeastern Brazil, inferences from marine core GeoB 3104-1. *Quaternary Science Reviews*, *19*(10), 981-994.

Böhme, W. (1991). New findings on the hemipenial morphology of monitor lizards and their systematic implications. Pp. 42-49. In Böhme, W. & H.G. Horn (eds.), *Advances in Monitor Research,* Mertensiella 2. Deutsche Gesellschaft für Herpetologie und Terrarienkunde e.V., Rheinbach,

Borges-Nojosa, D.M. & Caramaschi, U. (2003). Composição e análise comparativa da diversidade e das afinidades biogeográficas dos lagartos e anfisbenídeos (Squamata) dos Brejos Nordestinos. Pp. 489-540. In: I.R. Leal, M. Tabarelli & J.M.C. Silva (eds.). *Ecologia e conservação da Caatinga.* Universidade Federal de Pernambuco, Recife, PE.

Carnaval, A. C., Hickerson, M. J., Haddad, C. F., Rodrigues, M. T., & Moritz, C. (2009). Stability predicts genetic diversity in the Brazilian Atlantic forest hotspot. *Science*, *323*(5915), 785-789.

Cheng, Hai, et al. "Climate change patterns in Amazonia and biodiversity." *Nature communications* 4 (2013): 1411.

Colinvaux, P. A., & De Oliveira, P. E. (2001). Amazon plant diversity and climate through the Cenozoic. *Palaeogeography, Palaeoclimatology, Palaeoecology*, *166*(1), 51-63.

De Oliveira, P.E., Franca Barreto, A.M. & Suguio, K. (1999). Late Pleistocene/Holocene climatic and vegetational history of the Brazilian caatinga: the fossil dunes of the middle Sao Francisco River. *Palaeogeography Palaeoclimatology Palaeoecology*, 152,319–337.

D'Angiolella, A. B., Gamble, T., Avila-Pires, T. C., Colli, G. R., Noonan, B. P., & Vitt, L. J. (2011). *Anolis chrysolepis* Duméril and Bibron, 1837 (Squamata: Iguanidae), revisited: molecular phylogeny and taxonomy of the *Anolis chrysolepis* species group. *Bulletin of the Museum of Comparative Zoology*, *160*(2), 35–63.

Diniz-Filho, J. A. F., Terribile, L. C., de Oliveira, G., & Rangel, T. F. L. V. B. (2009). Padrões e processos ecológicos e evolutivos em escala regional. *Megadiversidade*, *5*, 5-16.

Domingos, F. M., Bosque, R. J., Cassimiro, J., Colli, G. R., Rodrigues, M. T., Santos, M. G., & Beheregaray, L. B. (2014). Out of the deep: Cryptic speciation in a Neotropical gecko (Squamata, Phyllodactylidae) revealed by species delimitation methods. *Molecular Phylogenetics and Evolution*, *80*, 113-124.

Dowling H.G., Savage J.M. (1960). A guide to the Snake hemipenis: a survey of basic structure and systematic characteristics. *Zoologica 45*:17–28.

Emerson, B. C., Paradis, E., & Thébaud, C. (2001). Revealing the demographic histories of species using DNA sequences. *Trends in Ecology & Evolution, 16(12),* 707-716.

Figueredo, J., Hoorn, C., van der Ven, P. & Soares, E. 2009. Late Miocene onset of the Amazon River and the Amazon deep-sea fan: Evidence from the Foz do Amazonas Basin. *Geology 37(7):* 619–622.

Gamble, T., Colli, G. R., Rodrigues, M. T., Werneck, F. P., & Simons, A. M. (2012). Phylogeny and cryptic diversity in geckos (*Phyllopezus*; Phyllodactylidae; Gekkota) from South America's open biomes. *Molecular Phylogenetics and Evolution*, *62*(3), 943-953.

Gaston, K. J. (2000). Global patterns in biodiversity. *Nature*, *405*(6783), 220-227

Gehara, M., Crawford, A. J., Orrico, V. G., Rodríguez, A., Lötters, S., Fouquet, A., & Köhler, J. (2014).

Gehara, M., Crawford, A.J., Orrico, V.G.D., Rodríguez, A., Lötters, S., Fouquet, A., Barrientos, L.S., Brusquetti, F., De-la-Riva, I., Ernst, R., Urrutia, G.G., Glaw, F., Guayasamin, J.M., Hölting, M., Jansen, M., Kok, P.J.R., Kwet, A., Lingnau, R., Lyra, M., Moravec, J., Pombal-Jr., J.P., Rojas-Runjaic, F.J.M., Schulze, A., CelsaSeñaris, J., Solé, M., Rodrigues, M.T., Twomey, E., Haddad, C.F.B., Vences, M., Köhler J. (2014): High levels of diversity uncovered in a widespread nominal taxon: continental phylogeography of the Neotropical tree frog *Dendropsophus minutus*. Plos One, 9: e103958.

Geurgas, S. R., & Rodrigues, M. T. (2010). The hidden diversity of *Coleodactylus amazonicus* (Sphaerodactylinae, Gekkota) revealed by molecular data. *Molecular Phylogenetics and Evolution*, *54*(2), 583-593.

Glor, R. E., Vitt, L. J., & Larson, A. (2001). A molecular phylogenetic analysis of diversification in Amazonian *Anolis* lizards. *Molecular Ecology*, *10*(11), 2661-2668.

Glor, R. E., & Laport, R. G. (2012). Are subspecies of *Anolis* lizards that differ in dewlap color and pattern also genetically distinct? A mitochondrial analysis. *Molecular Phylogenetics and Evolution*, *64*(2), 255-260.

Goyannes-Araújo, P., Almeida-Gomes, M., Borges-Junior, V. N. T., Albuquerque, H. G., Vrcibradic, D., & Rocha, C. F. D. (2009). Notes on Geographic Distribution. *Check List, 5(3)*, 746-748.

Haffer, J. (1969). Speciation in Amazonian forest birds. *Science 165*: 131–137

Haffer, J. (2008). Hypotheses to explain the origin of species in Amazonia. Brazilian *Journal of Biology, 68*(4), 917-947.

Hoorn, C., Guerrero, J., Sarmiento, G.A., & Lorente, M.A., 1995, Andean tectonics as a cause for changing drainage patterns in Miocene northern South America*: Geology 5*(23): 237–240

Hoorn, Carina, et al. (2010). Amazonia through time: Andean uplift, climate change, landscape evolution, and biodiversity. *Science* 330.6006: 927-931.

Keogh S. (1999). Evolutionary implications of hemipenial morphology in the terrestrial Australian elapid snakes. *Zoological Journal of the Linnean Society* 125: 239–278.

Köhler, G., & Sunyer, J. (2008). Two new species of anoles formerly referred to as *Anolis limifrons* (Squamata: Polychrotidae). *Herpetologica*, *64*(1), 92-108.

Köhler, G. (2009). New species of *Anolis* formerly referred to as *Anolis altae* from Monteverde, Costa Rica (Squamata: Polychrotidae). *Journal of Herpetology, 43*(1), 11-20.

Köhler, G. (2011). A new species of anole related to *Anolis altae* from Volcán Tenorio, Costa Rica (Reptilia, Squamata, Polychrotidae). *Zootaxa.* (3120), 29-42.

Köhler, J., Hahn, M., & Köhler, G. (2012). Divergent evolution of hemipenial morphology in two cryptic species of mainland anoles related to *Anolis polylepis. Salamandra, 48*(1), 1-11.

Latrubesse, E.M., Cozzuol, M., Silva-Caminha, S.A.F., Rigsby, C.A., Absy, M.L. & Jaramillo, C. 2010. The Late Miocene paleogeography of the Amazon Basin and the evolution of the Amazon River system. *Earth-Science Reviews 99*: 99–124.

Loebmann, D. e Haddad, C.F.B. 2010. Amphibians and reptiles from a highly diverse area of the Caatinga domain: composition and conservation implications. *Biota Neotropica 10(3)*: 227–256.

Losos J.B. & Schneider C.J. (2009). *Anolis* lizards. Current Biology. 19:R316–R318.

Losos, J. B. (2009). *Lizards in an evolutionary tree: ecology and adaptive radiation of anoles* (Vol. 10). Univ of California Press.

Macedonia, J. M., Clark, D. L., & Tamasi, A. L. (2014). Does selection favor dewlap colors that maximize detectability? A test with five species of Jamaican *Anolis* lizards. *Herpetologica*, *70*(2), 157-170.

Mayle, F. E., & Beerling, D. J. (2004). Late Quaternary changes in Amazonian ecosystems and their implications for global carbon cycling. *Palaeogeography, Palaeoclimatology, Palaeoecology*, *214*(1), 11-25.

Mayle, F. E. (2004). Assessment of the Neotropical dry forest refugia hypothesis in the light of palaeoecological data and vegetation model simulations. *Journal of Quaternary Science*, *19*(7), 713-720.

Moritz, C., Patton, J. L., Schneider, C. J., & Smith, T. B. (2000). Diversification of rainforest faunas: an integrated molecular approach. *Annual Review of Ecology and Systematics*, 533-563.

Morrone, J. J. 2004. Panbiogeografía, componentes bióticos y zonas de transición. *Revista Brasileira de Entomologia 48:* 149–162

Ng, J., Landeen, E. L., Logsdon, R. M., & Glor, R. E. (2013). Correlation between *Anolis* lizard dewlap phenotype and environmental variation indicates adaptive divergence of a signal important to sexual selection and species recognition. *Evolution*, *67*(2), 573-582.

Nicholson, K. E., Harmon, L. J., & Losos, J. B. (2007). Evolution of Anolis lizard dewlap diversity. *PLoS One*, *2*(3), e274.

Nicholson, K. E., Crother, B. I., Guyer, C., & Savage, J. M. (2012). It is time for a new classification of anoles (Squamata: Dactyloidae). *Zootaxa*, *3477*, 1-108.

Nores, M. (2004). The implications of Tertiary and Quaternary sea level rise events for avian distribution patterns in the lowlands of northern South America. *Global Ecology and Biogeography*, *13*(2), 149-161.

Nunes, P.M.S., Fouquet, A., Curcio, F. F., Kok P., & Rodrigues, M.T. (2012). Cryptic species in *Iphisa elegans* Gray, 1851 (Squamata: Gymnophthalmidae) revealed by hemipenial morphology and molecular data. *Zoological Journal of the Linnean Society, 166*(2), 361-376.

Prado, C., Haddad, C. F., & Zamudio, K. R. (2012). Cryptic lineages and Pleistocene population expansion in a Brazilian Cerrado frog. *Molecular Ecology*, *21*(4), 921-941.

Ribas, C.C.; Aleixo, A.; Nogueira, A.C.R.; Miyaki, C.Y. & Cracraft, J. 2012. A palaeobiogeographic model for biotic diversification within Amazonia over the past three million years. *Proceedings of the Royal Society B, 279*: 681–689.

Ricklefs, R. E. (2004). A comprehensive framework for global patterns in biodiversity. *Ecology Letters, 7*(1), 1-15.

Rossetti, D.F., Toledo, P.M. & Góes, A.M. 2005. New geological framework for Western Amazonia (Brazil) and implications for biogeography and evolution. *Quaternary Research 63*: 78-89.

Rosseti, D.F. & Valeriano, M.M. 2007. Evolution of the lowest Amazon basin modeled from the integration of geological and SRTM topographic data. *Catena 70*(2): 253–265.

Rull, V. (2007). On the origin of present Neotropical biodiversity: a preliminary meta-analysis about speciation timing using molecular phylogenies. In *Orsis: organismes i sistemes* (Vol. 22, pp. 105-119).

Rull, V. (2008). Speciation timing and neotropical biodiversity: the Tertiary–Quaternary debate in the light of molecular phylogenetic evidence. *Molecular Ecology*, *17*(11), 2722-2729.

Rull, V. (2011). Neotropical biodiversity: timing and potential drivers. *Trends in ecology & Evolution*, *26*(10), 508-513.

Rull, V. (2013). Palaeoclimates and Amazon biodiversity. *Journal of Biogeography*, *40*(8), 1413-1414.

Thomé, M. T. C., Zamudio, K. R., Giovanelli, J. G., Haddad, C. F., Baldissera, F. A., & Alexandrino, J. (2010). Phylogeography of endemic toads and post-Pliocene persistence of the Brazilian Atlantic Forest. *Molecular Phylogenetics and Evolution*, *55*(3), 1018-1031.

Townsend, T.M., Mulcahy, D.G., Noonan, B.P., Sites Jr., J.W., Kuczynski, C.A., Wiens, J.J., Reeder, T.W., 2011. Phylogeny of iguanian lizards inferred from 29 nuclear loci, and

a comparison of concatenated and species-tree approaches for an ancient, rapid radiation. *Molecular phylogenetics and evolution*. 61, 363–380.

Turchetto-Zolet, A.C., Pinheiro, F., Salgueiro, F., & Palma-Silva, C. (2013). Phylogeographical patterns shed light on evolutionary process in South America. *Molecular Ecology*, *22*(5), 1193-1213.

Van der Hammen, T., & Hooghiemstra, H. (2000). Neogene and Quaternary history of vegetation, climate, and plant diversity in Amazonia. *Quaternary Science Reviews, 19*(8), 725-742.

Vanhooydonck B, Herrel A, Meyers JJ, Irschick DJ. 2009. What determines dewlap diversity in *Anolis* lizards? An among-island comparison. *Journal of Evolutionary Biology 22*:293–305.

Vanzolini, P. E., & Williams, E. E. (1970). South American anoles: the geographic differentiation and evolution of the *Anolis chrysolepis* species group (Sauria, Iguanidae). *Arquivos de Zoologia*, *19*(1-2), 1-176.

Werneck, F.P. 2011. The diversification of eastern South American open vegetation biomes: Historical biogeography and perspectives. *Quaternary Science Reviews*, 1–19.

Werneck, F. P., Gamble, T., Colli, G. R., Rodrigues, M. T., & Sites Jr, J. W. (2012). Deep Diversification and long-term Persistence in the South American "Dry Diagonal": Integrating continent-wide Phylogeography and Distribution Modelling of geckos. *Evolution*, *66*(10), 3014-3034.

Ziegler, T., Vences, M., Glaw, F., & Böhme, W. (1997). Genital morphology and systematics of *Geodipsas* Boulenger, 1896 (Reptilia: Serpentes: Colubridae), with description of a new genus. *Revue Suisse de Zoologie*, *104*(1), 95-114.

POPULATION STRUCTURE AND DIVERSIFICATION OF THE MAINLAND RAINFOREST ANOLE *NOROPS FUSCOAURATUS* (SQUAMATA: DACTYLOIDAE)

Annelise B. D'Angiolella[1], Teresa C.S. Avila Pires[1,2], Miguel T.U. Rodrigues[3], Ivan Prates[4], and Ana C. Carnaval[4]

[1] Programa de Pós Graduação em Zoologia UFPA/MPEG, Belém, Pará, Brazil,

Author for correspondence: annelise.dangiolella@gmail.com.

[2] Museu Paraense Emilio Goeldi, Belém, Pará, Brazil.

[3] Universidade de São Paulo, USP, São Paulo, Brazil

4 The City College of New York, Division of Science, Biology Department, CUNY, New York, USA.

ABSTRACT

Molecular data has proven to be a useful tool in recovering crytic diversity and identifying independent evolutionary units in single and widely distributed taxa. *Norops fuscoauratus* is a widespread mainland anole species that occurs throughout the Amazonian and Atlantic rainforests in South America. In the present study, we perform multilocus analyses to identify the possible existence of spatial clusters of individuals, describe demographic parameters, phylogeographical structure, and quantify the importance of geography and climate in the genetic structure of *N. fuscoauratus*. Our results indicate that the species diversified during late Pliocene-early Pleistocene transition, showing a general pattern of recent population expansion. Population genetics and phylogenetic analysis indicate low geographic and genetic structure, in concordance with the relative recent diversification of the specie.

Keywords: Neotropical region, Population structure, Phylogeography, *Norops fuscoauratus*, Dactyloidae.

1. INTRODUCTION

The astonishing diversity of the Neotropical region is well known and understanding the processes that promoted diversification and shaped distributions of existing taxa is the focus of many evolutionary studies (Avila-Pires et al. 2012; Ribas et al. 2012; Werneck et al. 2012; Smith et al, 2014). Many factors are known to influence the diversification patterns in the Neotropics, but two main aspects have been proposed and debated: Tertiary paleogeographic changes and Quaternary climatic oscillations (Van der Hammen & Hooghiemstra, 2000; Colinvaux & De Oliveira, 2001; Rull, 2007; Carnaval et al. 2009; Hoorn et al. 2010; Cheng et al. 2013). However, as our knowledge increases it becomes clear that Neotropical biodiversity is the result of complex ecological and evolutionary histories, with both processes being important in generating and maintaining this diversity (Moritz et al. 2000; Rull, 2007, 2008).

The increasing utilization of molecular data in phylogenetic and phylogeographic studies has proven to be an excellent tool in identifying species and describing biological diversity, revealing the existence of a large number of cryptic species, especially in relation to South American widespread herpetofauna (Fouquet et al. 2007; Camargo et al. 2006; Geurgas & Rodrigues, 2010; Gamble et al. 2012; Prado et al. 2012; Werneck et al. 2012; Domingos et al. 2014; Gehara et al. 2014). However, studying widespread species across vast continental areas is not an easy task, given limited genetic sampling and the difficulty in retrieving material from all countries that encompass the species' distributions

An example of a widespread Neotropical species is *Norops fuscoauratus* (Duméril & Bibron, 1837), a small Dactyloid lizard of 49-54 mm of snouth-vent lengh and a common inhabitant of forested areas in cis-Andean South America. The species is distributed throughout the Amazonian and Atlantic forests, also occurring in isolated patches of humid forests situated between 600-1000 meters of altitude, surrounded by the semi-arid Caatinga matrix, known *as brejos de altitude* or *brejos nordestinos* (references?). Males of this species have a large dewlap that extends posteriorly beyond the chest and shows variation in color: shades of grey, olive, yellow, red and bicolored dewlaps were reported

by Avila-Pires (1995). Considering that anole dewlap has been frequently associated with reproductive isolation and speciation (Nicholson et al. 2007; Losos & Schneider, 2009) the variation found in *N. fuscoauratus* could be an indicative of cryptic diversity. However, Glor et al. (2001) found the smallest amount of genetic variation in *N. fuscoauratus* in relation to other Amazonian anoles, when comparing five localities throughout Amazonia. They suggested the species to be a relatively recent (late Pliocene) invader of South America from Central America.

In this study, we look more thoroughly at *N. fuscoauratus* to understand the evolutionary history of the species, as a possible example of recent invaders with a history mainly during the Plio-Pleistocene, which nevertheless succeeded in colonizing large forested areas. We also look for genetic geographic structure that might indicate cryptic species and maybe an older history for the species than previously suggested.

To this end, we 1) estimate phylogenetic relationships among populations of *Norops fuscoauratus* based on five molecular markers (one mtDNA and four nDNA); 2) estimate the divergence time of the species; 3) employ a Bayesian clustering method to identify possible spatial clusters of individuals, 4) assess demographic parameters and phylogeographical structure of mtDNA haplotypes across its geographical range and 5) quantify the relative contribution of climate and geography in *N. fuscoauratus* genetic structure.

2. MATERIAL AND METHODS

2.1 Sampling and molecular data collection

A total of 243 new sequences of *N. fuscoauratus* were generated from 112 localities throughout the species distribution including both the Amazon and Atlantic forests (Appendix 1; Figure 1). Three sequences from previous studies were also included (Glor et al. 2001; Prates et al. 2014). Tissues samples covered most of the distribution of *N. fuscoauratus*, including localities from Amazonia, Atlantic forest and *Brejos do Nordeste*.

Genomic DNA was extracted from muscle, liver, or tail clips following a standard phenol/chloroform protocol (Sambrook & Russel, 2001) or with the DNeasy Blood and Tissue Kit (Qiagen, Valencia, California). We amplified the mithocondrial gene ND2 (NADH dehydrogenase subunit 2) and adjacent tRNAs as well as four additional nuclear markers: RAG1 (recombination-activating gene 1), DNAH3 (dynein axonemal heavy

chain), MKL1 (megakaryoblastic leukemia 1) and SNCAIP (synuclein alpha interacting protein).

Polymerase Chain Reaction (PCR) profile followed an initial 5-min denaturation at 95 °C, proceeded by 32 cycles of denaturation (30 s at 95 °C), annealing (45 s at 52–56 °C), extension (1 min at 72 °C), and a final extension of 5 min at 72 °C. The PCR products were purified with the Polyethylene glycol protocol (PEG). Sequencing was carried out on an ABI 3130 automated capillary sequencer (Applied Biosystems, Foster City, California, USA) with the ABI Prism Big Dye terminator Kit. To confirm observed mutations, both strands of each sample were sequenced.

Sequences were edited and aligned using Muscle in Geneious Pro 6 (Biomatters, Auckland) and protein-coding sequences were translated into aminoacids to confirm alignment and ensure there were no premature stop codons. For nuclear loci, heterozygous nucleotide positions were inferred by the presence of double peaks of the same size in the electropherogram. The Bayesian approach implemented in PHASE 2.1 1 (Stephens & Scheet, 2005) was used to solve the gametic phase of haplotypes of the heterozygous individuals and the haplotypes with the highest probabilities were selected for analysis.

Models of nucleotide evolution and best-fit partition schemes, including partitions by codon position, were determined with Partition Finder 1.1.1 (Lanfear et al., 2012), implementing the Akaike information criterion (Akaike, 1974) for Maximun Likelihood (ML) and Bayesian Inference (BI) inference. The concatenated dataset was generated in Sequence Matrix (Vaidya et al., 2011) and it was partitioned by gene, with a sixth partition for tRNAs.

2.2 Genetic diversity, population structure and demography

We performed a spatial Bayesian clustering approach in GENELAND v.3.1.4 (Guillot et al, 2005) to infer the number of populations and their spatial boundaries using the ND2 dataset. The model uses genotype or haplotype data and spatial coordinates of sampled individuals to cluster them into populations (k clusters) that are approximately at Hardy–Weinberg equilibrium, considering linkage equilibrium between loci (Guillot et al. 2009) and without any a priori knowledge on the populational units and limits. The general assumption of the model is that a small number of polygons, determined using the colored

Poisson-Voronoi tessellation, can approximate the spatial domain occupied by the inferred clusters (Guillot et al, 2005). The spatial model is suitable to detect cryptic spatial genetic structure, to map borders between the identified populations and to detect migrants between those populations (Guillot et al, 2005). The model assumes that the overall population under study consists of several groups separated by barriers to gene flow; these barriers could be either physical barriers such as rivers, roads, urban areas, or barriers induced by climate (Stenseth et al. 2004).

For this analysis, the correlated model of allele frequency was used with 100,000 MCMC iterations, thinning of 100, with 10 independent runs, minimum number of populations set to one and maximum set to 10. We set the maximum Poisson process equal to the number of samples, the number of nuclei in the Poisson–Voronoi tessellation at 3 times the sample size (Guillot & Estoup, et al. 2005; Guillot, Mortier & Estoup 2005), and the *delta.coord* parameter (the uncertainty parameter to account for the possibility of bias in geographic coordinates) to 0.05, which corresponds to 3.5 km. Previous tests were made with longer runs of the Markov chain and alternative values for the *delta.coord*, but they did not significantly influence either the number of populations inferred or the posterior probability of membership for individual samples. Once K was inferred, a final run was completed to establish population boundaries. Clusters identified in GENELAND were used in all subsequent population analyses and within population measures of genetic diversity.

We calculated standard indices of population genetic diversity (number of haplotypes and of segregating sites, haplotype and nucleotide diversity), for each estimated cluster and for the entire dataset using ARLEQUIN v.3.1 (Excoffier et al. 2005). We investigated genetic differentiation between pairs of putative populations through the computation of *Fst* (significance assessed by 10,000 permutations). *Fst* statistics can be interpreted as a measure of how much genetic diversity exists between subpopulations compared to the diversity in the entire population, so an *Fst* value around 0 indicates that compared populations are undistinguishable, while a value around or equal to 1 indicates that populations are maximally differentiated (Peter & Slatkin 2013). Net between group distance for the mitochondrial data (Tamura, Nei & Kumar, 2004) was calculated using MEGA version 5.05 (Tamura et al. 2011) for the GENELAND estimated populations, calculating the standard error using 1000 bootstrap replicates. For visualization purposes, we constructed haplotype networks for each gene analyzed, highlighting the clusters

recovered by GENELAND analysis using the software haploview (Barret et al, 2005) for nDNA and the software SplitsTree (Huson & Bryant, 2006) for mtDNA. We also used ARLEQUIN to conduct an Analysis of molecular variance (AMOVA) to estimate genetic differentiation between clusters recovered by GENELAND and to estimate the demographic history of the same clusters through Fu's Fs neutrality test and Tajimas's D test with 10.000 permutations.

For ND2, both using the entire data set and the clusters recovered by GENELAND, we investigated mismatch distribution of pairwise genetic differences using ARLEQUIN. The observed distributions were compared to a unimodal expectation under a model of recent population expansion. The raggedness index (Harpending 1994) between observed and expected mismatch distributions were calculated and used to validate the estimated expansion model (Schneider & Excoffier, 1999), with a non-significant value of the raggedness index not allowing to exclude the null hypothesis of an expansion model. Significance was accessed using a parametric bootstrap analysis, and we considered p values >0.05 as significants. We also performed the coalescent-based Extended Bayesian Skyline Plot approach (EBSP; Heled & Drummond, 2008) as implemented in the software BEAST version 1.8.1 (Drummond et al. 2012), which analyzes multiple unlinked loci to estimate the demographic history of each cluster recovered by GENELAND.

2.3 Phylogenetic analysis and molecular dating

Outgroup taxa used in the following analysis were selected from Nicholson et al. (2012) and Prates et al. (2014). We constructed independent phylogenetic trees for the mtDNA molecular marker (not shown) and for the nuclear concatenated dataset using the maximum likelihood (ML) criteria in RAxML (Stamakis, 2006). Additionally, an mtDNA Bayesian tree was estimated with MrBayes 3.2.1 (Ronquist et al. 2012) through two independent runs and four Markov chains of 20 million generations each, sampling every 1000 steps. In both MrBayes and RAxML analyses, protein-coding genes were partitioned by codon position as indicated by Partition Finder and both analyses (ML and Bayesian inference) were conducted in CIPRES Web Portal (Miller et al. 2010).

To estimate divergence times, we performed simultaneous phylogenetic reconstruction and divergence time estimation under a concatenation approach using BEAST v.1.8.1 (Drummond et al. 2012). For this analysis, we implemented the partition

by gene, once BEAST analyses regularly failed to reach stationarity when applying the partition by codon position used in previous analysis.

As a calibration point, we set a normally-distributed prior to the node corresponding to the most recent common ancestor of *N. fuscoauratus* and *N. trachyderma* (mean = 11.83 Ma, standard deviation = 2.85 Ma) following Prates et al. (2014), who provided divergence times between pleurodont iguanian lizards based on five nuclear genes and well-known fossils. We ran three independent chains of 100 million steps, sampling every 10,000 steps. Convergence and stationarity of model parameters were assessed using Tracer 1.5, the runs were combined in LogCombiner 1.8 (with a 25% burn-in), and we summarized a maximum clade credibility tree in TreeAnnotator 1.8 (Drummond et al. 2012). We unlinked parameters of substitution rates and nucleotide frequencies between partitions. The resulting topologies were visualized in FigTree 1.4 (available from http://tree.bio.ed.ac.uk/software/figtree/).

We implemented both a strict and an uncorrelated lognormal clock strategy (Drummond et al. 2006), but a strict clock was favored over an uncorrelated lognormal relaxed clock as indicated by Bayes factors (logBayes = 3.75) estimated in Tracer with 1000 bootstrap replicates. The strict molecular clock was implemented with an uniform prior distribution (interval = 0 to 1) to the mean rate of the molecular clock while implementing default settings for the parameters relative to substitution rates, nucleotide frequencies, and the Coalescent constant tree prior.

2.4 Influence of climate and geographic distance in genetic variation

In order to quantify the relative contribution of climate and geographic distance in *N. fuscoauratus* genetic structure at the sampled locations, we performed a Redundancy Analysis (RDA). The RDA is a form of constrained ordination, being related to canonical correspondence analysis (CCA) and is useful when the expected relationship between dependent and independent variables is linear (Legendre & Legendre, 2012). Considering mating is likely to occur more often in nearby locations and that adjacent locations have similar climate, we opt to statistically control for this effect by doing a partial redundancy analysis (pRDA). The partial version of RDA allows removing the effect of undesirable variables through multiple regression before applying the computation of ordination analysis (Borcard et al, 1992). Even though partial Mantel tests have been used to perform partial regression analyses for genetic distances (Malhotra & Thorpe 2000;

Guillot et al. 2009), the strength of this method has been questioned (Legendre, 2000; Raufaste & Rousset, 2001; Castellano & Balletto, 2002; Legendre & Fortin, 2010). Legendre & Fortin (2010) demonstrated that methods as regression, linear correlation and ordination analysis are more likely to detect a relationship (when one is present in the data) than the Mantel test and derived forms.

So, at first, we downloaded Bioclimatic layers from WorldClim (Hijmans et al. 2005) and extracted values for each variable at every locality from where tissue samples were available using ArcGIS (ESRI). To quantify correlation among site climate variables, we performed a Pearson's correlation analysis and excluded those highly correlated ($r > 0.8$), keeping the ones we considered relevant biologically (Rissler & Apodaca, 2007). At the end, eleven environmental variables were selected and used in the subsequent analysis. We then compared genetic data (corrected distances under TN93 model as dependent matrix) and individual-specific climate data in a partial RDA, specifying geography (latitude and longitude) as a third conditioned matrix using the vegan package in R (R Development Core Team, 2013).

In order to examine how much of the genetic variation in *N. fuscoauratus* is exclusively explained by climate, how much by geography, and how much is due to the combined effect of both geography and climate, we partitioned the variance components of our RDA by running three models. The first was a full model with all climate and geographic variables as explanatory variables and the last two represented partial models: one in which geography explains genetic data conditioned on climate variables and another one in which climate variables explain genetic data conditioned on geography.

In addition, to examine how the genetic variation in *N. fuscoauratus* was spatially distributed, we plotted pairwise geographic distance vs. genetic distance.

3. RESULTS

3.1 Molecular diversity and population genetic structure

The spatial model of GENELAND inferred three genetically distinct clusters of individuals of *Norops fuscoauratus* (Figures 1– 3), categorized as follows: P1, including samples from Guiana, Imeri and Napo (n=14) Amazonian areas of endemism (Silva et al.

2005); P2, including the majority of *N. fuscoauratus* samples used, both in Amazonia and in Atlantic Forest, in Colombia, Peru, Bolívia and Brazil (n=197); and P3, comprising samples from northeastern Amazonia in Belém area of endemism and Marajó island (n=33), plus one sample in Alagoas state, northeastern Brazil, with higher probability of being a member of this cluster (Figure 1.1). Most individuals had high posterior probability (above 0.9) of occurrence in the assigned cluster (see appendix 1 for details and individual posterior probabilities of membership), except for 12 samples from seven different localities in Brazil (Table 1). For our subsequent population genetic analyses, each of them was considered in the cluster where it received higher posterior probability.

GENELAND tessellation maps did not identify possible migrants based on population boundaries (Figure 2.1). Nerveless, the analysis estimated three well-delimited points of genetic discontinuities among clusters, even in relation to the geographically nearest clusters P2 and P3 (Figures 2.1 and 3.1).

Table 1. *Norops fuscoauratus* samples with < 0.9 of posterior probability of membership to one of the three clusters (P1, P2, P3) identified by GENELAND.

Ammount of samples	Biome	Locality	Posterior probability		
			P1	P2	P3
1	Amazonia	Brazil: PA: Alto Mendae, Tapajós river	0	0.87	0.13
5	Amazonia	Brazil: PA: Vitória do Xingu	0	0.80	0.20
2	Amazonia	Brazil: PA: Paragominas, Capim river	0	0.65	0.35
1	Atlantic Forest	Brazil: Ceará: Pacoti	0.14	0.60	0.26
1	Atlantic Forest	Brazil: Alagoas: Passo de Camaragibe	0.02	0.16	0.82
1	Atlantic Forest	Brazil: Bahia: Serra do Teimoso	0	0.76	0.24
1	Atlantic Forest	Brazil: Espírito Santo: Linhares	0.04	0.70	0.26
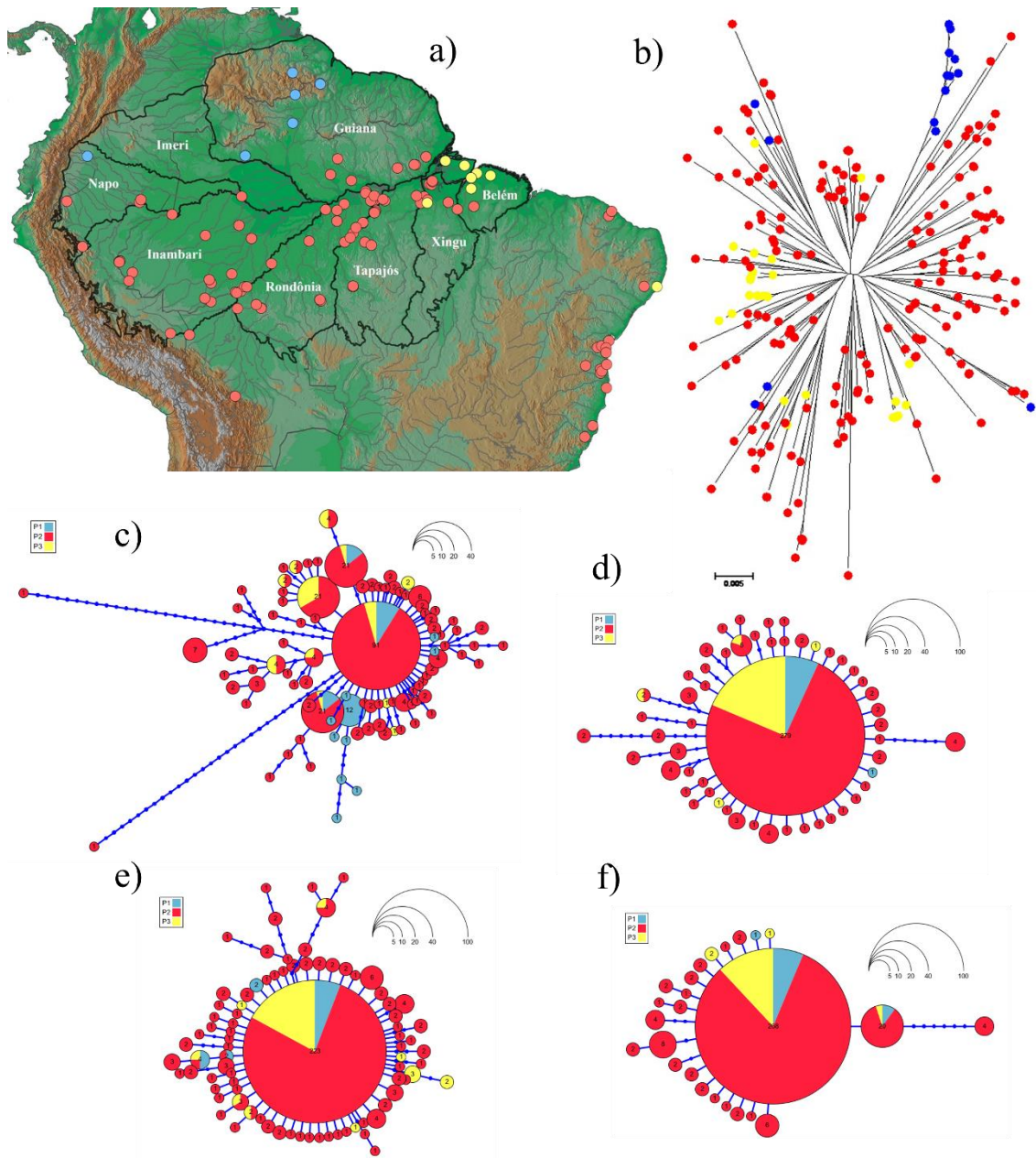
Figure 1.1: Records of studied samples of *Norops fuscoauratus* (a) and haplotype networks (b:ND2; c:Mkl1; d:Sincaip; e:RAG1; f:DNAH3), with points colored according to clusters determined by GENELAND v. 3.14 (Guillot & Estoup, et al. 2005).
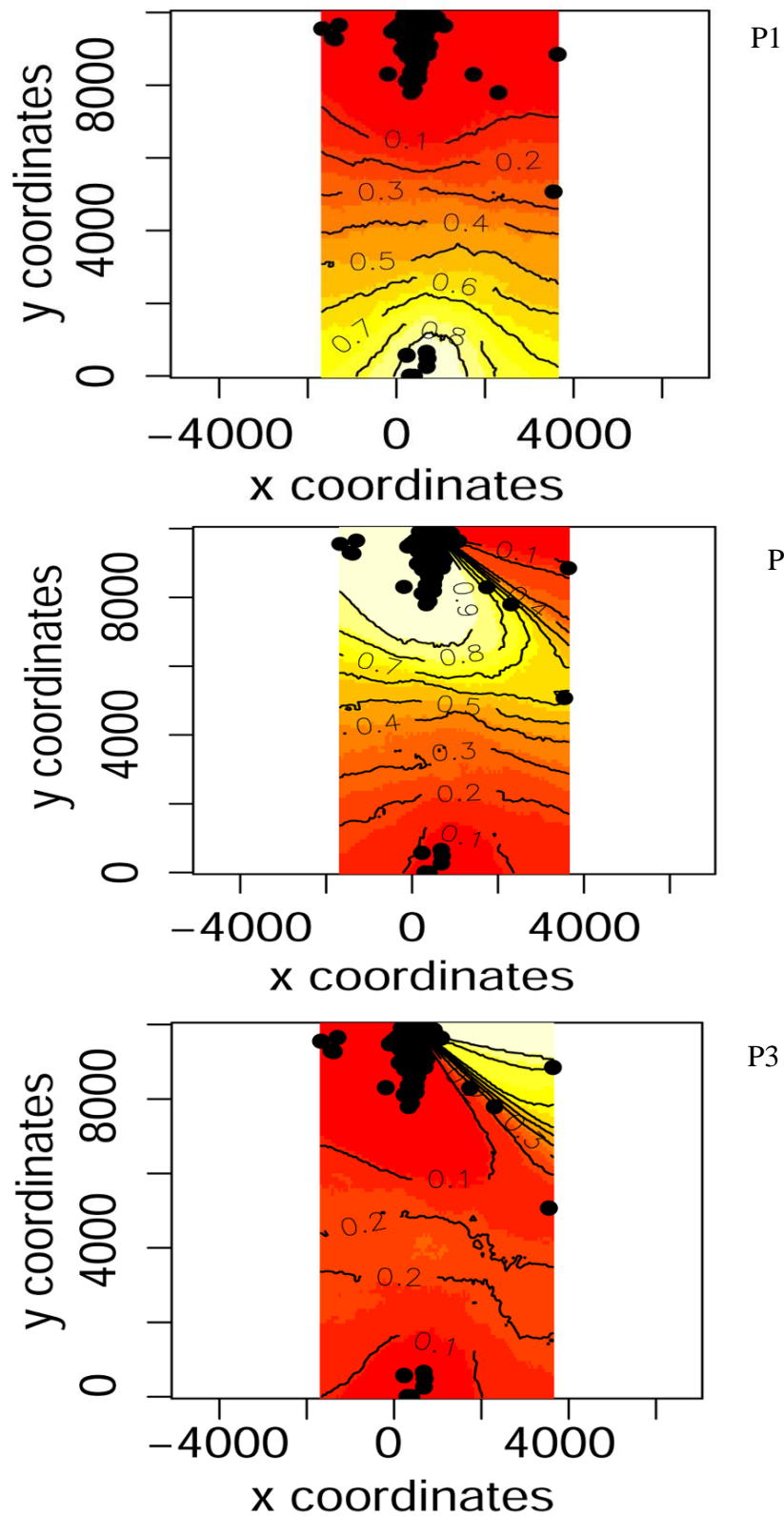
Figure 2.1: Maps showing posterior probabilities of cluster membership and location of genetic discontinuities for each of the three inferred clusters, P1, P2 and P3, as determined by GENELAND version 3.14 (Guillot & Estoup, et al. 2005). Lighter shading (from white, through yellow, to red) indicates higher probability of cluster membership and lines represent posterior probability values.
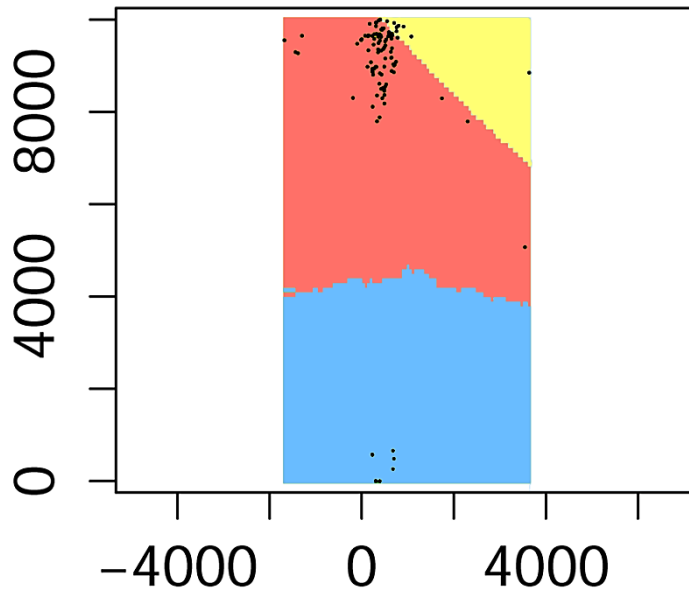
Figure 3.1: Map representing the estimated cluster membership and location of genetic discontinuities for each of the three inferred clusters, P1 (blue), P2 (red) and P3 (yellow), as determined by GENELAND version 3.14 (Guillot & Estoup, et al. 2005).

An overview of the genetic data is shown in Table 2. We sequenced a total of 1101 and 3228 bp of mtDNA and nDNA respectively. ND2 exhibited higher values of diversity (*h*, *Hd, Pi%, k and S*) than any of the nDNA. Among nDNA, MKL1 presented the highest values of *Pi%, k*, and *Hd,* while *h* and *S* were highest in RAG1. ND2 showed high haplotype diversity, with an elevated number of unique haplotypes (176 from 243 sequences analyzed) restricted to single localities. However, haplotypes were shared by nine localities, including distant ones like Pacoti-CE and Barra do Choça-BA in the Atlantic Forest, and Coari-AM and Aveiros-PA in the Amazonian forest, in Brazil (Figure 1.1).

Table 2. Molecular markers studied in *Norops fuscoauratus* and their respective molecular diversity indexes. DNA = type of molecular marker, if mitochondrial or nuclear; Bp = number of amplified base pairs; n = number of sequences used for each gene (for nDNA phased sequences were used); *h* = number of haplotypes; *Hd* = haplotype diversity; *Pi* = nucleotide diversity (%); *k* = average number of nucleotide differences between sequences; *S* = number of polymorphic (segregating) sites.

Molecular Marker	Primer Reference	DNA	Bp	*n*	*h*	*Hd*	*Pi%*	*k*	*S*
ND2	Jeskova et al. 2009	mtDNA	1101	243	176	0.9958	3.42%	14.68	186
MKL1	Townsend et al. 2011	nDNA	980	284	58	0.7131	0.13%	1.21	60
RAG1	Gartner et al. 2013	nDNA	1029	360	70	0.5438	0.09%	0.88	76
DNAH3	Townsend et al. 2008	nDNA	726	342	24	0.3771	0.07%	0.52	24
SINCAIP	Townsend et al. 2011	nDNA	493	360	39	0.3236	0.09%	0.41	36

Table 3. Analysis of Molecular Variance (AMOVA) performed with the clusters identified by GENELAND, showing genetic variation among and within clusters.

ND2 (*Fst* = 0.13933)		
	Among clusters	**Within clusters**
df	2	240
Var. comp.	1.12805 Va	6.96826 Vb
% variation	13.93 %	86.07 %

According to the AMOVA results, genetic variation is largest within clusters than among them (Table 3). Pairwise *Fst* comparisons presented low and non-significant values between P1, P2 and P3 clusters, indicating lack of population structure. Corrected and uncorrected genetic distances between P1, P2 and P3 clusters, all low, attest the same, with P2 and P3 being genetically more similar (Table 4).

Table 4. Net between group distances for ND2 among the clusters identified by GENELAND (P1, P2 and P3). Distances above the diagonal were maximum likelihood-corrected using the TN93 model and distances below the diagonal are uncorrected p-distances.

	P1	P2	P3
P1	—	0.012	0.016
P2	0.012	—	0.004
P3	0.015	0.004	—

For the entire ND2 dataset, values of Fs (Fu, 1997) and of D (Tajima, 1989) were significantly negative (Fs = −23.7929, p = 0.00; D = −1.6223, p = 0.01), indicating the non-neutral nature of the marker and favoring the hypothesis of demographic expansion of *N. fuscoauratus.* In relation to GENELAND clusters, *Fs* and *D* values were negative for all populations, but only significant for P2, supporting the hypothesis of demographic expansion in this cluster.

Table 5. Mitochondrial (ND2) molecular diversity indexes of *Norops fuscoauratus* clusters determined by GENELAND analysis. n = number of sequences used in the analysis, *h* = number of haplotypes; *Hd* = haplotype diversity; *Pi* = nucleotide diversity (%); *k* = average number of nucleotide differences between sequences; *S* = number of polymorphic (segregating) sites.

Clusters	n	*S*	*h*	*Hd* ± SD	*Pi*	*k*	*Fst*
P1	14	85	12	0.96 ± 0.04	0.02785	21.45	0.15
P2	197	177	150	0.99 ± 0.00	0.03432	14.79	0.14
P3	33	89	20	0.93 ± 0.02	0.02527	18.95	0.14

ND2 mismatch distribution plots (Figure 4.1) were unimodal for P2 and the whole sample, in agreement with the model of population expansion. P1 showed a bimodal distribution, indicating a departure from the model of population expansion, while P3 presented a more irregular and almost bimodal distribution. However, raggedness index was significant only for P3 (Table 6), which means that population expansion cannot be denied even for P1, that had a high index, probably due to the small sample size of this cluster. P3 raggedness index was higher than in P2, but still moderately low.
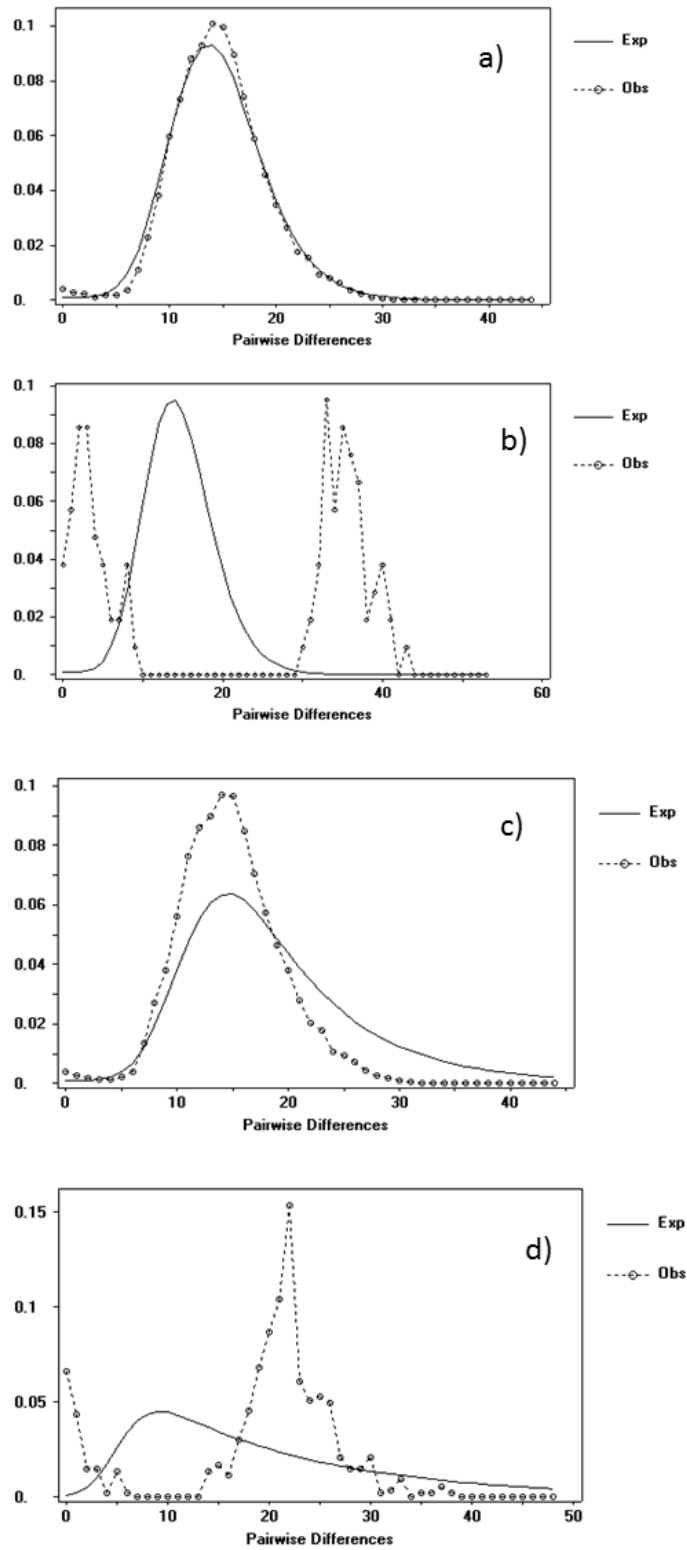
Figure 4.1: Mismatch distributions of expected (continuous line) and observed values of pairwise differences of haplotypes for the mtDNA (ND2) data set in *N. fuscoauratus*. a) Complete mtDNA dataset; b) Cluster P1, c) Cluster P2 and d) Cluster P3 from GENELAND analysis.

Table 6. Values of Fu's Fs, Tajima's D statistics, Harpending's Raggedness index and p-values estimated for clusters identified by GENELAND analysis in *Norops fuscoauratus*. P-values in bold are considered significant.

Clusters	n	Raggedness	Raggedness p-value	Fu's F_s		Tajima's D	
				F_s	p-value	D	p-value
P1	14	0.067	0.35	-0.53	0.4	-0.58	0.29
P2	197	0.002	0.99	-23.87	**0**	-1.61	**0.02**
P3	33	0.033	**0.00**	-0.73	0.4	-0.10	0.52

The EBSP's (Figure 5.1) were somewhat congruent with the neutrality tests, mismatch distribution and raggedness index, inferring a relatively stable P1, with a clear population expansion in P2 and P3 (starting around 1.5 Ma in P3) until approximately 0.6 Ma. All clusters showed a population decline spanning from about 0.5 to 0.2 Ma followed by a bottleneck and subsequent population expansion starting at about 0.1 (P1 and P2) to 0.05 Ma (P3) to the present.
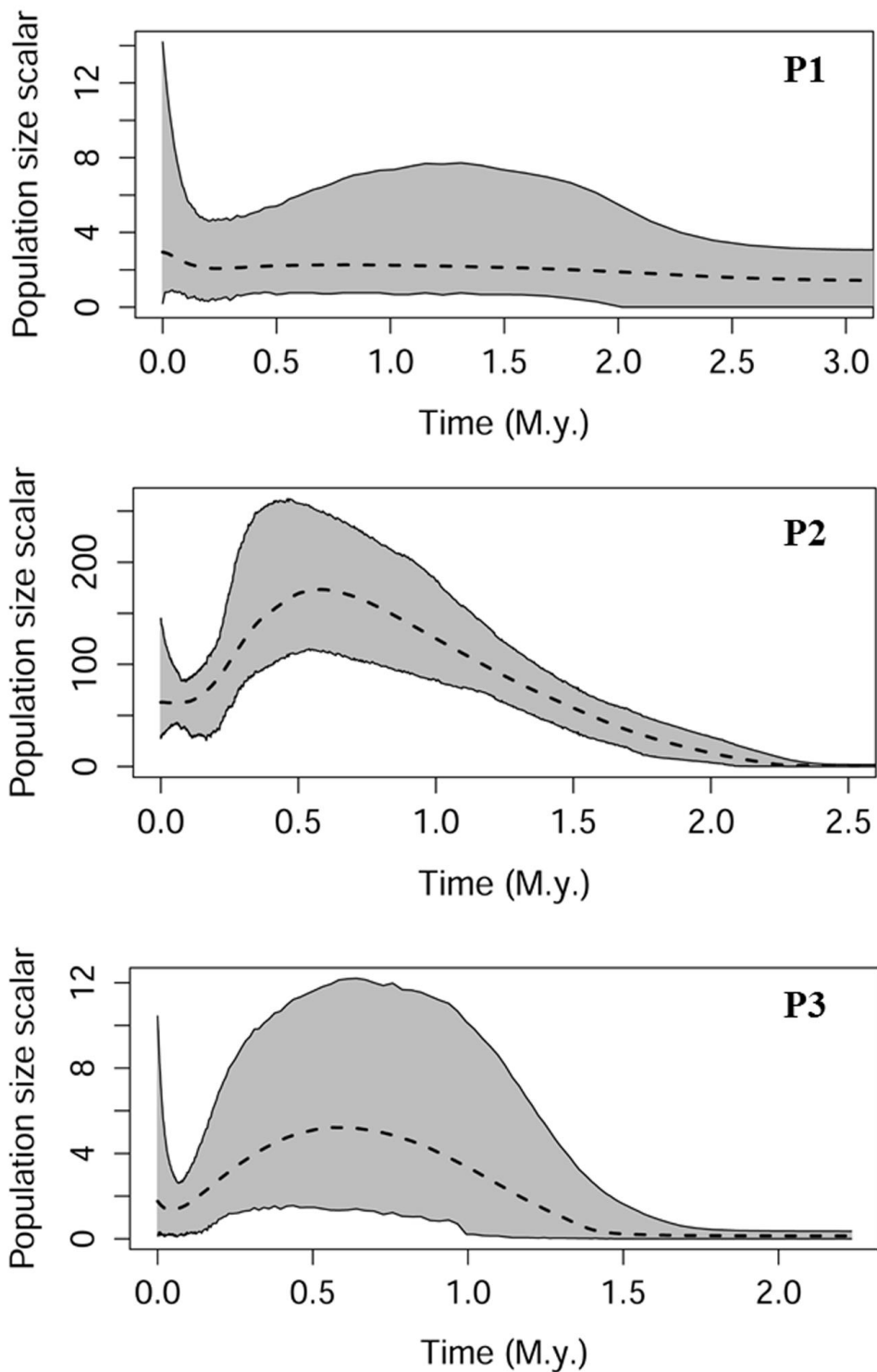
Figure 5.1: Extended Bayesian Skyline Plots representing demographic histories of *Norops fuscoauratus* clades (P1, P2 and P3) recovered by GENELAND analysis. Dashed lines represent median values while grey area corresponds to 95% confidence intervals.

3.2 Phylogenetic analysis and divergence dating

The individual topology of each nuclear marker (dnah3, sincaip, rag1 and mkl1, results not shown) does not support any particular relationship among individuals of *N. fuscoauratus*. Both mtDNA and concatenated nDNA phylogenies recovered a monophyletic *N. fuscoauratus*, with well-supported small demes at the tip of the tree, while basal nodes had low bootstrap/posterior probability values (results not shown) with a similar topology of our dated Bayesian inference (see below). The individuals composing the clusters identified by GENELAND were partially grouped in the phylogenetic trees, but not forming any particular well-supported clade, not allowing any inference about their relationships.

The dated Bayesian inference of concatenated dataset also recovered a monophyletic *N. fuscoauratus* with high statistical support (Figures 6.1 and 7.1). In this analysis, the same pattern of well-supported demes at the tip of tree contrasting with non-supported basal nodes was observed, except for three clades that were recovered with high statistical support. The first (1) clade is composed by three specimens from Rio Abacaxis, in Amazonas state, in the left bank of Tapajós river; eight specimens from the left and right bank of Tapajós River in Pará; two specimens from Vitória do Xingu at the right bank of Xingu river; seven specimens from Apiacás and Aripuanã in Mato Grosso and one specimen from Cochabamba, Bolivia. The second (2) and largest well supported clade is composed by specimens from Ecuador, Colombia, Peru, and in Brazil, by specimens from the states of Amazonas and Pará, in Amazonia, and specimens from brejos de altitude in Ceará state. The last and smaller clade (3) is composed by three specimens from localities in Pará, Brazil, situated between the Tapajós and Xingu Rivers

The molecular dating suggests that diversification of *N. fuscoauratus* occurred during the Pleistocene, between 1.99 and 2.56 Ma (mean 2.22 Ma). The split between *N. trachyderma* and *N. fuscoauratus* is suggested to have occurred between 27.5 – 20.97 Ma (mean 20.97). The low support at the basal nodes of the tree does not allow any inference about the time of diversification of other clades, but in relation to the three well supported clades, it seems that the first clade described above diverged during Early Pleistocene (2.08–1.7 Ma, mean 1.73 Ma), while the second clade diversified through Early-Middle Pleistocene (1.83-1.39 Ma, mean 1.52 Ma) and the third and smaller clade diversified in Middle to Late Pleistocene (1.35 – 0.82 Ma, mean 1.04 Ma).
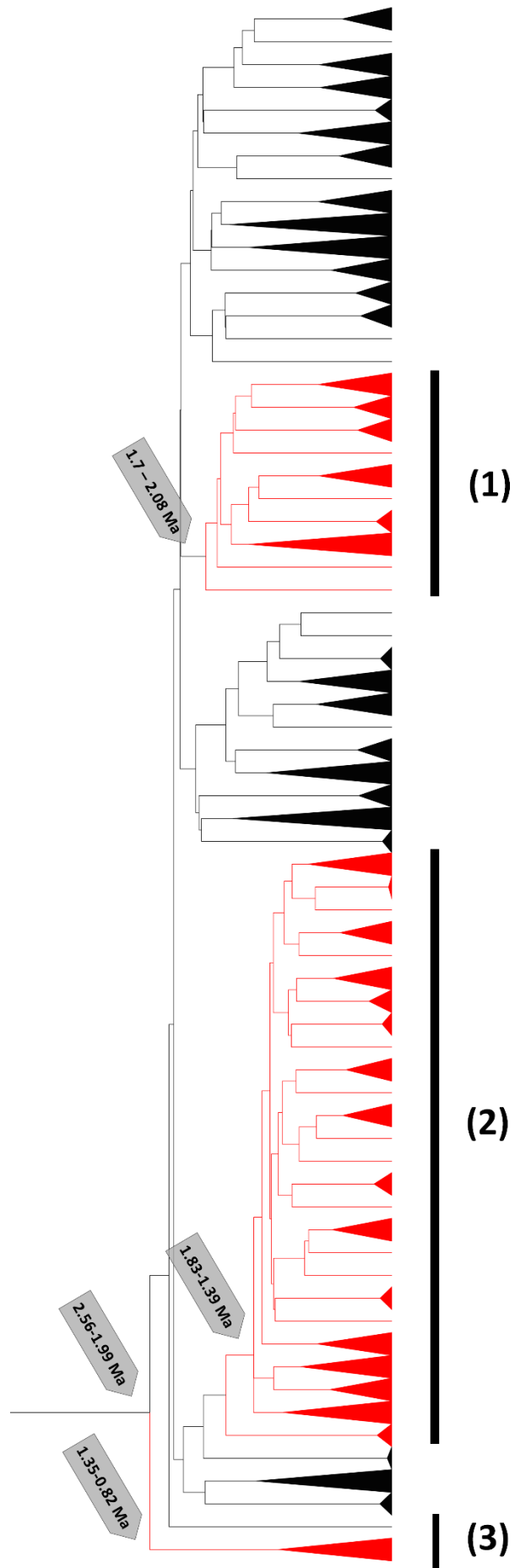
Figure 6.1: Results of the concatenated Bayesian analysis partitioned by gene. Clades in red represent the three well-supported clades (1), (2) and (3) mentioned in the text with posterior probability=1. Nodes in black and collapsed represent clades with posterior probabily=1 formed by nearby samples. Grey arrows indicate height 95% HPD in million years of well-supported clades. For better visualization purpuses, *N. trachyderma* was removed from the figure.

3.3 Influence of climate and geographic distance in genetic variation

Partial RDA analysis conditioned on geography (latitude/longitude), found a non-significant association between climate and genetic distance in *N. fuscoauratus*. Partitioning of total variance analysis (comparing the full model with a partial model conditioned on climate and a partial model conditioned on geography) indicated that climate accounts for 14% of the total explained genetic variance observed, when removing the effect of geography. On the other hand, geography is responsible for 3% of the genetic variation found after removing the variation explained by climate. The interaction between both climate and geography accounts for 5% of the genetic variation observed and 78% represents the residuals, which are the amount of variation that cannot be explained either by climate, geography or by their interaction due to multicollinearity.

The plot of the relationship between geographic and genetic distance agrees with the pRDA analysis (Figure 7.1) and demonstrates that genetic variation is not dependent on geographic distance. Geographically close samples are more distinct genetically than geographically distant samples.
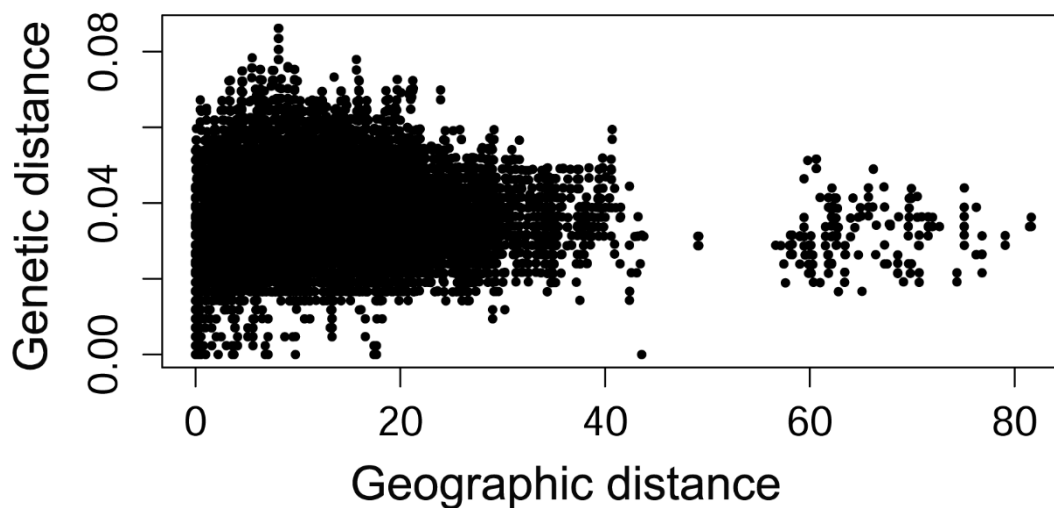
Figure 7.1: Plot of the relationship between geographic and corrected genetic distance generated under model TN93 (Tamura & Nei, 1993).

4. DISCUSSION

Apart of its widespread range, *N. fuscoauratus* shows an overall low genetic diversity and low geographical differentiation. Our data supports the suggestion by Glor et al. (2001) that it is a recent invader that has undergone rapid population expansion. Haplotype networks, AMOVA, and Fst comparisons between populational clusters identified confirm the panmixia in *N. fuscoauratus*, suggesting the occurrence of gene flow. In addition, the elevated number of mtDNA unique haplotypes, with a low frequency of association of one common haplotype with others, represents a typical pattern of populations that have undergone recent range expansion (Slatkin & Hudson, 1991; Rogers & Harpending, 1992; Peter & Slatkin, 2013).

Similar to *N. fuscoauratus*, the study of the endemic Atlantic forest bird *Basileuterus leucoblepharus* did not recover any phylogenetic structure in the species, but found a significant signal of demographic expansion (Batalha-Filho et al., 2012). In the Common Sandpiper *Actitis hypoleucos* neither individual nuclear gene trees nor analyses based on the five genes combined recovered geographic structure, and the lack of differentiation was attributed to the recent population expansion as suggested by the EBSP (Hung et al. 2013). Similarly, the wide-ranging microhylid frog *Gastrophryne*

carolinensis was studied using both mtDNA and AFLP nuclear markers, and showed very little phylogeographic structure (Makowski et al. 2009). However, in *G. carolinensis* there is evidence for isolation by distance with geographically restricted gene flow, while, in *N. fuscoauratus*, geographic distance does not seem an important factor in determining genetic differentiation.

Nevertheless, GENELAND analysis recovered three well-delimited clusters considering mtDNA haplotype divergence and spatial information. This might be related to the non-recombinant nature of mtDNA, as well as its matrilineal descent, that may lead to the recognition of distinct lineages even without detectable barriers to gene flow (Irwin, 2002). Therefore, one possibility is that these phylogeographic breaks found in *N. fuscoauratus* would not be the result of specific climatic or geographic barriers, but rather a result of stochastic processes. Another possibility is that population clusters might represent an initial stage of differentiation among *N. fuscoauratus* populations. In this sense, the genetic differentiation and stability of the northwestern Amazonian cluster (P1) would contrast with P2 and P3, which appear to be more genetically similar and have undergone a recent population expansion. These results, and the close relationship of *N. fuscoauratus* with *N. kemptoni* and *N. altae*, which are inhabitants of Panama and Costa Rica respectively, suggests the northwestern region of Amazonian forest might be the ancestral area of the species, as proposed by Glor et al. (2001) and Vanzolini & Williams (1970).

Despite the widespread distribution and pronounced dewlap color variation found in *N. fuscoauratus*, the lack of genetic population structure seems to indicate the absence of cryptic diversity whithin the species. Color polymorphisms are commonly evidenced in dendrobatid frogs, as a result of the interaction between sexual and natural selection, but not always supported by genetic differentiation (Hoogmoed & Avila-Pires, 2012; Rojas & Endler, 2013). In anoles, variation in dewlap colors are thought to evolve because of selection in signal detectability under different habitat conditions, not always reflecting a genetic divergence behind it (Leal & Fleishman, 2004; Stapley et al. 2011, Macedonia, 2014). However, processes that underlie divergent dewlap colors are still a matter of debate and need further investigation, especially in mainland taxa, where such information is scarce.

The lack of phylogeographical structure observed in *N. fuscoauratus* contrasts with the pattern observed for other mainland rainforest widespread species. Previously

recognized subspecies of *Norops chrysolepis* complex were elevated to species on the basis of concordant morphological and mitochondrial molecular (ND2) data (D'Angiolella et al. 2011). Distributed across central and eastern Amazonia, *Chatogekko amazonicus* illustrates how high molecular diversity can be underestimated in a morphologically similar species (Geurgas & Rodrigues, 2010). In addition, the molecular and morphological diversity present in the widespread skink *Copeoglussum nigropunctatum* rendered its recognition as a species complex, with at least three highly divergent and largely allopatric lineages (Mirales & Carranza, 2010; Hedges & Conn, 2012). However, in all previous cited examples, the species seem to be much older than *N. fuscoauratus*, with the diversification starting during Miocene for *Chatogekko amazonicus* (40.1 to 9.4 Ma; Geurgas & Rodrigues, 2008), *Norops chrysolepis* species group (20.8 to 11.4 Ma; D'Angiolella et al. *in prep*.) and *Copeoglussum nigropunctatum* (10.3 to 8.8 Ma; Mirales & Carranza, 2010).

In *N. fuscoauratus*, phylogenetic and populational analyses recovered with high posterior probability, individuals from ''*Brejos de Altitude*'' and from the Atlantic Forest nested within an Amazonian clade. This same pattern was evidenced by previous studies, which reported that individuals from the Atlantic forest might be closely related to individuals inhabiting the entire Amazonian forest or only the northeastern part of it (Costa, 2003; Lynch-Alfaro et al. 2012; Batalha-Filho et al. 2013; Prates et al. 2014).

Therefore, even though our results do not allow a firm reconstruction of the history of *N. fuscoauratus*, a possible scenario would be that the species originated in northwestern Amazonia during early Pleistocene and further dispersed to south Amazonia. By the estimated time of diversification, the Amazon River as we know was fully established, draining from the Andes to the Atlantic Ocean (Figueiredo et al. 2009; Latrubesse et al. 2010, Ribas et al. 2012) but land rearrangements in the course of the Amazon River, as well as in its tributaries, may have favored the southwards dispersion of the species. Considering the estimated divergence dates of the three well-supported clades in Bayesian analysis, the subsequent expansion occurred eastwards, with all three clades diverging almost simultaneously. According to previous studies (De Oliveira et al. 1999; Behling et al. 2000; Costa, 2003; Batalha-Filho et al. 2013), colonization of Atlantic forest may have occurred during forest expansion in humid and wet climate periods of late Pleistocene through the northern costal zones of Maranhão and Piauí, reaching "*Brejos de Altitude*" in Ceará state, in Brazil. The low-supported phylogenetic position

of other Atlantic Forest samples do not allow any interpretation of their phylogenetic relationship with other *N. fuscoauratus* samples, as well as their divergence time.

The present work presents the population structure of a polymorphic widespread species that have undergone recent population expansion throughout the Pleistocene. We undestand that molecular studies of recently diverged taxa can be challenging, such that few molecular markers may not capture the real demographic signal of divergence inside a species (McCormack et al. 2012). Comparable molecular data from closely related *Norops* species, in addition to demographic and ecological analyses, will certainly improve our knowledge about patterns of genetic diversity and the processes driving phylogeographic diversity in recent diverged taxa in the Neotropics.

REFERENCES

Akaike, H., 1974. A new look at the statistical model identification. *IEEE Transactions on Automatic Control. 19*, 716–723.

Avila-Pires, T. C., Mulcahy, D. G., Werneck, F. P., & Sites Jr, J. W. (2012). Phylogeography of the teiid lizard *Kentropyx calcarata* and the Sphaerodactylid *Gonatodes humeralis* (Reptilia: Squamata): testing a geological scenario for the lower Amazon-Tocantins basins, Amazonia, Brazil. *Herpetologica*, *68*(2), 272-287.

Barrett, J. C., Fry, B., Maller, J. D. M. J., & Daly, M. J. (2005). Haploview: analysis and visualization of LD and haplotype maps. *Bioinformatics, 21*(2), 263-265.

Borcard D, Legendre P, Drapeau P (1992) Partialling out the spatial component of ecological variation. *Ecology 73*: 1045–1055.

Camargo, A., De Sa, R. O., & Heyer, W. R. (2006). Phylogenetic analyses of mtDNA sequences reveal three cryptic lineages in the widespread neotropical frog *Leptodactylus fuscus* (Schneider, 1799) (Anura, Leptodactylidae). *Biological Journal of the Linnean Society*, *87*(2), 325-341.

Carnaval, A. C., Hickerson, M. J., Haddad, C. F., Rodrigues, M. T., & Moritz, C. (2009). Stability predicts genetic diversity in the Brazilian Atlantic forest hotspot. *Science*, *323*(5915), 785-789.

Castellano, S., & Balletto, E. (2002). Is the partial Mantel test inadequate? *Evolution*, *56*(9), 1871-1873.

Cheng, H., Sinha, A., Cruz, F.W., Wang, X., d'Horta, F.M., Ribas, C.C., Vuille, M. Stott, L.D. & Auler, A.S. (2013). Climate change patterns in Amazonia and biodiversity. *Nature communications* 4:1411.

Colinvaux, P. A., & De Oliveira, P. E. (2001). Amazon plant diversity and climate through the Cenozoic. *Palaeogeography, Palaeoclimatology, Palaeoecology*, *166*(1), 51-63.

Costa, L. P. (2003). The historical bridge between the Amazon and the Atlantic Forest of Brazil: a study of molecular phylogeography with small mammals. *Journal of Biogeography*, *30*(1), 71-86.

De Oliveira, P.E., Franca Barreto, A.M. & Suguio, K. (1999). Late Pleistocene/Holocene climatic and vegetational history of the Brazilian caatinga: the fossil dunes of the middle Sao Francisco River. *Palaeogeography Palaeoclimatology Palaeoecology*, 152,319–337.

Domingos, F. M., Bosque, R. J., Cassimiro, J., Colli, G. R., Rodrigues, M. T., Santos, M. G., & Beheregaray, L. B. (2014). Out of the deep: Cryptic speciation in a Neotropical gecko (Squamata, Phyllodactylidae) revealed by species delimitation methods. *Molecular phylogenetics and evolution*, *80*, 113-124.

Drummond, A. J., Suchard, M. A., Xie, D., & Rambaut, A. (2012). Bayesian phylogenetics with BEAUti and the BEAST 1.7. *Molecular biology and evolution*, *29*(8), 1969-1973.

Drummond, A. J., Ho, S. Y., Phillips, M. J., & Rambaut, A. (2006). Relaxed phylogenetics and dating with confidence. *PLoS biology*, *4*(5), e88.

Excoffier, L., & Schneider, S. (1999). Why hunter-gatherer populations do not show signs of Pleistocene demographic expansions. *Proceedings of the National Academy of Sciences*, *96*(19), 10597-10602.

Excoffier, L., Laval, G., & Schneider, S. (2005). Arlequin (version 3.0): an integrated software package for population genetics data analysis. *Evolutionary bioinformatics online*, *1*, 47.

Figueredo, J., Hoorn, C., van der Ven, P. & Soares, E. (2009). Late Miocene onset of the Amazon River and the Amazon deep-sea fan: Evidence from the Foz do Amazonas Basin. *Geology 37(7):* 619–622.

Fouquet, A., Vences, M., Salducci, M. D., Meyer, A., Marty, C., Blanc, M., & Gilles, A. (2007). Revealing cryptic diversity using molecular phylogenetics and phylogeography in frogs of the *Scinax ruber* and *Rhinella margaritifera* species groups. *Molecular phylogenetics and evolution*, *43*(2), 567-582.

Gamble, T., Colli, G. R., Rodrigues, M. T., Werneck, F. P., & Simons, A. M. (2012). Phylogeny and cryptic diversity in geckos (*Phyllopezus*; Phyllodactylidae; Gekkota) from South America's open biomes. *Molecular Phylogenetics and Evolution*, *62*(3), 943-953.

Gartner, G. E., Gamble, T., Jaffe, A. L., Harrison, A., & Losos, J. B. (2013). Left–right dewlap asymmetry and phylogeography of *Anolis lineatus* on Aruba and Curaçao. *Biological Journal of the Linnean Society*, *110*(2), 409-426.

Gehara, M., Crawford, A. J., Orrico, V. G., Rodríguez, A., Lötters, S., Fouquet, A., ... & Köhler, J. (2014). High levels of diversity uncovered in a widespread nominal taxon: continental phylogeography of the Neotropical tree frog *Dendropsophus minutus*. *PloS one*, *9*(9), e103958.

Geurgas, S. R., & Rodrigues, M. T. (2010). The hidden diversity of *Coleodactylus amazonicus* (Sphaerodactylinae, Gekkota) revealed by molecular data. *Molecular Phylogenetics and Evolution*, *54*(2), 583-593.

Glor, R. E., Vitt, L. J., & Larson, A. (2001). A molecular phylogenetic analysis of diversification in Amazonian *Anolis* lizards. *Molecular Ecology*, *10*(11), 2661-2668.

Guillot, G., Leblois, R., Coulon, A., & Frantz, A. C. (2009). Statistical methods in spatial genetics. *Molecular Ecology*, *18*(23), 4734-4756.

Guillot, G., Santos, F., & Estoup, A. (2008). Analysing georeferenced population genetics data with Geneland: a new algorithm to deal with null alleles and a friendly graphical user interface. *Bioinformatics*, *24*(11), 1406-1407.

Guillot, G., Mortier, F., & Estoup, A. (2005). GENELAND: a computer package for landscape genetics. *Molecular ecology notes*, *5*(3), 712-715.

Harpending, H. C. (1994). Signature of ancient population growth in a low-resolution mitochondrial DNA mismatch distribution. *Human biology*, 591-600.

Heled, J., & Drummond, A. J. (2008). Bayesian inference of population size history from multiple loci. *BMC Evolutionary Biology*, *8*(1), 289

Hewitt, G. (2000). The genetic legacy of the Quaternary ice ages. *Nature*, *405*(6789), 907-913.

Hijmans, R. J., Cameron, S. E., Parra, J. L., Jones, P. G., & Jarvis, A. (2005). Very high resolution interpolated climate surfaces for global land areas. *International journal of climatology*, *25*(15), 1965-1978.

Hoogmoed, M. S., & Avila, T. C. A. P. C. (2012). Inventory of color polymorphism in populations of *Dendrobates galactonotus* (Anura: Dendrobatidae), a poison frog endemic to Brazil. *Phyllomedusa: Journal of Herpetology,* 11(2), 95-115.

Hoorn, Carina, et al. (2010). Amazonia through time: Andean uplift, climate change, landscape evolution, and biodiversity. *Science* 330.6006: 927-931.

Huson, D.H. & Bryant, D. (2006) Application of Phylogenetic Networks in Evolutionary Studies, *Molecular Biology and Evolution. 23*(2):254-267.

Irwin, D. E. (2002). Phylogeographic breaks without geographic barriers to gene flow. *Evolution*, *56*(12), 2383-2394.

Lanfear, R., Calcott, B., Ho, S. Y., & Guindon, S. (2012). PartitionFinder: combined selection of partitioning schemes and substitution models for phylogenetic analyses. *Molecular biology and evolution*, *29*(6), 1695-1701.

Latrubesse, E.M., Cozzuol, M., Silva-Caminha, S.A.F., Rigsby, C.A., Absy, M.L. & Jaramillo, C. (2010). The Late Miocene paleogeography of the Amazon Basin and the evolution of the Amazon River system. *Earth-Science Reviews* 99: 99–124.

Leal, M., & Fleishman, L. J. (2004). Differences in visual signal design and detectability between allopatric populations of *Anolis* lizards. *The American Naturalist, 163*(1), 26-39.

Ledru, M. P. (1993). Late Quaternary environmental and climatic changes in central Brazil. *Quaternary research*, *39*(1), 90-98.

Legendre, P. (2000). Comparison of permutation methods for the partial correlation and partial Mantel tests. *Journal of Statistical Computation and Simulation*, *67*(1), 37-73.

Legendre, P., & Fortin, M. J. (2010). Comparison of the Mantel test and alternative approaches for detecting complex multivariate relationships in the spatial analysis of genetic data. *Molecular Ecology Resources*, *10*(5), 831-844.

Legendre, P., & Legendre, L. F. (2012). *Numerical ecology* (Vol. 24). Elsevier.

Lynch-Alfaro, J.W.; Boubli, J.P.; Olson, L.E.; Di Fiore, A.; Wilson, B.; Gutierrez-Espeleta, G.A.; Chiou, K.L.; Schulte, M.; Neitzel, S.; Ross, V.; Schwochow D.; Nguyen, M.T.T; Farias, I.; Janson, C.H. & Alfaro, M.E. (2012). Explosive Pleistocene range expansion leads to widespread Amazonian sympatry between robust and gracile capuchin monkeys. *Journal of Biogeography.* 39, 272–288.

Macedonia, J. M., Clark, D. L., & Tamasi, A. L. (2014). Does Selection Favor Dewlap Colors that Maximize Detectability? A Test with Five Species of Jamaican *Anolis* Lizards. *Herpetologica, 70*(2), 157-170.

Makowsky, R., Chesser, J. & Rissler, L.J. (2009). A striking lack of genetic diversity across the wide-ranging amphibian *Gastrophryne carolinensis* (Anura: Microhylidae). *Genetica* 135, 169–183.

Malhotra, A., & Thorpe, R. S. (2000). The dynamics of natural selection and vicariance in the Dominican anole: patterns of within-island molecular and morphological divergence. *Evolution*, *54*(1), 245-258.

Mayle, F. E., & Beerling, D. J. (2004). Late Quaternary changes in Amazonian ecosystems and their implications for global carbon cycling. *Palaeogeography, Palaeoclimatology, Palaeoecology*, *214*(1), 11-25.

Mayle, F. E. (2004). Assessment of the Neotropical dry forest refugia hypothesis in the light of palaeoecological data and vegetation model simulations. *Journal of Quaternary Science*, *19*(7), 713-720.

McCormack, J. E., Hird, S. M., Zellmer, A. J., Carstens, B. C., & Brumfield, R. T. (2013). Applications of next-generation sequencing to phylogeography and phylogenetics. *Molecular Phylogenetics and Evolution*, *66*(2), 526-538.

Miller, M. A., Pfeiffer, W., & Schwartz, T. (2010). Creating the CIPRES Science Gateway for inference of large phylogenetic trees. In *Gateway Computing Environments Workshop (GCE), 2010* (pp. 1-8). IEEE.

Miralles A, & Carranza S. (2010) Systematics and biogeography of the Neotropical genus *Mabuya*, with special emphasis on the Amazonian skink *Mabuya nigropunctata* (Reptilia, Scincidae) *Molecular Phylogenetics and Evolution 54*:857-869.

Moritz, C., Patton, J. L., Schneider, C. J., & Smith, T. B. (2000). Diversification of rainforest faunas: an integrated molecular approach. *Annual Review of Ecology and Systematics*, 533-563.

Nicholson, K. E., Harmon, L. J., & Losos, J. B. (2007). Evolution of *Anolis* lizard dewlap diversity. *PLoS One*, *2*(3), e274.

Nicholson, K. E., Crother, B. I., Guyer, C., & Savage, J. M. (2012). It is time for a new classification of anoles (Squamata: Dactyloidae). *Zootaxa*, *3477*, 1-108.

Pennington, T.R., Prado, D. E., & Pendry, C. A. (2000). Neotropical seasonally dry forests and Quaternary vegetation changes. *Journal of Biogeography*, *27*(2), 261-273.

Peter, B. M., & Slatkin, M. (2013). Detecting range expansions from genetic data. *Evolution*, *67*(11), 3274-3289.

Prado, C., Haddad, C. F., & Zamudio, K. R. (2012). Cryptic lineages and Pleistocene population expansion in a Brazilian Cerrado frog. *Molecular Ecology*, *21*(4), 921-941.

Prates, I., Rodrigues, M. T., Melo-Sampaio, P. R., & Carnaval, A. C. (2014). Phylogenetic relationships of Amazonian anole lizards (Dactyloa): Taxonomic implications, new

insights about phenotypic evolution and the timing of diversification. *Molecular phylogenetics and evolution*, *82*, 258-268.

Raufaste, N., & Rousset, F. (2001). Are partial mantel tests adequate? *Evolution*, *55*(8), 1703-1705.

Ribas, C. C., Aleixo, A., Nogueira, A. C., Miyaki, C. Y., & Cracraft, J. (2011). A palaeobiogeographic model for biotic diversification within Amazonia over the past three million years. *Proceedings of the Royal Society B: Biological Sciences*, rspb20111120.

Rissler, L. J., & Apodaca, J. J. (2007). Adding more ecology into species delimitation: ecological niche models and phylogeography help define cryptic species in the black salamander (*Aneides flavipunctatus*). *Systematic Biology*, *56*(6), 924-942.

Rodríguez-Robles, J. A., Jezkova, T., & García, M. A. (2007). Evolutionary relationships and historical biogeography of *Anolis desechensis* and *Anolis monensis,* two lizards endemic to small islands in the eastern Caribbean Sea. *Journal of Biogeography*, *34*(9), 1546-1558.

Rogers, A. R., & Harpending, H. (1992). Population growth makes waves in the distribution of pairwise genetic differences. *Molecular biology and evolution*, *9*(3), 552-569.

Ronquist, Fredrik, et al. (2012). MrBayes 3.2: efficient Bayesian phylogenetic inference and model choice across a large model space. *Systematic biology* 61.3: 539-542.

Rull, V. (2007). On the origin of present Neotropical biodiversity: a preliminary meta-analysis about speciation timing using molecular phylogenies. In *Orsis: organismes i sistemes* (Vol. 22, pp. 105-119).

Rull, V. (2008). Speciation timing and neotropical biodiversity: the Tertiary–Quaternary debate in the light of molecular phylogenetic evidence. *Molecular Ecology*, *17*(11), 2722-2729.

Sambrook, J., & Russell, D. W. (2001). Molecular cloning: a laboratory manual, 3rd eds. *New York: Cold Spring Harbor Laboratory Press*, *6*, 4-6.

Scheet, P., & Stephens, M. (2006). A fast and flexible statistical model for large-scale population genotype data: applications to inferring missing genotypes and haplotypic phase. *The American Journal of Human Genetics*, *78*(4), 629-644.

Schneider, S., & Excoffier, L. (1999). Estimation of past demographic parameters from the distribution of pairwise differences when the mutation rates vary among sites: application to human mitochondrial DNA. *Genetics*, *152*(3), 1079-1089.

Slatkin, M., & Hudson, R. R. (1991). Pairwise comparisons of mitochondrial DNA sequences in stable and exponentially growing populations. *Genetics*, *129*(2), 555-562.

Slatkin, M., & L. Excoffier. 2012. Serial founder effects during range expansion: a spatial analog of genetic drift. *Genetics* 191:171–181.

Smith, B. T., McCormack, J. E., Cuervo, A. M., Hickerson, M. J., Aleixo, A., Cadena, C. D., Pérez-Emán, J., Burney, C.W., Xie, X., Harvey, M.G., Faircloth, B.C., Glen, T.C., Derryberry, E.P., Prejan, J., Fields, S. & Brumfield, R. T. (2014). The drivers of tropical speciation. *Nature*, *515*(7527), 406-409.

Stamatakis, A. (2006). RAxML-VI-HPC: maximum likelihood-based phylogenetic analyses with thousands of taxa and mixed models. *Bioinformatics*, *22*(21), 2688-2690.

Stapley, J., Wordley, C., & Slate, J. (2011). No evidence of genetic differentiation between anoles with different dewlap color patterns. *Journal of Heredity*, *102*(1), 118-124.

Stenseth, N.C. A. Shabbar, K.S. Chan, S. Boutin, E.K. Rueness, D. Ehrich, J.W. Hurrell, O.C. Lingjæde, & Jacobsen, K.S. (2004). Snow conditions may create an invisible barrier for lynx. *Proceedings of the National Academy of Sciences*, 101:10632–10634.

Townsend, T.M., Mulcahy, D.G., Noonan, B.P., Sites Jr., J.W., Kuczynski, C.A., Wiens, J.J. & Reeder, T.W. (2011). Phylogeny of iguanian lizards inferred from 29 nuclear loci,

and a comparison of concatenated and species-tree approaches for an ancient, rapid radiation. *Molecular phylogenetics and evolution*. 61, 363–380.

Vaidya, G., Lohman, D. J., & Meier, R. (2011). SequenceMatrix: concatenation software for the fast assembly of multi‐gene datasets with character set and codon information. *Cladistics*, *27*(2), 171-180.

Vanzolini, P. E., & Williams, E. E. (1970). South American anoles: the geographic differentiation and evolution of the *Anolis chrysolepis* species group (Sauria, Iguanidae). *Arquivos de Zoologia*, *19*(1-2), 1-176.

Van der Hammen, T., & Hooghiemstra, H. (2000). Neogene and Quaternary history of vegetation, climate, and plant diversity in Amazonia. Quaternary Science Reviews, 19(8), 725-742.

Werneck, F. P., Nogueira, C., Colli, G. R., Sites, J. W., & Costa, G. C. (2011). Climatic stability in the Brazilian Cerrado: implications for biogeographical connections of South American savannas, species richness and conservation in a biodiversity hotspot. *Journal of Biogeography*, *39*(9), 1695-1706.

Werneck, F. P., Gamble, T., Colli, G. R., Rodrigues, M. T., & Sites Jr, J. W. (2012). Deep Diversification and long-term Persistence in the South American "Dry Diagonal": Integrating continent-wide Phylogeography and Distribution Modelling of geckos. *Evolution*, *66*(10), 3014-3034.

APPENDIX

Appendix 1: Tissues samples included in the study, procedence, ND2 haplotype number, GENELAND cluster and geographical coordinates. Besides those listed here, some additional sequences were obtained from GenBank. Acronyms refer to field numbers or Museum numbers. An asterisk indicates the individuals with posterior probability of assignment in GENELAND cluster membership below 0.9.

ID	ND2 haplotype	Locality	Country	GENELAND clusters	Posterior probabilities of cluster membership	Latitude	Longitude
BM002	01	UHE Belo Monte, Vitória do Xingu, Rio Xingu, PA	Brazil	P2	0.99	-2.8587	-52.0316
BM144	02	UHE Belo Monte, Vitória do Xingu, Rio Xingu, PA	Brazil	P2	0.99	-2.8587	-52.0316
BM260	03	UHE Belo Monte, Vitória do Xingu, Rio Xingu, PA	Brazil	P2	0.99	-2.8587	-52.0316
BM261	03	UHE Belo Monte, Vitória do Xingu, Rio Xingu, PA	Brazil	P2	0.99	-2.8587	-52.0316
BM365	04	Altamira, PA	Brazil	P2	0.98	-3.3229	-52.2711
BM527	05	Anapu, Belo Monte, PA	Brazil	P2	0.99	-3.0919	-51.7772
BON03	06	Bonito, PA	Brazil	P3	0.99	-1.3580	-47.3199
BON04	06	Bonito, PA	Brazil	P3	0.99	-1.3580	-47.3199
BON06	06	Bonito, PA	Brazil	P3	0.99	-1.3580	-47.3199
BON07	06	Bonito, PA	Brazil	P3	0.99	-1.3580	-47.3199
BON12	06	Bonito, PA	Brazil	P3	0.99	-1.3580	-47.3199

BP01	06	Agropalma, Tailandia, PA	Brazil	P3	0.90	-2.2877	-48.6984
BP02	01	Bacia Rio Capim, Paragominas, PA	Brazil	P2	0.65 *	-3.5466	-48.4977
BP05	01	Bacia Rio Capim, Paragominas, PA	Brazil	P2	0.65 *	-3.5466	-48.4977
CAX166	08	Floresta Nacional de Caxiuanã, PA	Brazil	P2	0.99	-1.7363	-51.4531
CAX167	09	Floresta Nacional de Caxiuanã, PA	Brazil	P2	0.99	-1.7363	-51.4531
CN0250	10	Flota Faro, PA	Brazil	P2	0.99	-1.7036	-57.2026
CN0525	11	Flota Faro, PA	Brazil	P2	0.99	-1.7036	-57.2026
CN0571	12	Esec Grão Pará Sul, Alenquer	Brazil	P2	0.94	-0.1655	-58.1864
CN0842	12	Esec Grão Pará Sul, Alenquer	Brazil	P2	0.94	-0.1655	-58.1864
CN1021	13	Serra do Acari, Oriximiná, PA	Brazil	P2	0.99	-1.2811	-58.6950
CN1133	14	Serra do Acari, Oriximiná, PA	Brazil	P2	0.99	-1.2811	-58.6950
CN1424	15	Rebio Maicuru, Almerim, PA	Brazil	P2	0.98	-0.8286	-53.9314
CN1616	16	Rebio Maicuru, Almerim, PA	Brazil	P2	0.98	-0.8286	-53.9314
CORBIDI8715	17	Region Loreto, Datem Province.	Peru	P2	0.99	-3.1870	-77.4333
FS055	18	RDS do Uacari,Monte Carmelo, Rio Juruá, AM	Brazil	P2	0.97	-5.6078	-67.5833
FS081	19	RDS do Uacari, Varadouro do Ouro Preto, Rio Juruá, AM	Brazil	P2	0.97	-5.6078	-67.5833
H0805	20	UHE Jirau, Abunã, RO	Brazil	P2	0.98	-9.6421	-65.4471
H1043	21	UHE Jirau, Abunã, RO	Brazil	P2	0.98	-9.6421	-65.4471
H1817	22	UHE Jirau, Mutum, RO	Brazil	P2	0.98	-9.5669	-65.0627

H1888	23	UHE Jirau, Caiçara, RO	Brazil	P2	0.98	-9.2654	-64.8110
H1964	23	UHE Jirau, Caiçara, RO	Brazil	P2	0.98	-9.2654	-64.6386
H2137	24	UHE Jirau, Mutum, RO	Brazil	P2	0.98	-9.2654	-64.6386
H3120	22	UHE Jirau, Mutum, RO	Brazil	P2	0.98	-9.2654	-64.6386
H3210	21	UHE Jirau, Abunã, RO	Brazil	P2	0.98	-9.6984	-65.3605
HERP5943	25	Tucumatuba, Tapajós, PA	Brazil	P2	0.91	-3.0948	-55.5230
HERP5944	26	Tucumatuba, Tapajós, PA	Brazil	P2	0.91	-3.0948	-55.5230
HERP5949	27	Tucumatuba, Tapajós, PA	Brazil	P2	0.91	-3.0948	-55.5230
HJ0066	28	UHE Jirau, Porto Velho, RO	Brazil	P2	0.98	-9.2654	-64.6386
HJ0466	21	UHE Jirau, Abunã, RO	Brazil	P2	0.98	-9.6984	-65.3605
HJ0479	21	UHE Jirau, Abunã,RO	Brazil	P2	0.98	-9.6984	-65.3605
IRSNB17832	29	Kaieteur National Park, Potaro-Siparuni District.	Guyana	P1	0.90	5.2000	-59.4500
IRSNB17851	30	Kaieteur National Park, Potaro-Siparuni District.	Guyana	P1	0.90	5.1333	-59.4167
JFT726	31	Santa Teresa, ES	Brazil	P2	0.98	19.9268	-40.6101
JOG541	32	Mina do Palito, Itaituba, PA	Brazil	P2	0.99	-6.3117	-55.7831
JUR060	33	Alcoa, Platô Capiranga, Juruti,PA	Brazil	P2	0.92	-2.4936	-56.1614
JUR070	34	Alcoa, Platô Capiranga, Juruti,PA	Brazil	P2	0.92	-2.4936	-56.1614
JUR503	35	Pacoval, Juruti, PA	Brazil	P2	0.93	-2.5444	-56.1672
JUR660	33	Adutora, Igarapé Prudente, Juruti, PA	Brazil	P2	0.92	-2.4642	-56.1914
JUR756	36	Mutum, Juruti, PA	Brazil	P2	0.93	-2.6094	-56.1961

LG1002	37	Porto Seguro, BA	Brazil	P2	0.98	16.4482	-39.0719
LG1028	38	Plácido de castro, AC	Brazil	P2	0.98	10.3218	-67.1847
LG1040	38	Plácido de castro, AC	Brazil	P2	0.98	10.3218	-67.1847
LSUMZH12538	39	Reserva Faunistica Cuyabeno, Neotropic Turis, Sucumbios.	Ecuador	P1	0.96	0.0119	-75.9695
LSUMZH12545	40	Reserva Faunistica Cuyabeno, Neotropic Turis, Sucumbios.	Ecuador	P1	0.96	0.0119	-75.9695
LSUMZH13566	41	Porto Walter, Rio Juruá, AC	Brazil	P2	0.98	-8.2509	-72.7677
LSUMZH13801	42	Porto Walter, Rio Juruá, AC	Brazil	P2	0.98	-8.2509	-72.7677
LSUMZH14094	43	Lábrea: Rio Ituxi Madeirera Scheffer, AM	Brazil	P2	0.98	-8.3464	-65.7161
LSUMZH14327	44	Belterra: Agropecuária Treviso LTDA , PA	Brazil	P2	0.98	-3.1467	-54.8296
LSUMZH15471	45	Nova Mamoré: Parque Estadual Guajará Mirim, RO	Brazil	P2	0.98	10.7992	-65.3087
MAR0536	46	Plot PPBIO Caxiuanã, PA	Brazil	P2	0.99	-1.9639	-51.6667
MAR0762	47	Plot PPBIO Caxiuanã, PA	Brazil	P2	0.99	-1.9639	-51.6667
MAR1342	46	Plot PPBIO Caxiuanã, PA	Brazil	P2	0.99	-1.9639	-51.6667
MAR1477	48	Afua, Rio Preto, Ilha do Marajó, PA	Brazil	P3	0.99	-0.3098	-50.5284
MAR1523	48	Afua, Rio Preto, Ilha do Marajó, PA	Brazil	P3	0.99	-0.3098	-50.5284
MAR1528	48	Afua, Rio Preto, Ilha do Marajó, PA	Brazil	P3	0.99	-0.3098	-50.5284
MAR1533	48	Afua, Rio Preto, Ilha do Marajó, PA	Brazil	P3	0.99	-0.3098	-50.5284
MAR1554	48	Afua, Rio Preto, Ilha do Marajó, PA	Brazil	P3	0.99	-0.3098	-50.5284

MAR1569	48	Afua, Rio Preto, Ilha do Marajó, PA	Brazil	P3	0.99	-0.3098	-50.5284
MAR1587	49	Afua, Rio Preto, Ilha do Marajó, PA	Brazil	P3	0.99	-0.3098	-50.5284
MAR1846	48	Afua, Rio Preto, Ilha do Marajó, PA	Brazil	P3	0.99	-0.3098	-50.5284
MBS11	50	Parque Nacional Serra do Divisor, AC	Brazil	P2	0.98	-8.8487	-73.0237
MBS14	51	Parque Nacional Serra do Divisor, AC	Brazil	P2	0.98	-8.8487	-73.0237
MBS17	51	Parque Nacional Serra do Divisor, AC	Brazil	P2	0.98	-8.8487	-73.0237
MBS19	52	Parque Nacional Serra do Divisor, AC	Brazil	P2	0.98	-8.8487	-73.0237
MBS34	53	Parque Nacional Serra do Divisor, AC	Brazil	P2	0.98	-8.8487	-73.0237
MBS46	54	Parque Nacional Serra do Divisor, AC	Brazil	P2	0.98	-8.8487	-73.0237
MJS011	55	Monte Dourado, Almerim, Estação, PA	Brazil	P2	0.99	-0.5908	-52.7358
MJS015	56	Monte Dourado, Almerim, Estação, PA	Brazil	P2	0.99	-0.5908	-52.7358
MJS053	57	Monte Dourado, Almerim, Estação, PA	Brazil	P2	0.99	-0.5908	-52.7358
MJS059	58	Monte Dourado, Almerim, Estação, PA	Brazil	P2	0.99	-0.5908	-52.7358
MJS075	59	Monte Dourado, Almerim, Estação, PA	Brazil	P2	0.99	-0.5908	-52.7358
MJS108	60	Comunidade Aldeia Nova, Antiga Boa Fé, Rio Tapajós, PA	Brazil	P2	0.98	-4.7191	-56.3843
MJS113	61	Comunidade Aldeia Nova, Antiga Boa Fé, Rio Tapajós, PA	Brazil	P2	0.98	-4.7034	-56.3841
MNCN04099	62	Camino los Guácharos - El Palmar. A 8 Km de los Guácharos, Cochabamba.	Bolivia	P2	0.98	17.0500	-65.4667

MNCN26614	63	Umarital, Río Ampiyacu, Loreto.	Peru	P2	0.98	-3.2666	-72.2673
MNCN26649	64	Confluencia de los Ríos Supai y Sábalo, Loreto.	Peru	P2	0.98	-3.0648	-72.1684
MNCN26691	65	Confluencia de los Ríos Supai y Sábalo, Loreto.	Peru	P2	0.98	-3.0648	-72.1684
MNCN26692	66	Confluencia de los Ríos Supai y Sábalo, Loreto.	Peru	P2	0.98	-3.0648	-72.1684
MNCN27173	67	Cataratas Auashiyacu, carretera Tarapoto-Yurimaguas, San Martin.	Peru	P2	0.98	-6.4119	-76.3175
MNCN27174	68	Cataratas Auashiyacu, carretera Tarapoto-Yurimaguas, San Martin.	Peru	P2	0.98	-6.4119	-76.3175
MNCN27175	67	Cataratas Auashiyacu, carretera Tarapoto-Yurimaguas, San Martin.	Peru	P2	0.98	-6.4119	-76.3175
MNCN34624	69	Heath River Wildlife Centre, en la orilla boliviana del río Heath. Iturralde, La Paz.	Bolivia	P2	0.98	12.6801	-68.7118
MNCN34625	70	Heath River Wildlife Centre, en la orilla boliviana del río Heath. Iturralde, La Paz.	Bolivia	P2	0.98	12.6801	-68.7118
MNCN34717	70	Heath River Wildlife Centre, en la orilla boliviana del río Heath. Iturralde, La Paz.	Bolivia	P2	0.98	12.6801	-68.7118
MNCN34738	71	Heath River Wildlife Centre, en la orilla boliviana del río Heath. Iturralde, La Paz.	Bolivia	P2	0.98	12.6801	-68.7118
MNCN46629	72	Leticia. Kilómetro 11 Tanimboca, carretera junto a la reserva, Amazonas.	Colombia	P2	0.98	-4.1195	-69.9510

MNCN46829	73	Leticia. Kilómetro 13, Amazonas.	Colombia	P2	0.98	-4.1195	-69.9510
MNCN48920	74	Campamento III km119, Primavera baja, Qda Jayave, Dist. Inambari, prov. Tambopata. Madre de Dios.	Peru	P2	0.98	-12.5769	-70.0710
MNCN48978	72	Leticia. Varzea del arroyo Huallar ka ka junto a Tanimboca, Amazonas.	Colombia	P2	0.98	-4.1195	-69.9510
MPEG11032	75	Resex Tapajós Arapiuns, Nova Canaã, PA	Brazil	P2	0.98	-2.8006	-52.5777
MPEG22766	76	Monte Dourado, PA	Brazil	P2	0.99	-0.5870	-52.6500
MPEG24510	77	Tucuruí, PA	Brazil	P2	0.93	-3.7508	-49.6675
MPEG24580	78	Faz. Riacho Monte Verde, Precious Woods, Portel, PA	Brazil	P2	0.97	-3.2658	-50.3249
MPEG24583	79	Faz. Riacho Monte Verde, Precious Woods, Portel, PA	Brazil	P2	0.97	-3.2658	-50.3249
MPEG24585	80	Faz. Riacho Monte Verde, Precious Woods, Portel, PA	Brazil	P2	0.97	-3.2658	-50.3249
MPEG24589	81	Faz. Riacho Monte Verde, Precious Woods, Portel, PA	Brazil	P2	0.97	-3.2658	-50.3249
MPEG24590	79	Faz. Riacho Monte Verde, Precious Woods, Portel, PA	Brazil	P2	0.97	-3.2658	-50.3249
MPEG24593	79	Faz. Riacho Monte Verde, Precious Woods, Portel, PA	Brazil	P2	0.97	-3.2658	-50.3249
MPEG26929	82	Coari, Porto Urucu, AM	Brazil	P2	0.98	-4.8955	-65.1892
MPEG26946	83	Coari, Porto Urucu, AM	Brazil	P2	0.98	-4.8955	-65.1892
MPEG27022	84	Vila dos Cabanos, Barcarena, PA	Brazil	P3	0.99	-1.5103	-48.6968
MPEG27665	26	Maués, AM	Brazil	P2	0.99	-3.3817	-57.7152
MPEG27693	85	Porto Urucu, AM	Brazil	P2	0.98	-4.8955	-65.1892
MPEG28043	06	Parque do Gunma, PA	Brazil	P3	0.99	-1.2007	-48.2901

MSH07851	86	Estação Sul, área Jari 112, Almerim, PA	Brazil	P2	0.99	-0.5907	-52.7355
MSH10714	87	Nova Canaã, Santarém, PA	Brazil	P2	0.92	-3.1667	-55.7372
MSH10730	88	Nova Canaã, Santarém, PA	Brazil	P2	0.92	-3.1591	-55.8255
MSH11140	89	Resex Tapajós Arapiuns, PA, Alto Mentae.	Brazil	P2	0.87*	-2.8005	-55.5853
MSH11539	90	Floresta Nacional de Caxiuanã, PA	Brazil	P2	0.99	-2.0096	-51.5021
MSH11570	91	Floresta Nacional de Caxiuanã, PA	Brazil	P2	0.99	-1.7959	-51.4351
MSH11625	92	Floresta Nacional de Caxiuanã, PA	Brazil	P2	0.99	-1.7380	-51.4558
MSH12240	93	Santa Isabel do Rio Negro, AM	Brazil	P1	0.96	0.0456	-64.7596
MSH12316	94	Santa Isabel do Rio Negro, AM	Brazil	P1	0.96	0.0446	-64.7565
MTR0152	95	Pacoti, CE	Brazil	P2	0.99	-4.2263	-38.9217
MTR04279	96	Pacoti, CE	Brazil	P2	0.60 *	-4.2263	-38.9217
MTR04528	97	Pacoti, CE	Brazil	P2	0.99	-4.2263	-38.9217
MTR04531	97	Pacoti, CE	Brazil	P2	0.99	-4.2263	-38.9217
MTR06037	98	Serra do Teimoso, Jussari, BA	Brazil	P2	0.76 *	15.1333	-39.5167
MTR06262	99	Igarapé Camaipi, AP	Brazil	P2	0.90	-0.0242	-51.8972
MTR06329	100	Igarapé Camaipi, AP	Brazil	P2	0.90	-0.0242	-51.8972
MTR11085	101	Floresta Nacional do Tapajós	Brazil	P2	0.98	-3.0492	-54.9622
MTR12159	102	Linhares, ES	Brazil	P2	0.98	19.1517	-40.0644
MTR12298	102	Linhares, ES	Brazil	P2	0.70 *	19.1516	-40.0669
MTR12860	103	Rio Abacaxis, AM	Brazil	P2	0.98	-4.5969	-58.2206

MTR13088	104	Rio Abacaxis, Pacamiri, AM	Brazil	P2	0.98	-4.5969	-58.2206
MTR13253	105	Maruim, Rio Abacaxis, AM	Brazil	P2	0.97	-3.8251	-58.2243
MTR13628	106	Camacan (Fazenda são carlos), BA	Brazil	P2	0.98	15.4085	-39.4934
MTR15591	96	Barra do Choça, BA	Brazil	P2	0.98	14.8647	-40.5581
MTR16316	107	Serra das Lontras, Arataca, BA	Brazil	P2	0.98	15.2566	-39.4140
MTR18124	108	Passo de Camaragibe, AL	Brazil	P3	0.82 *	-9.2576	-35.4891
MTR18621	109	Rio Purus, AM	Brazil	P2	0.98	-5.8341	-64.3087
MTR18622	110	Rio Purus, AM	Brazil	P2	0.98	-5.8341	-64.3087
MTR18636	109	Rio Purus, AM	Brazil	P2	0.98	-5.8341	-64.3087
MTR19048	111	Rio Purus, AM	Brazil	P2	0.98	-5.8341	-64.3087
MTR19062	112	Rio Purus, AM	Brazil	P2	0.98	-5.8341	-64.3087
MTR19066	112	Rio Purus, AM	Brazil	P2	0.98	-5.8341	-64.3087
MTR20738	113	Pacaraima, RR	Brazil	P2	0.98	4.3807	-61.1995
MTR20773	114	Pacaraima, RR	Brazil	P1	0.98	4.3807	-61.1995
MTR20797	114	Pacaraima, RR	Brazil	P1	0.98	4.3807	-61.1995
MTR20799	114	Pacaraima, RR	Brazil	P1	0.98	4.3807	-61.1995
MTR23059	115	Serra da Maroquinha, RR	Brazil	P1	0.98	4.3807	-61.1995
MTR23096	116	Serra da Maroquinha, RR	Brazil	P1	0.99	2.3679	-61.3735

MTR23155	116	Serra da Maroquinha, RR	Brazil	P1	0.99	2.3679	-61.3735
MTR25524	117	Parque Nacional Pacaás Novos, Base Candeias, RO	Brazil	P2	0.99	10.7732	-63.6210
MTR25537	118	Parque Nacional Pacaás Novos, Base Candeias, RO	Brazil	P2	0.98	10.7732	-63.6210
MTR25538	119	Parque Nacional Pacaás Novos, Base Candeias, RO	Brazil	P2	0.98	10.7692	-63.6225
MTR25597	120	Parque Nacional Pacaás Novos, Base Candeias, RO	Brazil	P2	0.98	10.7692	-63.6225
MTR25668	121	Parque Nacional Pacaás Novos, Base Candeias, RO	Brazil	P2	0.98	10.7868	-63.6281
MTR25978	122	Parque Nacional Pacaás Novos, Base do Jaci, RO	Brazil	P2	0.98	10.7868	-63.6281
MTR25984	122	Parque Nacional Pacaás Novos, Base do Jaci, RO	Brazil	P2	0.98	10.5275	-63.9734
MTR25985	122	Parque Nacional Pacaás Novos, Base do Jaci, RO	Brazil	P2	0.98	10.5275	-63.9734
MTR26007	122	Parque Nacional Pacaás Novos, Base do Jaci, RO	Brazil	P2	0.98	10.5273	-63.9735
MTR28056	123	Serra do Divisor, Pe da Serra, AC	Brazil	P2	0.98	-7.4431	-73.6577
MTR28194	123	Serra do Divisor, Pe da Serra, AC	Brazil	P2	0.98	-7.4458	-73.6576
MTR28201	123	Serra do Divisor, Pe da Serra, AC	Brazil	P2	0.98	-7.4267	-73.6622
MTR28206	123	Serra do Divisor, Pe da Serra, AC	Brazil	P2	0.98	-7.4458	-73.6576
MTR28368	124	Serra do Divisor, Pe da Serra, AC	Brazil	P2	0.98	-7.5031	-73.7208
MTR28392	124	Serra do Divisor, Pe da Serra, AC	Brazil	P2	0.98	-7.5044	-73.7083
MTR28393	125	Serra do Divisor, Pe da Serra, AC	Brazil	P2	0.98	-7.5044	-73.7083
MTR28413	123	Serra do Divisor, Pe da Serra, AC	Brazil	P2	0.98	-7.5044	-73.7083
MTR28414	124	Serra do Divisor, Pe da Serra, AC	Brazil	P2	0.98	-7.5044	-73.7083
MTR28534	126	Boca do Acre, ramal bode preto, AC	Brazil	P2	0.98	-9.0047	-67.1814

MTR28535	127	Boca do Acre, ramal bode preto, AC	Brazil	P2	0.98	-9.0050	-67.1815
MTR28538	128	Boca do Acre, ramal bode preto, AC	Brazil	P2	0.98	-9.0041	-67.1812
MTR28563	129	Boca do Acre, ramal Cruzeirinho, AC	Brazil	P2	0.98	-8.7598	-67.3089
MTR28564	130	Boca do Acre, ramal Cruzeirinho, AC	Brazil	P2	0.98	-8.7598	-67.3089
MTR28565	131	Boca do Acre, ramal Cruzeirinho, AC	Brazil	P2	0.98	-8.7598	-67.3089
MTR28576	132	Fazenda Experimental Catuaba, AC	Brazil	P2	0.98	10.0834	-67.6278
MTR28577	132	Fazenda Experimental Catuaba, AC	Brazil	P2	0.98	10.0834	-67.6278
MTR28578	132	Fazenda Experimental Catuaba, AC	Brazil	P2	0.98	10.0763	-67.6260
MTR28579	132	Fazenda Experimental Catuaba, AC	Brazil	P2	0.98	10.0841	-67.6280
MTR28680	133	FLONA Humaita, Igarape Buiussu	Brazil	P2	0.98	-7.6160	-62.8833
MTR967911	134	Aripuanã, MT	Brazil	P2	0.98	10.2719	-59.3883
MTR968155	135	Aripuanã, MT	Brazil	P2	0.98	10.1756	-59.4514
MTR977706	136	Aripuanã, MT	Brazil	P2	0.98	10.1767	-59.4503
PEU014	137	Wenceslau Guimarães, BA	Brazil	P2	0.98	13.5785	-39.7086
PEU075	138	Tancredo Neves, BA	Brazil	P2	0.98	13.4563	-39.4210
PEU120	139	Jaguaripe, BA	Brazil	P2	0.98	13.1030	-38.8953
PEU133	140	Jaguaripe, BA	Brazil	P2	0.98	13.1030	-38.8953
PEU276	141	Nilo Peçanha, BA	Brazil	P2	0.98	13.6036	-39.1039
PEU300	142	Camamu, BA	Brazil	P2	0.98	13.9375	-39.1046
PEU488	143	Ilhéus, BA	Brazil	P2	0.98	14.7767	-39.0632

PJA036	144	AHE Jatobá, Rio Tapajos, PA	Brazil	P2	0.98	-6.0838	-57.6904
PJA166	145	AHE Jatobá, Rio Tapajos, PA	Brazil	P2	0.98	-5.4535	-57.0851
PJC226	146	AHE Jatobá, Rio Tapajos, PA	Brazil	P2	0.99	-5.0623	-56.8779
PJD084	147	AHE Jatobá, Rio Tapajos, PA	Brazil	P2	0.98	-5.7660	-57.2771
PK2255	94	La Escalera, Bolivar State.	Venezuela	P1	0.97	5.9500	-61.3833
PMRT460	82	Aveiros-PA. Uricurituba	Brazil	P2	0.98	-3.8283	-55.4897
PMRT464	148	Aveiros-PA. Uricurituba	Brazil	P2	0.98	-3.8283	-55.4897
PMRT510	149	Aveiros-PA. Uricurituba	Brazil	P2	0.98	-3.8283	-55.4897
PMRT555	150	Aveiro, Brasil Legal, PA Ponto 1.	Brazil	P2	0.98	-3.9224	-55.5942
PMRT556	151	Aveiro, Brasil Legal, PA Ponto 2.	Brazil	P2	0.98	-3.9111	-55.5325
PMRT609	150	Aveiro, Brasil Legal, PA, Ponto 1.	Brazil	P2	0.98	-3.9224	-55.5942
PMRT642	150	Aveiro, Brasil Legal, PA, Ponto 1.	Brazil	P2	0.98	-3.9224	-55.5942
PMRT656	152	Aveiro, Brasil Legal, PA Ponto 2.	Brazil	P2	0.98	-3.9111	-55.5325
PMRT701	153	Aveiro, Brasil Legal, PA Ponto 4.	Brazil	P2	0.98	-4.0069	-55.5760
PMRT727	154	Aveiro, Brasil Legal, PA Ponto 3	Brazil	P2	0.98	-3.9731	-55.6193
PMRT775	155	Aveiro, Brasil Legal, PA Ponto 3	Brazil	P2	0.98	-3.9731	-55.6193
PMRT780	155	Aveiro, Brasil Legal, PA Ponto 4.	Brazil	P2	0.98	-4.0069	-55.5760
RDS064	156	Mamirauá, AM	Brazil	P2	0.98	-2.8412	-65.0070
RDS067	157	Mamirauá, AM	Brazil	P2	0.98	-2.8412	-65.0070
RDS276	158	Mamirauá, AM	Brazil	P2	0.98	-2.8412	-65.0070

RFB06	159	Vila dos Cabanos, Barcarena, PA	Brazil	P3	0.99	-1.5154	-48.6977
RFB07	160	Vila dos Cabanos, Barcarena, PA	Brazil	P3	0.99	-1.5154	-48.6977
RFB09	161	Vila dos Cabanos, Barcarena, PA	Brazil	P3	0.99	-1.5154	-48.6977
RFB10	161	Vila dos Cabanos, Barcarena, PA	Brazil	P3	0.99	-1.5154	-48.6977
RFB13	161	Vila dos Cabanos, Barcarena, PA	Brazil	P3	0.99	-1.5154	-48.6977
RFB21	161	Vila dos Cabanos, Barcarena, PA	Brazil	P3	0.99	-1.5154	-48.6977
RFB48	161	Vila dos Cabanos, Barcarena, PA	Brazil	P3	0.99	-1.5154	-48.6977
SMS608	162	São Sebastião dos Bargas, AM	Brazil	P2	0.98	-3.7894	-59.0340
SMS649	162	São Sebastião dos Bargas, AM	Brazil	P2	0.98	-3.7894	-59.0340
TCAP3192	163	Santa Cruz do Arari, Ilha do Marajó, PA	Brazil	P3	0.99	-0.6468	-49.1626
TCAP3384	164	Santa Cruz do Arari, Ilha do Marajó, PA	Brazil	P3	0.99	-0.6468	-49.1626
TCAP3399	164	Santa Cruz do Arari, Ilha do Marajó, PA	Brazil	P3	0.99	-0.6468	-49.1626
TCAP3400	148	Santa Cruz do Arari, Ilha do Marajó, PA	Brazil	P3	0.99	-0.6468	-49.1626
TEC0045	97	Planalto de Ibiapaba, Ubajara, CE	Brazil	P2	0.97	-6.0855	-56.2491
TEC0532	166	Tocantinzinho, Itaituba, PA	Brazil	P2	0.97	-6.3117	-55.7855
TEC2029	97	Serra de Maranguape, Maranguape, CE	Brazil	P2	0.99	-3.9018	-38.7160
TEC2087	167	Serra de Maranguape, Maranguape, CE	Brazil	P2	0.99	-3.9018	-38.7160
TEC2088	167	Serra de Maranguape, Maranguape, CE	Brazil	P2	0.99	-3.9018	-38.7160
TEC2089	97	Serra de Maranguape, Maranguape, CE	Brazil	P2	0.99	-3.9018	-38.7160
UFS038	168	Cachoeira da fumaça; UHE Foz do Apiacás, MT	Brazil	P2	0.98	-9.2474	-57.0888

UFS212	169	Cachoeira da fumaça; UHE Foz do Apiacás, MT	Brazil	P2	0.98	-9.2474	-57.0888
UFS557	168	Trilha eixo 1, Apiacas, MT	Brazil	P2	0.98	-9.2045	-57.0887
URCA319	169	REBIO Pedra Talhada, Quebrangulo, AL	Brazil	P2	0.98	-9.2341	-36.4077
URD572	170	Trilha eixo 1, Apiacas, MT	Brazil	P2	0.98	-9.2045	-57.0887
VOGT2028	171	Lago Açaí, AM	Brazil	P2	0.98	-6.0146	-60.2090
VXG01	172	Vitória do Xingu, PA	Brazil	P3	0.80 *	-3.3030	-51.8065
VXG16	173	Vitória do Xingu, PA	Brazil	P3	0.80 *	-3.3030	-51.8065
VXG17	174	Vitória do Xingu, PA	Brazil	P3	0.80 *	-3.3030	-51.8065
VXG20	175	Vitória do Xingu, PA	Brazil	P3	0.80 *	-3.3030	-51.8065
VXG21	176	Vitória do Xingu, PA	Brazil	P3	0.80 *	-3.3030	-51.8065

DEWLAP COLOR DIVERSITY IN THE MAINLAND ANOLE *NOROPS FUSCOAURATUS* (REPTILIA: DACTYLOIDAE)

Annelise B. D'Angiolella[1], Miguel T.U. Rodrigues[2], Ivan Prates[3], Ana C. Carnaval[3], Kirsten Nicholson[4] and Teresa C.S. Avila Pires[1,5]

[1] Programa de Pós Graduação em Zoologia UFPA/MPEG, Belém, Pará, Brazil,

Author for correspondence: annelise.dangiolella@gmail.com.

[2] Universidade de São Paulo, USP, São Paulo, Brazil

[3] The City College of New York, Division of Science, Biology Department, CUNY, New York, USA

[4] Department of Biology, Central Michigan University, Mt. Pleasant, MI 48859, USA.

[5] Museu Paraense Emilio Goeldi, Belém, Pará, Brazil.

ABSTRACT

The dewlaps of anoline lizards represent a complex signaling system that has been frequently associated to reproductive isolation and speciation. However, the potential causes of geographic variation in dewlap diversity and its role in speciation remain poorly understood. In the present study we perform a morphological and a multilocus phylogenetic analysis of geographic differentiation in dewlap color in *Norops fuscoauratus* a widespread mainland anole species that inhabits the Amazonian and Atlantic forests, attempting to understand if different dewlap color morphs would correspond to genetically and morphologically distinct groups on the basis of meristic, morphometrics and hemipenial characters and to verify if differences in dewlap color would be associated with climatic/environmental variation. Our results show that dewlap color morphs in *N. fuscoauratus* have no correspondence with genetic and morphology, including hemipenial characters. Allthough, the color variation seems to respond to climate variation in temperature and precipitation.

Keywords: Dewlap, anoles, Amazonia, hemipenes, *Norops fuscoauratus,* Dactyloidae.

1. INTRODUCTION

Diversity of intra and interespecific communication signals has generated extensive debates on the mechanisms behind it (Nicholson et al. 2007; Stapley et al. 2011; Ng et al. 2013). Dewlap in anoles represents an example of a complex signaling system, that has been regularly associated to reproductive isolation and speciation, frequently used as diagnostic character in anoles systematics and taxonomy (Losos & Schneider, 2009; Vanhooydonck et al. 2009; D'Angiolella et al. 2011; Glor & Laport, 2012). The dewlap is an extensible flap of skin located beneath the chin and present, in most species, in females and males (Nicholson et al. 2007). Several studies attempted to quantify the morphological diversity in dewlap shape, color and size and to understand the forces that shape dewlap evolution among and within anole species (Losos & Chu, 1998; Nicholson et al. 2007; Vanhooydonk et al. 2009; Stapley et al. 2011; Ng & Glor, 2011, Ng et al, 2013). However, the potential causes of geographic variation in dewlap diversity and its role in speciation remain poorly understood.

Several processes have been postulated to underlie geographic divergence in dewlap color, including sexual selection, genetic drift and adaptation to local signaling conditions (Macedonia, 2001; Lean & Fleishman 2002, 2004; Ord et al. 2010, 2011; Glor & Laport, 2012; Ng et al. 2013; Macedonia et al. 2014). Differences in dewlap coloration may be an indicative of speciation since this trait is directly associated with reproductive isolation (Losos, 2009; Ng & Glor, 2011).

Our focal organism is an inhabitant of Amazonian and Atlantic forests in South America. *Norops fuscoauratus* is a common lizard, found on the vegetation (occasionally on the ground), both in undisturbed and secondary forests (Avila-Pires 1995). In this species, only males have large dewlaps that extend almost to the midbody. Specimens of distinct occurrence localities of this species have dewlap colors in shades of grey, olive, yellow and red, with some specimens presenting a bicolored dewlap (Avila-Pires, 1995). As a common and easily collected inhabitant of forested areas, with a widespread distribution and an extensive dewlap color variation, *N. fuscoauratus* is an interesting model organism to investigate aspects related to dewlap color divergence.

Here, we conduct a morphological and a multilocus phylogenetic analysis of geographic differentiation in dewlap color in *N. fuscoauratus*, addressing the following questions: 1) Are groups of individuals with different dewlap colors genetically

differentiated? 2) Do different dewlap color morphs present variation in other morphological traits? 3) Do different dewlap color morphs present differences in hemipenial morphology? 4) Are differences in dewlap color associated with climatic/environmental variation?

2. MATERIAL AND METHODS

2.1 Dewlap color variation

We collected information on dewlap color from the literature (containing pictures or mentioning dewlap color in life), photographs taken in the field, and from personal communication by specialists. To make sure that observed shifts in color were not related to ontogenetic variation, we also collected dewlap color information of both juveniles and adult males from the same locality, when this information was available. Considering that personal observations and descriptions in the literature did not follow a standard scale, and that different environmental conditions (such as light reflectance and time of the day) to which dewlaps are exposed when photographed may influence final colors in a photo, we grouped them in five color categories that include the broad color gradients observed; besides, we considered only the skin color. Categories considered are: 1) Olive grey, 2) Yellow, 3) Red, 4) Bicolor and 5) Dark grey (Figure 1.2).

Figure 1.2: Dewlap color patterns found in *N. fuscoauratus* during the present study.

Sousa & Freire (2010) published the first record of *N. fuscoauratus* from the state of Rio Grande do Norte, Brazil, based on a male specimen with a "Red" dewlap collected in the locality of Timbau do Sul. From the photo presented, it is clear that this specimen is actually a male of *N. ortonii* and for this reason; we do not include it in our analyses.

2.2 Sampling and amplification of molecular data

A total of 147 new sequences were generated from 47 localities throughout the distribution of *N. fuscoauratus,* including both Amazonian and Atlantic forests (Appendix-Table 1). GenBank sequences with dewlap color information were also included (vouchers LSUMZH 12538, 12545 and 15471, from Glor et al. 2001). We used *Norops kemptoni* as outgroup due to its close relationship to *N. fuscoauratus* (Nicholson et al. 2005; 2012).

Genomic DNA was extracted from muscle, liver, or tail clips following a standard phenol/chloroform protocol (Sambrook et al. 1989) or with the DNeasy Blood and Tissue Kit (Qiagen, Valencia, California). We amplified the mitochondrial gene ND2 (*NADH dehydrogenase subunit 2*) and adjacent tRNAs (Rodriguez Robles et al. 2007) as well as three nuclear markers: RAG1 (*recombination-activating gene 1*; Gartner et al. 2013), DNAH3 (*dynein axonemal heavy chain*), MKL1 (*megakaryoblastic leukemia 1*) and SNCAIP (*synuclein alpha interacting protein*), as per Townsend et al. (2011).

Our Polymerase Chain Reaction (PCR) profile followed an initial 5-min denaturation at 95 °C, proceeded by 32 cycles of denaturation (30 s at 95 °C), annealing (45 s at 52–56 °C), extension (1 min at 72 °C), and a final extension of 5 min at 72 °C. The PCR products were purified with the Polyethylene glycol protocol (PEG). Sequencing was carried out on an ABI 3130 automated capillary sequencer (Applied Biosystems, Foster City, California, USA) with the ABI Prism Big Dye terminator Kit. To confirm observed mutations, both strands of each sample were sequenced.

Sequences were edited and aligned using Geneious Pro 6 (Biomatters, Auckland) and protein-coding sequences were translated into amino acids to confirm alignment and ensure there were no premature stop codons. For nuclear loci, heterozygous nucleotide positions were inferred by the presence of double peaks of the same size in the electropherogram. To obtain the gametic phase of haplotypes of the heterozygous individuals, we used a Bayesian approach as implemented in PHASE 2.1 1 (Scheet & Stephens, 2006).

2.3 Phylogenetic Analyses

Models of nucleotide evolution and best-fit partition schemes, including partitions by codon position, were determined with Partition Finder 1.1.1 (Lanfear et al. 2012),

implementing the Bayesian information criterion (BIC) for Bayesian Inference (BI). The concatenated dataset was generated in Sequence Matrix (Vaidya et al. 2011) and it was partitioned by gene, with a sixth partition for tRNAs.

We constructed independent phylogenetic trees for each molecular marker (results not shown) and for the concatenated dataset using the Bayesian criteria implemented in MrBayes v.3.1.2 (Ronquist & Huelsenbeck, 2003) by running tree independent chains for 100,000,000 generations, sampling every 10,000 generations. To assess burnin, stationarity and convergence, we used Tracer 1.8.1. The maximum credibility tree was summarized in Tree Annotator 1.8.1 and we visualized the annotated tree in FigTree 1.4.0. We also conducted partitioned Maximum Likelihood analysis in RAXML ver. 7.0.4 (Stamatakis, 2006) using the GTR+GAMMA model for all partitions. We conducted 1,000 ''fast bootstrap'' replicates and 10 separate maximum likelihood searches. Bootstrap values >70 were considered as indicating supported clades. Both MrBayes and RAxML analysis were conducted in CIPRES web portal (Miller et al. 2010).

We calculated net among group distances (Nei & Li, 1979) for ND2 gene between the different dewlap color morphs using MEGA 4 (Kumar et al. 2008) with pairwise exclusion of gapped and missing stretches of the sequences.

To visualize relationships among mtDNA and nDNA haplotypes and the distribution of the dewlap color patterns, we constructed haplotype networks for all five molecular markers using the median joining algorithm (Bandelt, Forster & Rohl, 1999) in the software PopArt (http://popart.otago.ac.nz.). The input file was generated using DNAsp v. 5.10.01 (Librado & Rozas, 2009) using the phased dataset for the nDNA markers.

The analysis of Molecular Variance (AMOVA) estimates population differentiation from molecular data and provides the possibility of testing hypotheses about such differentiation (Excoffier et al, 1992). In our case, we used AMOVA to estimate the genetic differentiation among the dewlap color morphs. The amount of genetic differentiation between dewlap morphs was quantified using the F-statistics (Wright, 1965) and the statistical significance of Fst estimates was determined using 10,000 permutations. These analyses were conducted in Arlequin v.3.11 (Excoffier et al, 1992).

2.4 External Morphological data analyses

To investigate the overall morphological variation in *N. fuscoauratus*, we collected meristic and morphometric data from 263 specimens (127 females and 136 males) deposited in the zoological collections of Museu de Zoologia da Universidade de São Paulo (MZUSP), Museu Paraense Emílio Goeldi (MPEG), and American Museum of Natural History (AMNH) (Figure 2.2).
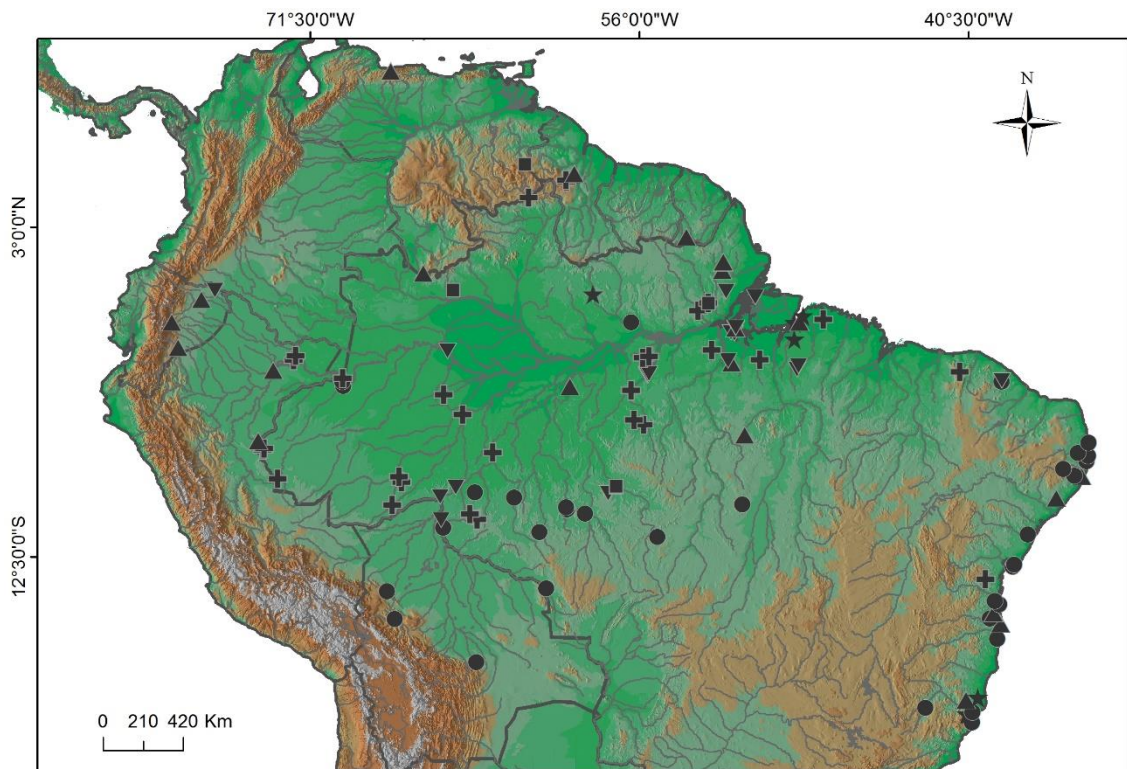
Figure 7 Distribution of *Norops fuscoauratus* samples used in morphological, molecular and hemipenial analysis. Circles represent samples used for morphology analysis; Cross represent tissues samples; Triangles represent samples that were used for both morphological and hemipenial analysis; Squares represent tissues and hemipenis samples; Stars represent tissies and morphology samples and Inverted triangle represents tissues, morphological and hemipenial samples.

We selected 13 and 10 morphometric and meristic characters respectively. The following morphometric data were recorded: snout–vent length (SVL), head width, head height, minimum distance between orbits, ear-opening diameter, minimum distance between nostrils, distance from mouth to ear (from posterior margin of mouth to anterior margin of ear opening), snout length (from tip of snout to anterior margin of orbit),

interparietal length, hand length (from wrist to base of finger IV), fourth finger length (from base to nail of finger IV), tibia length, foot length (from heel to base of toe IV), and fourth toe length (from base to tip of nail of toe IV). Additionally, the following meristic characters were recorded: number of postrostrals, supralabials, infralabials, loreals (in a vertical line under second canthal), canthals, scales between second canthals, minimum number of scales between supraorbital semicircles, minimum number of scales between interparietal and supraorbital semicircles, postmentals, fourth finger lamellae, and fourth toe lamellae.

Pholidosis and measurements were taken on the right side of the body, except when specimens were damaged (in this case, the left side was used). Measurements were recorded with digital calipers to the nearest 0.1 mm, taken at least twice, and the mean values were used for subsequent analysis. Scale and measurement terminology follows Avila-Pires (1995) and D'Angiolella et al. (2011). Individuals were sexed on basis of presence or absence of the dewlap.

To assess differences in body size between sexes, measurements of snout-vent-length (SVL) were checked for normality and homoscedasticity and evaluated through a one-way analysis of variance (ANOVA) using the package vegan in R v. 3.1.1 (R Core Team, 2013). To determine if other traits were varying between sexes, when controlling for the effect of size (SVL), we performed a multiple analysis of covariance (MANCOVA) using SVL as a covariate in SPSS v.17.0 (2008).

To investigate if different dewlap color morphs present variation in continuous and meristic traits, we performed a principal component analysis (PCA) in the package FactoMineR (Lê et al. 2008) in R v. 3.1.1 (R Core Team, 2013). This package allows the inclusion of supplementary variables (either continuous or categorical) that, even though have no influence on the principal components of the analysis, help to interpret the dimensions of variability. For this analysis, only specimens with dewlap color information were used (n=109) and we removed the effect of size in morphometric data through univariate regressions of each variable with SVL, subsequently using the residual values to perform the PCA. Individuals were grouped as Olive grey (n=66), Red (n=22), Yellow (n=12) and Bicolor (n=9). None individuals with Dark grey pattern were available for morphological analysis, and for that, were not included in the PCA analysis.

We employed the *estim_ncp* function to estimate the number of dimensions to interpret in the PCA analysis, applying the "GCV" (generalized cross-validation approximation) method and we included the dewlap color as categorical supplementary variable. We also applied the *dimdesc* function to interpret the dimensions of the PCA, considering the default statistical significance level of 0.05. This function describes which categorical and continuous variables are the most correlated to each axis, and is very useful when there is an elevated number of variables in the analysis. Even though this is not our case, it was useful in evaluating which categories of our categorical variable (dewlap color) better describe each axis.

2.5 Hemipenial preparation

To determine if different dewlap color morphs of *N. fuscoauratus* would also vary in relation to hemipenes morphology, 42 hemipenes were prepared. We selected hemipenes from localities of specimens/tissues with dewlap color information and from localities with no dewlap color information only for comparison purposes (Table 2).

Table 2: Museum numbers and localities of the prepared hemipenes of *N. fuscoauratus.*

ID	Locality	Country
AMNH115871	Napo	Ecuador
AMNH133697	Amazonas	Venezuela
AMNH138679	Amapa, AP	Brazil
AMNH151836	Guyana	Guyana
MPEG20589	P. Walter, Jurua, AC	Brazil
MPEG20590	P. Walter, Jurua, AC	Brazil
MPEG20598	P. Walter, Jurua, AC	Brazil
MPEG21611	Ourilandia do Norte, PA	Brazil
MPEG22367	ECFPN Caxiuana, PA	Brazil
MPEG22768	Monte Dourado, Almerin, PA	Brazil
MPEG25462	Caracol, UHE, Belo Monte, PA	Brazil
MPEG26095	Plot PPBIO, FN Caxiuana, PA	Brazil
MPEG27065	Juruti, PA	Brazil
MPEG28863	Floresta Nacional Caxiuana, PA	Brazil
MPEG28909	Floresta Nacional Caxiuana, PA	Brazil
MPEG28913	Floresta Nacional Caxiuana, PA	Brazil
MPEG29236	Terra Santa, PA	Brazil
MPEG29607	Afua, Ilha do Marajo, PA	Brazil
MPEG29612	Afua, Ilha do Marajo, PA	Brazil
MPEG29697	Mazagao, AP	Brazil
MPEG-BP02	Bacia Rio Capim, Paragominas, PA	Brazil

MPEG-PMRT556	Aveiro, PA Ponto 2.	Brazil
MPEG-PMRT602	Aveiro, PA, Ponto 1.	Brazil
MPEG-PMRT656	Aveiro, PA Ponto 2.	Brazil
MPEG-VXG14	Vitoria do Xingu, PA	Brazil
MPEG-VXG16	Vitoria do Xingu, PA	Brazil
MSH12316	Santa Isabel do Rio Negro, AM	Brazil
MSH12356	Santa Isabel do Rio Negro, AM	Brazil
MZUSP10043	Uhe Jirau, Porto Velho, RO	Brazil
MZUSP101624	UHE Jirau, Porto Velho, RO	Brazil
MZUSP103435	Potaro-siparuni	Guyana
MZUSP16182	Canavieiras, BA	Brazil
MZUSP27091	Napo, Limoncocha	Ecuador
MZUSP32784	Sto. Antonio do Içá	Brazil
MZUSP42569	Borba, AM	Brazil
MZUSP65666	Estação Ecológica de Saltinho, PE	Brazil
MZUSP66412	Fezenda Unacau, São José, BA	Brazil
MZUSP81620	Apiacás, MT	Brazil
MZUSP82885	Vila Rica, MT	Brazil
MZUSP87561	Pacoti, CE	Brazil
MZUSP87563	Pacoti CE	Brazil
MZUSP96073	Campo Alegre, AL	Brazil

For hemipenes preparation, we combined techniques described by Pesantes (1994), Keogh (1999) and Zaher & Prudente (2003). To minimize the variation that the eversion process may cause and since *N. fuscoauratus* hemipenes are very small and delicate, only partially or totally everted hemipenes were prepared. Once the preserved specimen was selected, one of the hemipenis was removed through a small incision at the base of the tail. Due to its very thin skin, the use of KAOH 2% was not possible, so if the hemipenis was not fully everted, it was repeatedly filled with hot water until the lobes were completely everted. When everted, the organ was filled with colored Vaseline, to allow better visualization of ornamentation structures, and subsequently conserved in 70% ethanol. We obtained digital images of hemipenes in sulcate, assulcate, and lateral views using a JVC camera, KYF75U, attached to a stereomicroscope with the aid of Auto-Montage Pro, 5.02.

2.6 Environmental data

To investigate if different dewlap colors in *N. fuscoauratus* were associated with different environmental conditions (precipitation and temperature), we conducted a Principal Components Analysis (PCA) in the package FactorMineR in R v.3.1.1 (R Core Team, 2013). At first, we obtained the locality data of all tissue samples containing information about the dewlap color through field GPS records, georeferenced museum data or published papers, and records from trusted collectors. Each point was verified with Google Earth to ensure it was not located outside forested areas. Then, the Bioclimatic layers were downloaded from the WorldClim database (Hijmans et al. 2005) and the values for each variable at every locality were extracted using ArcGIS (ESRI). To avoid the use of redundant variables, we performed a Pearson correlation analysis and excluded those highly correlated variables ($r > 0.8$), keeping the ones we considered relevant biologically (Rissler & Apodaca, 2007). From the original 19 environmental variables downloaded from the WorldClim database, twelve were selected and used in subsequent analyses. The parameters used to perform the PCA were the same described in the section "external morphological data analyses".

3. RESULTS

3.1 Quantifying Dewlap Color Variation

"Olive-grey" dewlaps were present in 56% (84 samples) of all tissue samples analyzed. The second most frequent dewlap color was "Red", present in 26% (39 samples) of all samples. The "Yellow" (13 samples), "Bicolor" (9 samples) and "Dark Grey" (5 samples) groups were less common, representing 8.7%, 6% and 3.3% of all tissue samples analyzed respectively. At each locality, the dewlap color was constant, with no variation found between juveniles and adults. The dewlap color in *N. fuscoauratus* does not reflect a geographic structure, with the "Olive grey" pattern present across the entire range of the species. "Red" dewlaps were found in specimens from Ecuador, Colombia, Venezuela, Guyana and in the states of Rondônia, Acre, Pará and Mato Grosso, in Brazil. "Yellow" dewlaps were found in individuals from Brazilian Amazonia, in Rio Purus-AM, Monte Dourado-PA and Almerin-PA, and in Santa Teresa-ES and Linhares-ES in the Atlantic Forest. "Bicolor" dewlaps were present in Acre and Amazonas, in Brazil, and "Dark Grey" dewlaps were observed only in two nearby localities along the Tapajós River, Pará, Brazil (Figure 3.2).

3.2 Phylogenetic analysis

All Bayesian analyses converged and data from three runs were combined for final analysis (results not shown). The partitioned ML analysis produced a single tree (ln L - 14.338.226075), with similar topology of the partitioned Bayesian consensus tree at well-supported nodes. Basal relationships were poorly supported and inconsistent across analyses, even though small demes had high posterior probabilities as well as high bootstrap values. The ML phylogenetic tree recovered a monophyletic *N. fuscoauratus* clade, but Bayesian analysis did not. Both analyses recovered a well supported division between a clade represented by specimens with "Red" dewlap from Parque Nacional Pacaás Novos, in Rondônia, southwestern Amazonia, and all other clades (Figure 4.2),
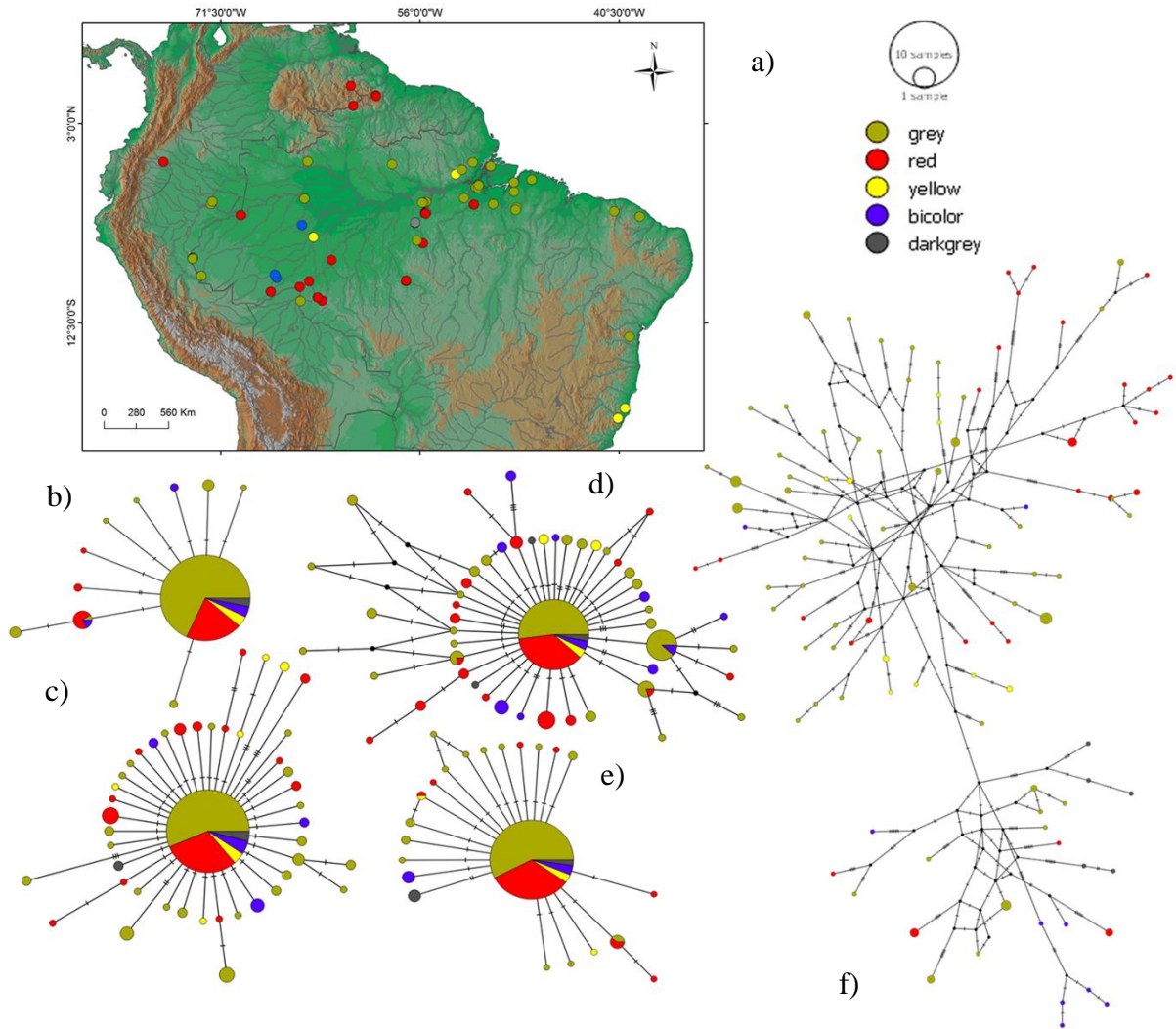
Figure 3.2 Map and haplotype networks generated for mtDNA and nDNA for sequences from N. fuscoauratus with known dewlap information. Colors represent different dewlap colors as indicated in the figure. a) Distribution of tissue samples of *N. fuscoauratus* with known dewlap color; b) DNAH3 haplotype network; c) RAG1 haplotype network; d) MKL1 haplotype network; e) SINCAIP haplotype network and f) ND2 haplotype network.
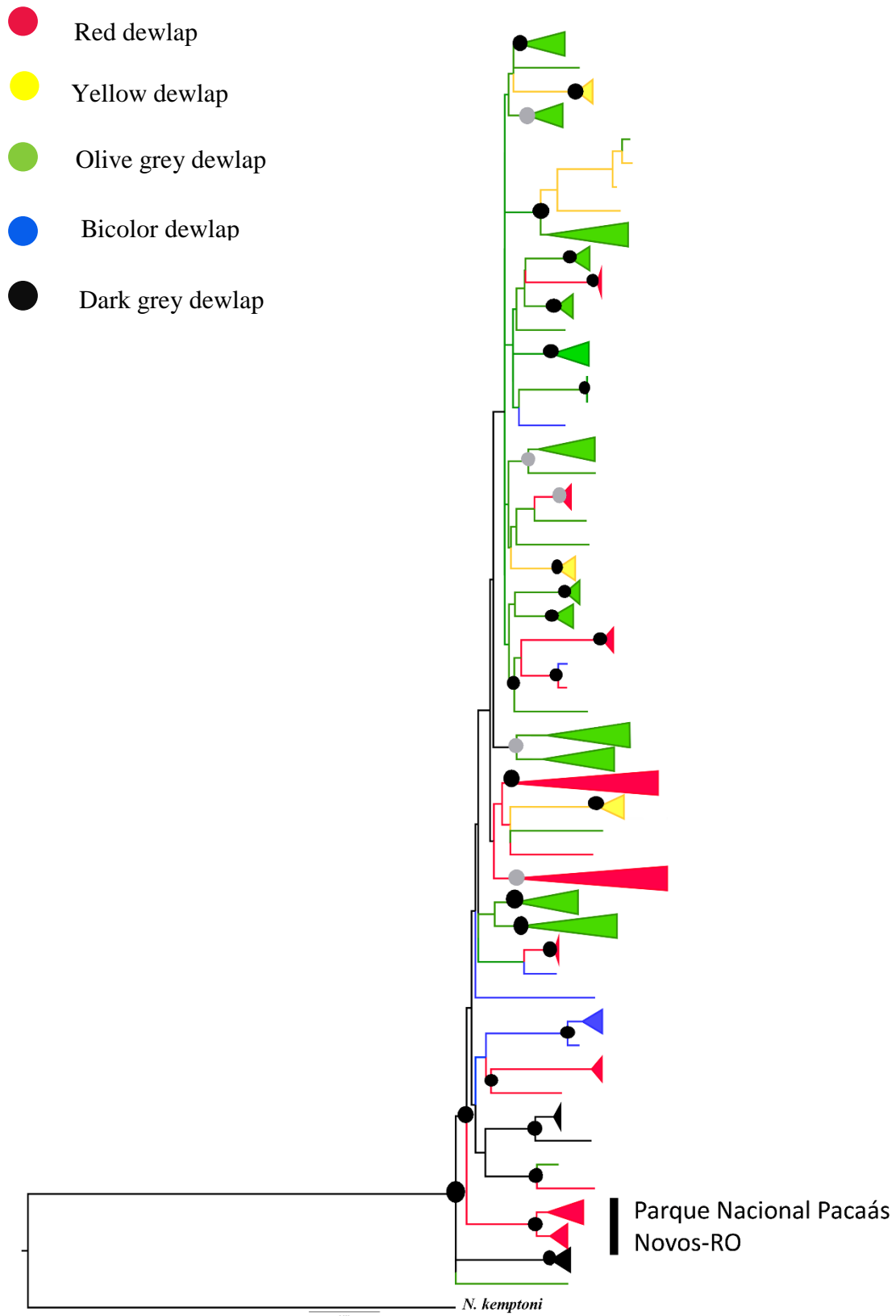
Figure 4.2: Maximun likelihood inference generated for the concatenated dataset, including one mtDNA and four nDNA, for sequences of specimens of *N. fuscoauratus* with dewlap color information. Black circles represent bootstrap values 90%-100% and

grey circles represent bootstrap values 80% - 89%. Colored clades correspond to dewlap color as pointed in the figure legend.

Uncorrected pairwise distances for ND2 gene among dewlap color morphs ranged from 0.3% between "Olive grey" and "Yellow", and "Olive grey" and "Red", to 1.3% between "Yellow" and "Dark grey" (Table 1). *Fst* values computed for pairwise comparisons also revealed low genetic differentiation (Table 2). AMOVA indicated a proportion of genetic variation among the different dewlap color morphs of 12.6% ($p<0.001$), with 87.4% of the variance attributable to within dewlap morph variation.

Table 1: Net between group distances for ND2 among the different dewlap color morphs. Distances above the diagonal are uncorrected p-distances. Distances below the diagonal were maximum likelihood-corrected using the TN93 model.

	Olive grey	Yellow	Red	Dark grey	Bicolor
Olive grey	—	0.003	0.003	0.011	0.008
Yellow	0.003	—	0.006	0.013	0.011
Red	0.003	0.006	—	0.009	0.008
Dark grey	0.012	0.014	0.01	—	0.012
Bicolor	0.009	0.012	0.008	0.012	—

Table 2. Analysis of Molecular Variance (AMOVA) performed with the different dewlap color morphs of *N. fuscoauratus* showing the genetic variation among and within groups.

ND2 ($Fst = 0.12641$; $P=0.00$)		
	Among clusters	Within clusters
df	4	145
Var. comp.	0.95552 Va	6.60308Vb
% variation	12.64%	87.36%
Fst **values**		
Olive grey	0.1280	
Red	0.1167	
Yellow	0.1336	
Bicolor	0.1392	
Dark grey	0.1394	

df =degree of freedom*; Var.comp.*= variance components.

Haplotype networks constructed for nDNA indicate that different dewlap color morphs share the same haplotypes (Figure 2b–f). However, ND2 had a high number of unique haplotypes (104 of 147 sequences analyzed), with only two haplotypes being shared between different localities: Pacoti-CE and Serra de Maraguape-CE (both localities with olive grey dewlap); Santa Isabel do Rio Negro-AM-Brazil (olive grey dewlap) and La Escalera-Venezuela (red dewlap).

3.3 Morphological variation in *Norops fuscoauratus*

Descriptive statistics of all morphological traits analyzed is presented in Table 3. The results of one-way ANOVA indicate a statistically significant difference between males and females in relation to SVL ($F_{(1,261)}$=14.381, p<0.001). A Tukey post-hoc test revealed that females are, on average, 1.38 mm larger than males (p<0.001). The one-way MANCOVA showed that even controlling for the effect of size, females have statistically significant longer foot and snout, wider head, and greater distance between nostrils than males. In relation to the PCA performed with individuals with dewlap color information, the "GCV" method selected the first two axis to interpret the PCA results and we

considered loading values >0.5 as significant. The two primary axes account for 21.43% of the morphological variation detected, with loreals and scales between supraorbital semicircles contributing negatively to the first axis variation and canthals contributing positively, while fourth finger length and lamellae of finger IV contributed positively to the second axis variation (Table 4). The *dimdesc* function did not identify any influence of dewlap color on the two-selected axis of PCA, suggesting that the groups of individuals with different dewlap color are not significantly different from the group as a whole.

Table 3. Morphometric and meristic traits studied in *N. fuscoauratus* specimens and MANCOVA results. In bold morphometric traits statistically significant for sexual dimorphism, even when controlling for the effect of size.

Mophological traits	Male (N = 136)			Female (N = 127)			Sex Effect (One-Way Mancova)	
							F	p
Max. SVL	49,87			54,02			-	-
Head W	6.355	±	0.373	6.698	±	0.462	**27.740**	**< 0.001**
Head H	5.033	±	0.433	5.206	±	0.447	1.845	0.176
Orbit D	4.522	±	0.395	4.617	±	0.314	0.140	0.709
Ear Dm	1.176	±	0.163	1.186	±	0.153	0.068	0.795
Nostrils D	1.439	±	0.181	1.550	±	0.192	**13.343**	**< 0.001**
Mouth–Ear D	1.622	±	0.252	1.634	±	0.288	0.006	0.940
Snout L	4.401	±	0.410	4.686	±	0.448	**15.985**	**< 0.001**
Itpar L	1.386	±	0.208	1.439	±	0.199	1.741	0.188
Hand L	6.348	±	0.465	6.473	±	0.603	0.021	0.885
Finger IV L	5.032	±	0.491	5.146	±	0.494	0.120	0.729
Tibia L	11.669	±	0.660	11.912	±	0.777	0.142	0.707
Foot L	13.519	±	0.899	14.079	±	0.828	**11.565**	**0.001**
Toe IV L	8.430	±	0.816	8.637	±	0.708	0.546	0.461
Ptrostrals	5.0	-	8.0	5.0	-	8.0	-	-
Splabials	8.0	-	12.0	8.0	-	13.0	-	-
Iflabials	8.0	-	12.0	8.0	-	12.0	-	-
Loreals	5.0	-	8.0	5.0	-	8.0	-	-

Canthals	4.0	-	8.0	5.0	-	8.0	-	-
Bet2°Cant	6.0	-	13.0	7.0	-	16.0	-	-
BetSporb	0.0	-	3.0	0.0	-	3.0	-	-
Itpar–Sporb	1.0	-	3.0	1.0	-	3.0	-	-
Ptmentals	5.0	-	8.0	4.0	-	8.0	-	-
LamFingIV	14.0	-	19.0	14.0	-	18.0	-	-
LamToeIV	22.0	-	30.0	24.0	-	30.0	-	-

Abbreviations: Abreviations: Bet2°Cant=scales between second canthals; BetSporb=scales between supraorbital semicircles; D= distance; Dm=diameter; Itpar=interparietal; H=height; Iflabials=infralabials; Itpar–Sporb=scales between interparietal and supraorbital semicircles; L=length; LamFingIV=lamellae under fourth finger; LamToeIV=lamellae under fourth toe; max. SVL=maximun snout–vent length; Ptmentals=postmentals; Ptrostrals=postrostrals; Sboculars=suboculars; Splabials= supralabials; W=width).

Table 4: Results of Principal Component Analysis with continuous and meristic traits collected for specimens of *N. fuscoauratus* with dewlap color information (n=109). Numbers in bold represent loading values >0.5. For abbreviations, see Table 3.

Morphometric traits	Axis 1	Axis 2
Tibia L	-0.280	0.190
Head W	-0.066	-0.458
Head H	0.218	-0.427
Orbit D	-0.094	-0.31
Ear Dm	0.178	-0.191
Nostrils D	0.306	-0.251
Snout L	0.402	-0.427
Itpar L	0.132	0.079
Finger IV L	0.417	**0.509**
Toe IV L	0.309	0.143
Hand L	0.122	0.329
Foot L	0.196	0.248
Meristic traits	**Axis 1**	**Axis 2**

Splabials	0.178	0.473
Iflabials	0.417	0.406
Loreals	**-0.507**	0.19
Canthals	**0.715**	0.035
Bet2ºCant	-0.465	-0.005
BetSorb	**-0.607**	-0.191
Itpar–Sporb	-0.471	0.162
Ptrostrals	0.03	0.475
Ptmentals	0.01	0.104
LamFingIV	-0.123	**0.511**
LamToeIV	-0.381	0.425
Eigenvalues	2.708	2.436
Variance explained (%)	11.28	10.15
Cumulative variance (%)	11.28	21.43

Hemipenial morphology of *N. fuscoauratus* is overall very conservative, with minimal differences that can be attributed as the result of the eversion and preparation processes. Different dewlap color morphs did not present divergent hemipenial morphology.

3.4 Environmental data

The PCA analysis performed with Bioclim variables indicate three primary axis of variation accounting for 80.5% of bioclimatic variation found. The first axis explained 37.4% of this variation with Annual Precipitation, Isothermality, Mean Temperature of Warmest Quarter, Precipitation of Wettest Quarter and Precipitation of Coldest Quarter accounting positively for most variation. The second axis was responsible for 23.3% of the variation observed, with the variable Precipitation Seasonality (Coefficient of Variation) influencing positively and the variables Precipitation of Warmest Quarter and Precipitation of Driest Quarter accounting negatively for most variation. The third axis explained 19.7% of the variation observed and Maximun Temperature of Warmest Month was the most important variable (Table 5).

The *dimdesc* function results showed that the dewlap color groups were significantly linked to the first (R^2=0.117, p<0.01) and third (R^2=0.080, p=0.01) axis, but showing a weak relationship. The color pattern "olive grey" was positively related (estimate=0.822, p=0.00) while "Red" was negatively related (estimate=-0.738, p=0.00) to the first axis. The third axis was positively linked to "Bicolor" (estimate=0.608, p=0.04) pattern and negatively linked to "olive grey" (estimate=-0.755, p=0.00) pattern. The results of *dimdesc* function for quantitative variables with correlations >0.7 in axis 1 and 3 are summarized in Table 6.

Table 5: Results of principal components analysis performed with Bioclim variables using the dewlap color morphs as categorical variable. Number is bold represent values of loadings >0.7.

Bioclim variables	Axis 1	Axis 2	Axis 3
Mean Diurnal Range	-0.411	0.202	0.664
Isothermality	**0.758**	-0.098	-0.299
Temperature Seasonality	-0.648	-0.056	0.014
Maximun Temperature of Warmest Month	0.411	0.480	**0.755**
Mean Temperature of Wettest Quarter	0.697	0.207	0.625
Mean Temperature of Warmest Quarter	**0.720**	0.327	0.509
Annual Precipitation	**0.835**	-0.302	-0.085
Precipitation Seasonality	-0.277	**0.879**	-0.261
Precipitation of Wettest Quarter	**0.740**	0.302	-0.343
Precipitation of Driest Quarter	0.53	**-0.806**	-0.002
Precipitation of Warmest Quarter	-0.026	**-0.822**	0.462
Precipitation of Coldest Quarter	**0.743**	0.298	-0.457
Eigenvalues	4.492	2.803	2.366
Variance explained (%)	37.436	23.356	19.719
Cumulative variance (%)	37.436	60.792	80.511

Table 6. Quantitative variables with correlations values >0.7 as results of the function *dimdesc* of principal components analysis performed with Bioclim variables using the dewlap color morphs as categorical variable.

Axis 1	
Bioclim variables	**Correlation**
Annual Precipitation	**0.8354694**
Isothermality	0.758191
Precipitation of Coldest Quarter	0.7425281
Precipitation of Wettest Quarter	0.7399593
Mean Temperature of Warmest Quarter	0.7201104
Axis 3	
Precipitation Seasonality	**0.8788178**
Precipitation of Driest Quarter	-0.8061925
Precipitation of Warmest Quarter	-0.8219269

4. DISCUSSION

Dewlap colors in *Norops fuscoauratus* do not seem to correspond to geographically, genetically or morphologically delimited groups. Hemipenial morphology, that if modified might represent a mechanical pre-mating barrier for reproduction, did not differ between groups of individuals with different dewlap colors. These data indicate that variation of dewlap color in *N. fuscoauratus* does not represent cryptic species, and apparently not even a beginning of a process of divergence that could lead to speciation. This is in agreement with the findings of Glor et al. (2001) and with the previous study about population structure and diversification of *N. fuscoauratus*, which reports low genetic differentiation for the species as a whole.

Most likely, variation in dewlap color seems to respond to external factors. A similar case of dewlap variation in color not linked to genetic differentiation was reported in *Norops apletophalus,* where spectrophotometry and microsatellite markers were used to measure gene flow in different dewlap morphs and different populations of the species (Stapley et al. 2011). Likewise, a study on *Norops roquet* found that variation in dewlap color did

not necessarily correspond to the genetic structure found, with this variation being related to a certain type of habitat (Thorpe & Stenson 2003). Some studies reported that different vegetational structure influences the habitat light that underlie some of the color variation observed in dewlaps (Fleishman, 1992, Leal & Fleishman, 2004; Fleishman et al. 2009). In this case, the dewlap color variation may be an adaptive response to variation in signaling environments in order to increase detectability (Leal & Fleishman 2002, Leal & Fleishman, 2004; Ng & Glor 2011; Ng et al. 2013).

We found significant association of climatic variation with different dewlap colors in *N. fuscoauratus*, with Annual Precipitation and Precipitation Seasonality being most important in explaining the bioclimatic variation among sampled localities. Dispite the significance, this association was weak as illustrated by the low coefficient of determination (R^2). This suggests that dewlap color variation found in *N. fuscoauratus* is rather a polymorphism maintained within a single and widespread panmictic population, than a reflection of independent evolutionary units.

ACKNOWLEDGEMENTS

REFERENCES

Avila-Pires, T. D. (1995). Lizards of Brazilian Amazonia (Reptilia: Squamata). *Zoologische Verhandelingen*, *299*, 1-706.

Bandelt, H. J.; Forster, P. & Rohl, A. (1999). Median-joining networks for inferring intraspecific phylogenies. *Molecular Biology and Evolution*. 16: 37-48.

Camargo, A., De Sa, R. O., & Heyer, W. R. (2006). Phylogenetic analyses of mtDNA sequences reveal three cryptic lineages in the widespread neotropical frog *Leptodactylus fuscus* (Schneider, 1799) (Anura, Leptodactylidae). *Biological Journal of the Linnean Society*, *87*(2), 325-341.

D'Angiolella, A.B., Gamble, T., Avila-Pires, T.C., Colli, G.R., Noonan, B.P., & Vitt, L.J. (2011). *Anolis chrysolepis* Duméril and Bibron, 1837 (Squamata: Iguanidae), revisited: molecular phylogeny and taxonomy of the *Anolis chrysolepis* species group. *Bulletin of the Museum of Comparative Zoology*, *160*(2), 35-63

Excoffier, L., Smouse, P. E., & Quattro, J. M. (1992). Analysis of molecular variance inferred from metric distances among DNA haplotypes: application to human mitochondrial DNA restriction data. *Genetics*, *131*(2), 479-491.

Fitch, H. S., & Hillis, D. M. (1984). The *Anolis* dewlap: interspecific variability and morphological associations with habitat. *Copeia*, *1984*(2), 315-323.

Fleishman, L. J. (1992). The influence of the sensory system and the environment on motion patterns in the visual displays of anoline lizards and other vertebrates. *American Naturalist*, S36-S61.

Fleishman, L. J., Leal, M., & Persons, M. H. (2009). Habitat light and dewlap color diversity in four species of Puerto Rican anoline lizards. *Journal of Comparative Physiology A*, *195*(11), 1043-1060.

Gartner, G. E., Gamble, T., Jaffe, A. L., Harrison, A., & Losos, J. B. (2013). Left–right dewlap asymmetry and phylogeography of *Anolis lineatus* on Aruba and Curaçao. *Biological Journal of the Linnean Society*, *110*(2), 409-426.

Glor, R. E., Vitt, L. J., & Larson, A. (2001). A molecular phylogenetic analysis of diversification in Amazonian *Anolis* lizards. *Molecular Ecology*, *10*(11), 2661-2668.

Hijmans, R. J., Cameron, S. E., Parra, J. L., Jones, P. G., & Jarvis, A. (2005). Very high resolution interpolated climate surfaces for global land areas. *International journal of climatology*, *25*(15), 1965-1978.

Keogh S. (1999). Evolutionary implications of hemipenial morphology in the terrestrial Australian elapid snakes. *Zoological Journal of the Linnean Society, 125*: 239–278.

Kumar, S., Nei, M., Dudley, J., & Tamura, K. (2008). MEGA: a biologist-centric software for evolutionary analysis of DNA and protein sequences. *Briefings in bioinformatics*, *9*(4), 299-306.

Lanfear, R., Calcott, B., Ho, S. Y., & Guindon, S. (2012). PartitionFinder: combined selection of partitioning schemes and substitution models for phylogenetic analyses. *Molecular biology and evolution*, *29*(6), 1695-1701.

Lê, S., Josse, J., & Husson, F. (2008). FactoMineR: an R package for multivariate analysis. *Journal of statistical software*, *25*(1), 1-18.

Leal, M., & Fleishman, L. J. (2002). Evidence for habitat partitioning based on adaptation to environmental light in a pair of sympatric lizard species. *Proceedings of the Royal Society of London B: Biological Sciences*, *269*(1489), 351-359.

Leal, M., & Fleishman, L. J. (2004). Differences in visual signal design and detectability between allopatric populations of *Anolis* lizards. *The American Naturalist*, *163*(1), 26-39.

Librado, P., & Rozas, J. (2009). DnaSP v5: a software for comprehensive analysis of DNA polymorphism data. *Bioinformatics*, *25*(11), 1451-1452.

Losos, J. B., & Chu, L. R. (1998). Examination of factors potentially affecting dewlap size in Caribbean anoles. *Copeia*, 430-438.

Losos J.B. & Schneider C.J. (2009). *Anolis* lizards. *Current Biology.* 19:316–318.

Losos, J. B. (2009). *Lizards in an evolutionary tree: ecology and adaptive radiation of anoles* (Vol. 10). Univ of California Press.

Macedonia, J. M., James, S., Wittle, L. W., & Clark, D. L. (2000). Skin pigments and coloration in the Jamaican radiation of *Anolis* lizards. *Journal of Herpetology*, 99-109.

Macedonia, J. M. (2001). Habitat light, colour variation, and ultraviolet reflectance in the Grand Cayman anole, *Anolis conspersus*. *Biological Journal of the Linnean Society*, *73*(3), 299-320.

Macedonia, J. M., Clark, D. L., & Tamasi, A. L. (2014). Does Selection Favor Dewlap Colors that Maximize Detectability? A Test with Five Species of Jamaican *Anolis* Lizards. *Herpetologica*, *70*(2), 157-170.

Miller, M. A., Pfeiffer, W., & Schwartz, T. (2010, November). Creating the CIPRES Science Gateway for inference of large phylogenetic trees. In *Gateway Computing Environments Workshop (GCE), 2010* (pp. 1-8). IEEE

Ng, J., & Glor, R. E. (2011). Genetic differentiation among populations of a Hispaniolan trunk anole that exhibit geographical variation in dewlap colour. *Molecular ecology*, *20*(20), 4302-4317.

Ng, J., Landeen, E. L., Logsdon, R. M., & Glor, R. E. (2013). Correlation between *Anolis* lizard dewlap phenotype and environmental variation indicates adaptive divergence of a signal important to sexual selection and species recognition. *Evolution*, *67*(2), 573-582

Nicholson, K. E., Glor, R. E., Kolbe, J. J., Larson, A., Blair Hedges, S., & Losos, J. B. (2005). Mainland colonization by island lizards. *Journal of Biogeography*, *32*(6), 929-938.

Nicholson, K. E., Harmon, L. J., & Losos, J. B. (2007). Evolution of *Anolis* lizard dewlap diversity. *PLoS One*, *2*(3), e274

Nicholson, K. E., Crother, B. I., Guyer, C., & Savage, J. M. (2012). It is time for a new classification of anoles (Squamata: Dactyloidae). *Zootaxa*, *3477*, 1-108.

Nei, M., & Li, W. H. (1979). Mathematical model for studying genetic variation in terms of restriction endonucleases. *Proceedings of the National Academy of Sciences*, *76*(10), 5269-5273.

Nunes, P.M.S., Fouquet, A., Curcio, F. F., Kok P., & Rodrigues, M.T. (2012). Cryptic species in *Iphisa elegans* Gray, 1851 (Squamata: Gymnophthalmidae) revealed by hemipenial morphology and molecular data. *Zoological Journal of the Linnean Society, 166*(2), 361-376.

Ord, T. J., Stamps, J. A., & Losos, J. B. (2010). Adaptation and plasticity of animal communication in fluctuating environments. *Evolution*, *64*(11), 3134-3148.

Ord, T. J., Charles, G. K., & Hofer, R. K. (2011). The evolution of alternative adaptive strategies for effective communication in noisy environments. *The American Naturalist*, *177*(1), 54-64.

Pesantes O.S. 1994. A method for preparing the hemipenis of preserved snakes. *Journal of Herpetology 28*:93–95.

Rissler, L. J., & Apodaca, J. J. (2007). Adding more ecology into species delimitation: ecological niche models and phylogeography help define cryptic species in the black salamander (*Aneides flavipunctatus*). *Systematic Biology*, *56*(6), 924-942.

Rodríguez-Robles, J. A., Jezkova, T., & García, M. A. (2007). Evolutionary relationships and historical biogeography of Anolis desechensis and Anolis monensis, two lizards endemic to small islands in the eastern Caribbean Sea. *Journal of Biogeography*, *34*(9), 1546-1558.

Ronquist, F., & Huelsenbeck, J. P. (2003). MrBayes 3: Bayesian phylogenetic inference under mixed models. *Bioinformatics*, *19*(12), 1572-1574.

Scheet, P., & Stephens, M. (2006). A fast and flexible statistical model for large-scale population genotype data: applications to inferring missing genotypes and haplotypic phase. *The American Journal of Human Genetics*, *78*(4), 629-644.

Sousa, P. A. G., & Freire, E. M. X. (2010). Reptilia, Squamata, Polychrotidae, *Anolis fuscoauratus* DOrbigny, 1837: Distribution extension for the state of Rio Grande do Norte, Brazil. *Check List*, *6*(4).

SPSS Inc. Released (2008). SPSS Statistics for Windows, Version 17.0. Chicago: SPSS Inc.

Stamatakis, A. (2006). RAxML-VI-HPC: maximum likelihood-based phylogenetic analyses with thousands of taxa and mixed models. *Bioinformatics*, *22*(21), 2688-2690.

Stapley, J., Wordley, C., & Slate, J. (2011). No evidence of genetic differentiation between anoles with different dewlap color patterns. *Journal of Heredity*, *102*(1), 118-124.

Thorpe, R. S. & Stenson, A. G. (2003). Phylogeny, paraphyly and ecological adaptation of the colour and pattern in the *Anolis roquet* complex on Martinique. *Molecular Ecology*, *12*(1), 117-132.

Townsend, T.M., Mulcahy, D.G., Noonan, B.P., Sites Jr., J.W., Kuczynski, C.A., Wiens, J.J., Reeder, T.W., (2011). Phylogeny of iguanian lizards inferred from 29 nuclear loci, and a comparison of concatenated and species-tree approaches for an ancient, rapid radiation. *Molecular phylogenetics and evolution*. 61, 363–380.

Vaidya, G., Lohman, D. J., & Meier, R. (2011). SequenceMatrix: concatenation software for the fast assembly of multi-gene datasets with character set and codon information. *Cladistics*, *27*(2), 171-180.

Vanhooydonck B, Herrel A, Meyers JJ & Irschick DJ. (2009).What determines dewlap diversity in *Anolis* lizards? An among-island comparison. *Journal of Evolutionary Biology* 22:293–305.

Vitt, L. J., Avila-Pires, T. C. S., Zani, P. A., Sartorius, S. S., & Espósito, M. C. (2003). Life above ground: ecology of *Anolis fuscoauratus* in the Amazon rain forest, and comparisons with its nearest relatives. *Canadian Journal of Zoology*, *81*(1), 142-156.

Wright, S. (1965). The interpretation of population structure by F-statistics with special regard to systems of mating. *Evolution*, 395-420.

Zaher, H., & Prudente, A.L.C. (2003). Hemipenes of *Siphlophis* (Serpentes, Xenodontinae) and techniques of hemipenial preparation in snakes: a response to Dowling. *Herpetological Review*, *34*(4), 302-306.

APPENDIX

Table 1: Tissue samples, locality, geographic coordinates and dewlap color from *Norops fuscoauratus* individuals analyzed.

Sample ID	lat	long	Dewlap	Locality	Country	Genbank
BON03	-1.36	-47.32	grey	Bonito, PA	BRAZIL	
BON04	-1.36	-47.32	grey	Bonito, PA	BRAZIL	
BON06	-1.36	-47.32	grey	Bonito, PA	BRAZIL	
BON07	-1.36	-47.32	grey	Bonito, PA	BRAZIL	
BON12	-1.36	-47.32	grey	Bonito, PA	BRAZIL	
BP01	-2.29	-48.70	grey	Agropalma, Tailandia	BRAZIL	
BP02	-3.55	-48.50	grey	Bacia Rio Capim, Paragominas, PA	BRAZIL	
BP05	-3.71	-48.56	grey	Bacia Rio Capim, Paragominas, PA	BRAZIL	
CAX166	-1.74	-51.45	grey	Floresta Nacional de Caxiuana, Portel, PA	BRAZIL	
CAX167	-1.74	-51.45	grey	Floresta Nacional de Caxiuana, Portel, PA	BRAZIL	
CAX181	-1.74	-51.45	grey	Floresta Nacional de Caxiuana, Portel, PA	BRAZIL	
CN0571	-1.74	-51.45	grey	Esec Grão Pará Sul, Alenquer	BRAZIL	
CN0842	-0.17	-58.19	grey	Esec Grão Pará Sul, Alenquer	BRAZIL	
CN2021	-0.94	-53.24	yellow	Flota Paru, Almerim, PA	BRAZIL	

H3210	-9.70	-65.36	red	UHE Jirau, Abunã, RO	BRAZIL
HERP5943	-3.09	-55.52	grey	Tucumatuba, Tapajós, PA	BRAZIL
HERP5944	-3.09	-55.52	grey	Tucumatuba, Tapajós, PA	BRAZIL
HERP5949	-3.09	-55.52	grey	Tucumatuba, Tapajós, PA	BRAZIL
HJ0066	-9.27	-64.64	red	Porto Velho, Jirau, RO	BRAZIL
HJ0466	-9.70	-65.36	red	UHE Jirau, Abunã, RO	BRAZIL
HJ0479	-9.70	-65.36	red	UHE Jirau, Abunã, RO	BRAZIL
IRSNB17832	5.20	-59.45	red	Kaieteur National Park, Potaro-Siparuni District, Guyana	GUYANA
IRSNB17851	5.13	-59.42	red	Kaieteur National Park, Potaro-Siparuni District, Guyana	GUYANA
JFT726	-19.93	-40.61	yellow	Santa Teresa, ES	BRAZIL
JOG541	-6.31	-55.78	red	Mina do Palito, Itaituba PA	BRAZIL
JOG555	-6.31	-5578	red	Mina do Palito, Itaituba PA	BRAZIL
LSUMZH12538	0.01	-75.97	red	Ecuador: Sucumbio Province, Reserva Faunistica Cuyabeno (RPF-Cuyabeno), Neotropic Turis	ECUADOR
LSUMZH12545	0.01	-75.97	red	Ecuador: Sucumbio Province, Reserva Faunistica Cuyabeno (RPF-Cuyabeno), Neotropic Turis	ECUADOR

LSUMZH15471	-10.80	-65.31	grey	Nova Mamoré: RO Guajará Mirim	BRAZIL
MAR0536	-1.96	-51.67	grey	Plot PPBIO Caxiuanã, PA	BRAZIL
MAR0762	-1.96	-51.67	grey	Plot PPBIO Caxiuanã, PA	BRAZIL
MAR1342	-1.96	-51.67	grey	Plot PPBIO Caxiuanã, PA	BRAZIL
MAR1477	-0.31	-50.53	grey	Afua, Rio Preto, Ilha do Marajo, PA	BRAZIL
MAR1523	-0.31	-50.53	grey	Afua, Rio Preto, Ilha do Marajo, PA	BRAZIL
MAR1528	-0.31	-50.53	grey	Afua, Rio Preto, Ilha do Marajo, PA	BRAZIL
MAR1533	-0.31	-50.53	grey	Afua, Rio Preto, Ilha do Marajo, PA	BRAZIL
MAR1554	-0.31	-50.53	grey	Afua, Rio Preto, Ilha do Marajo, PA	BRAZIL
MAR1569	-0.31	-50.53	grey	Afua, Rio Preto, Ilha do Marajo, PA	BRAZIL
MAR1587	-0.31	-50.53	grey	Afua, Rio Preto, Ilha do Marajo, PA	BRAZIL
MAR1846	-0.31	-50.53	grey	Afua, Rio Preto, Ilha do Marajo, PA	BRAZIL
MBS11	-8.85	-73.02	grey	Parna Serra do Divisor, AC	BRAZIL
MBS14	-8.85	-73.02	grey	Parna Serra do Divisor, AC	BRAZIL
MBS17	-8.85	-73.02	grey	Parna Serra do Divisor, AC	BRAZIL

MBS19	-8.85	-73.02	grey	Parna Serra do Divisor, AC	BRAZIL
MBS34	-8.85	-73.02	grey	Parna Serra do Divisor, AC	BRAZIL
MBS46	-8.85	-73.02	grey	Parna Serra do Divisor, AC	BRAZIL
MJS015	-0.59	-52.74	yellow	Monte Dourado, Almerim, Estação, PA	BRAZIL
MJS053	-0.59	-52.74	yellow	Monte Dourado, Almerim, Estação, PA	BRAZIL
MJS059	-0.59	-52.74	yellow	Monte Dourado, Almerim, Estação, PA	BRAZIL
MJS108	-4.72	-56.38	dark grey	Comunidade Aldeia Nova, Antiga Boa Fé, Rio Tapajós, PA	BRAZIL
MJS113	-4.70	-56.38	dark grey	Expedição Tapajós-Arapiuns, PA	BRAZIL
MNCN26614	-3.27	-72.27	grey	Umarital, Río Ampiyacu, Loreto, Peru	PERU
MNCN26649	-3.06	-72.17	grey	Confluencia de los Ríos Supai y Sábalo, Loreto, Peru	PERU
MNCN26691	-3.06	-72.17	grey	Confluencia de los Ríos Supai y Sábalo, Loreto, Peru	PERU
MNCN26692	-3.06	-72.17	grey	Confluencia de los Ríos Supai y Sábalo, Loreto, Peru	PERU
MNCN46629	-4.12	-69.95	red	Leticia. Kilómetro 11 Tanimboca, carretera junto a la reserva, Amazonas, Colombia.	COLOMBIA

MNCN46829	-4.12	-69.95	red	Leticia. Kilómetro 13, Amazonas, Colombia.	COLOMBIA
MNCN48978	-4.12	-69.95	red	Leticia. Varzea del arroyo Huallar ka ka junto a Tanimboca, Amazonas, Colombia.	COLOMBIA
MPEG11032	-2.80	-52.58	grey	Resex Tapajós Arapiuns, Nova Canaã, PA	BRAZIL
MPEG24580	-3.27	-50.32	grey	Faz. Riacho Monte Verde, Precious Woods, Portel, PA	BRAZIL
MPEG24583	-3.27	-50.32	grey	Faz. Riacho Monte Verde, Precious Woods, Portel, PA	BRAZIL
MPEG24589	-3.27	-50.32	grey	Faz. Riacho Monte Verde, Precious Woods, Portel, PA	BRAZIL
MPEG24590	-3.27	-50.32	grey	Faz. Riacho Monte Verde, Precious Woods, Portel, PA	BRAZIL
MPEG26929	-4.90	-65.19	Bicolor	Coari, Porto Urucu, AM	BRAZIL
MPEG26946	-4.90	-65.19	Bicolor	Coari, Porto Urucu, AM	BRAZIL
MPEG27693	-4.90	-65.19	Bicolor	Porto Urucu, AM	BRAZIL
MSH07851	-0.59	-52.74	grey	Estação Sul, área Jari 112, Almerim, PA	BRAZIL
MSH10714	-3.17	-55.74	grey	Nova Canaã, Santarém, PA	BRAZIL
MSH10730	-3.16	-55.83	grey	Nova Canaã, Santarém, PA	BRAZIL
MSH11539	-2.01	-51.50	grey	Floresta Nacional de Caxiuana, Portel, PA	BRAZIL

MSH11570	-1.80	-51.44	grey	Floresta Nacional de Caxiuana, Portel, PA	BRAZIL
MSH12233	0.05	-64.76	grey	Santa Isabel do Rio Negro, AM	BRAZIL
MTR00152	-4.23	-38.92	grey	Pacoti, CE	BRAZIL
MTR04528	-4.23	-38.92	grey	Pacoti, CE	BRAZIL
MTR04531	-4.23	-38.92	grey	Pacoti, CE	BRAZIL
MTR06037	-4.23	-38.92	grey	Pacoti, CE	BRAZIL
MTR06262	-0.02	-51.90	grey	Igarapé Camaipi, AP	BRAZIL
MTR06329	-0.02	-51.90	grey	Igarapé Camaipi, AP	BRAZIL
MTR12159	-19.15	-40.06	yellow	Linhares, ES	BRAZIL
MTR12298	-19.15	-40.07	yellow	Linhares, ES	BRAZIL
MTR18621	-5.83	-64.31	yellow	Rio Purus, AM	BRAZIL
MTR18622	-5.83	-64.31	yellow	Rio Purus, AM	BRAZIL
MTR18636	-5.83	-64.31	yellow	Rio Purus, AM	BRAZIL
MTR19048	-5.83	-64.31	yellow	Rio Purus, AM	BRAZIL
MTR19062	-5.83	-64.31	yellow	Rio Purus, AM	BRAZIL
MTR19066	-5.83	-64.31	yellow	Rio Purus, AM	BRAZIL
MTR20738	4.38	-61.20	red	Pacaraima, RR	BRAZIL
MTR20773	4.38	-61.20	red	Pacaraima, RR	BRAZIL
MTR20797	4.38	-61.20	red	Pacaraima, RR	BRAZIL

MTR25524	-10.77	-63.62	red	P. N. Pacaás Novos, Base Candeias	BRAZIL
MTR25537	-10.77	-63.62	red	P. N. Pacaás Novos, Base Candeias	BRAZIL
MTR25538	-10.77	-63.62	red	P. N. Pacaás Novos, Base Candeias	BRAZIL
MTR25597	-10.79	-63.63	red	P. N. Pacaás Novos, Base Candeias	BRAZIL
MTR25668	-10.79	-63.63	red	P. N. Pacaás Novos, Base Candeias	BRAZIL
MTR25978	-10.53	-63.97	red	P. N. Pacaás Novos, Base do Jaci	BRAZIL
MTR25984	-10.53	-63.97	red	P. N. Pacaás Novos, Base do Jaci	BRAZIL
MTR25985	-10.53	-63.97	red	P. N. Pacaás Novos, Base do Jaci	BRAZIL
MTR26007	-10.53	-63.97	red	P. N. Pacaás Novos, Base do Jaci	BRAZIL
MTR28056	-7.44	-73.66	grey	Serra do Divisor, Pe da Serra, AC	BRAZIL
MTR28194	-7.45	-73.66	grey	Serra do Divisor, Pe da Serra, AC	BRAZIL
MTR28201	-7.43	-73.66	grey	Serra do Divisor, Pe da Serra, AC	BRAZIL
MTR28206	-7.45	-73.66	grey	Serra do Divisor, Pe da Serra, AC	BRAZIL

MTR28368	-7.50	-73.72	grey	Serra do Divisor, Pe da Serra, AC	BRAZIL
MTR28392	-7.50	-73.71	grey	Serra do Divisor, Pe da Serra, AC	BRAZIL
MTR28393	-7.50	-73.71	grey	Serra do Divisor, Pe da Serra, AC	BRAZIL
MTR28413	-7.50	-73.71	grey	Serra do Divisor, Pe da Serra, AC	BRAZIL
MTR28414	-7.50	-73.71	grey	Serra do Divisor, Pe da Serra, AC	BRAZIL
MTR28534	-9.00	-67.18	Bicolor	Boca do Acre, ramal bode preto	BRAZIL
MTR28535	-9.01	-67.18	Bicolor	Boca do Acre, ramal bode preto	BRAZIL
MTR28538	-9.00	-67.18	Bicolor	Boca do Acre, ramal bode preto	BRAZIL
MTR28563	-8.76	-67.31	Bicolor	Boca do Acre, ramal Cruzeirinho	BRAZIL
MTR28564	-8.76	-67.31	Bicolor	Boca do Acre, ramal Cruzeirinho	BRAZIL
MTR28565	-8.76	-67.31	Bicolor	Boca do Acre, ramal Cruzeirinho	BRAZIL
MTR28576	-10.08	-67.63	red	Fazenda Experimental Catuaba, AC	BRAZIL
MTR28577	-10.08	-67.63	red	Fazenda Experimental Catuaba, AC	BRAZIL
MTR28578	-10.08	-67.63	red	Fazenda Experimental Catuaba, AC	BRAZIL

MTR28579	-10.08	-67.63	red	Fazenda Experimental Catuaba, AC	BRAZIL
MTR28680	-7.62	-62.88	red	FLONA Humaita, Igarape Buiussu	BRAZIL
PEU014	-13.58	-39.71	grey	Wenceslau Guimarães, BA	BRAZIL
PK2255	5.95	-61.38	red	La Escalera, Bolivar State	VENEZUELA
PMRT555	-3.92	-55.59	red	Aveiro, Brasil Legal, PA Ponto 1	BRAZIL
PMRT556	-3.91	-55.53	dark grey	Aveiro, Brasil Legal, PA Ponto 2	BRAZIL
PMRT609	-3.92	-55.59	red	Aveiro, Brasil Legal, PA, Ponto 1	BRAZIL
PMRT642	-3.92	-55.59	red	Aveiro, Brasil Legal, PA Ponto 1	BRAZIL
PMRT656	-3.91	-55.53	dark grey	Aveiro, Brasil Legal, PA Ponto 2	BRAZIL
PMRT701	-4.01	-55.58	dark grey	Aveiro, Brasil Legal, PA Ponto 4	BRAZIL
PMRT727	-3.97	-55.62	red	Aveiro, Brasil Legal, PA Ponto 3	BRAZIL
PMRT775	-3.97	-55.62	red	Aveiro, Brasil Legal, PA Ponto 4	BRAZIL
PMRT780	-4.01	-55.58	red	Aveiro, Brasil Legal, PA Ponto 3	BRAZIL
RDS064	-2.84	-65.01	grey	Mamirauá, AM	BRAZIL
RDS067	-2.84	-65.01	grey	Mamirauá, AM	BRAZIL
RDS276	-2.84	-65.01	grey	Mamirauá, AM	BRAZIL

RFB06	-1.56	-48.70	grey	Vila dos Cabanos, Barcarena, PA	BRAZIL
RFB07	-1.56	-48.70	grey	Vila dos Cabanos, Barcarena, PA	BRAZIL
RFB09	-1.56	-48.70	grey	Vila dos Cabanos, Barcarena, PA	BRAZIL
RFB10	-1.56	-48.70	grey	Vila dos Cabanos, Barcarena, PA	BRAZIL
RFB13	-1.56	-48.70	grey	Vila dos Cabanos, Barcarena, PA	BRAZIL
RFB21	-1.56	-48.70	grey	Vila dos Cabanos, Barcarena, PA	BRAZIL
RFB48	-1.56	-48.70	grey	Vila dos Cabanos, Barcarena, PA	BRAZIL
TEC0045	-3.83	-40.90	grey	Planalto de Ibiapaba, Ubajara, CE	BRAZIL
TEC0532	-3.83	-40.90	grey	Tocantinzinho, Itaituba, PA	BRAZIL
TEC2089	-6.09	-56.25	grey	Planalto de Ibiapaba, Ubajara, CE	BRAZIL
UFS212	-9.25	-57.09	red	Apiacás, MT	BRAZIL
UFS557	-9.20	-57.09	red	Apiacás, MT	BRAZIL
URD572	-9.20	-57.09	red	Apiacás, MT	BRAZIL
VXG01	-3.30	-51.81	red	Volta Grande do Xingu, Vitória do Xingu, PA	BRAZIL
VXG16	-3.30	-51.81	red	Volta Grande do Xingu, Vitória do Xingu, PA	BRAZIL
VXG17	-3.30	-51.81	red	Volta Grande do Xingu, Vitória do Xingu, PA	BRAZIL
VXG20	-3.30	-51.81	red	Volta Grande do Xingu, Vitória do Xingu, PA	BRAZIL

| VXG21 | -3.30 | -51.81 | red | Volta Grande do Xingu, Vitória do Xingu, PA | BRAZIL |

HEMIPENIAL MORPHOLOGY AND DIVERSITY IN BRAZILIAN ANOLES (SQUAMATA: DACTYLOIDAE)

Annelise Batista D´Angiolella[1], Julia Klaczko[2], Miguel Trefaut U. Rodrigues[3], Teresa C. S. Avila-Pires[4]

[1] Programa de Pós Graduação em Zoologia UFPA/MPEG, Belém, Pará, Brazil,

Author for correspondence: annelise.dangiolella@gmail.com

[2] Museum of Comparative Zoology and Department of Organismic and Evolutionary Biology, Harvard University, Cambridge, USA.

[3] Universidade de São Paulo, USP, São Paulo, Brazil

[4] Museu Paraense Emilio Goeldi, Belém, Pará, Brazil.

ABSTRACT

Hemipenial morphology has provided useful characters that help elucidating species identification and phylogenetic relationships in Squamate systematics. Here we provide the hemipenial description of Brazilian anoles, discussing the diversity of this structure in light of the available phylogenetic hypothesis. Generally, intraspecific variation was low, while at the generic and specific levels several differences were observed, mainly related to the form and ornamentation of hemipenes.

1. INTRODUCTION

Morphology of male genitalia and its species-specific traits provide helpful taxonomic characters in many groups of vertebrates and invertebrates (Keogh, 1999; Luepold et al, 2004; Yoshizawa & Jonhson, 2006; Song & Bicheli, 2010, Kohler et al, 2007; Kohler, 2010). This structure is particularly important in groups where external morphology is conservative and levels of parallelism are high, so it has been of great help in differentiating closely related species and elucidating their relationships (Keogh, 1999). Hemipenes are directly involved in the copulation process and modifications in its morphology can be considered a physical mechanism of reproductive isolation (Arnold, 1986, Köhler & Sunyer 2008, Köhler 2009; Nunes et al. 2012).

In Squamates, hemipenes are paired, blind and tubular structures that act as the male copulatory organ; they show differences in size, shape and ornamentation (Dowling & Savage, 1960). In some groups, there is extensive conservatism in hemipenial morphology (Klaver & Böhme, 1986; Keogh, 1999) while others display significant intraspecific variation (Zaher & Prudente, 1999; Kohler, 2009; Nunes et al, 2012). The study of hemipenial morphology has provided important insights in the systematics of Squamate reptiles, elucidating questions about species identification and phylogenetic relationships (Dowling & Savage 1960, Böhme 1991, Ziegler & Böhme 1997, Keogh, 1999; Kohler et al. 2012).

Among lizards, Gymnophtalmidae, Lacertidae, Agamidae, Varanidae and Chamaleonidae are among the most studied in relation to hemipenes characters (Arnold, 1973, 1986; Cope, 1986; Kohler & Vesely, 2007; Böhme & Ziegler, 2008; Rodrigues et al. 2008; Myers et al, 2009, Nunes et al, 2012; Maduwage & Silva, 2012; Nunes et al, 2014). However, anole hemipenes have gained much more attention in the last decade thanks to the work of G. Köhler and colleagues in mainland Central America. These authors found several cases of geographically separated populations with very distinct hemipenial morphology — usually a large and bilobate organ in one population contrasting with a smaller and unilobate one in the other population (Köhler et al. 2012). These studies reveal the importance of hemipenis in identifying cryptic diversity, showing it is a useful tool to help elucidate the taxonomy and phylogenetic relationships at species level (e.g., Köhler & Sunyer 2008; Köhler & Vesely 2010).

In the past decades, molecular data has become increasingly available and new techniques continue to enhance the rate at which this process occurs. Combination of molecular and morphological data maximizes our basis to understand the evolution and relationships between organisms and aids to uncover hidden biodiversity (Hillis, 1987; Wiens, 2004; Schneider et al. 2009). In our study, we compile phylogenetic relationship hypotheses available for Brazilian mainland anoles and characterize their hemipenial variation and diversity. Our main objective is to provide the first description of this structure in the selected species, discussing its diversity in light of their phylogenetic relationships.

2. MATERIAL AND METHODS

We examined the hemipenes of 13 out of 18 anole species that occur in Brazil (Caldera-Costa & Bérnils, 2014): *Norops auratus* (Daudin, 1802), *N. meridionalis* (Boettger,

1885), *N. tandai* (Avila-Pires, 1995), *N. chrysolepis* (Duméril & Bibron, 1837)*, N. planiceps* (Troschel, 1848), *N. brasiliensis* (Vanzolini &Williams, 1970), *N. scypheus* (Cope, 1864), *N. trachyderma* (Cope, 1875), *N. ortonii* (Cope, 1868), *N. fuscoauratus* (Duméril & Bibron,1837), *Dactyloa punctata* (Daudin, 1802), *D. transversalis* (Duméril, 1851) and *D. phyllorhina* (Myers & Carvalho, 1945). We prepared from three to ten hemipenes per species, mostly four (Appendix 3.1, Table 3.1), except for *D. phyllorhina*, of which description and comparisons were based on photos of a hemipenis prepared by Gabriel Skuk. For hemipenes preparation, we followed a combination of techniques described in Pesantes (1994), Keogh (1999), Myers & Cadle (2003) and Zaher & Prudente (2003). To minimize possible variation caused by the eversion process, only partially or totally everted hemipenes were prepared. Once the preserved specimen was selected, one of the hemipenes was removed through a small incision at the base of the tail. In general, anole hemipenes have a very thin skin and to avoid possible damages, KAOH 2% was used only when the specimen was too old or when the lobes could not be totally everted with hot water. When fully everted, the organ was filled with colored vaseline to allow better visualization of ornamentation structures, and subsequently conserved in 70% ethanol. We obtained digital images of hemipenes in sulcate, assulcate, and lateral views using a JVC camera KYF75U, attached to a stereomicroscope with the aid of Auto-Montage Pro 5.02, for the smaller hemipenes, and all other hemipenes were photographed using a Nikon D90, macro lens of 105mm.

In order to analyze the hemipenial morphology of Brazilian anole species in a phylogenetic context, we use the Bayesian phylogenetic hypothesis proposed by Nicholson et al. (2012), combined with the phylogenies proposed by D'Angiolella et al. (2011) and Prates et al. (2014) for data on Brazilian *Norops* and *Dactyloa* species, respectively. These latter two studies are more complete for Brazilian species than the much broader analysis by Nicholson et al. (2012), which included 231 species grouped in eight genera. Considering our purposes, the tree that we present is only a graphical representation of the above-mentioned phylogenetic hypothesis involving Brazilian anole species. It does not contain information about branch lengths or posterior probability, but illustrates the relationship among the species we focus on and their South and Central American counterparts.

3. RESULTS

All hemipenis are bilobed, with globular or tubular calyculated lobes presenting a naked area and with bifurcated sulcus spermaticus. No mineralized structures are present. Generally, intraspecific variation is low, while at the generic and specific levels several differences are observed. Below we present the hemipenial description of all species studied, following an alphabetical order (Figure 1.3).
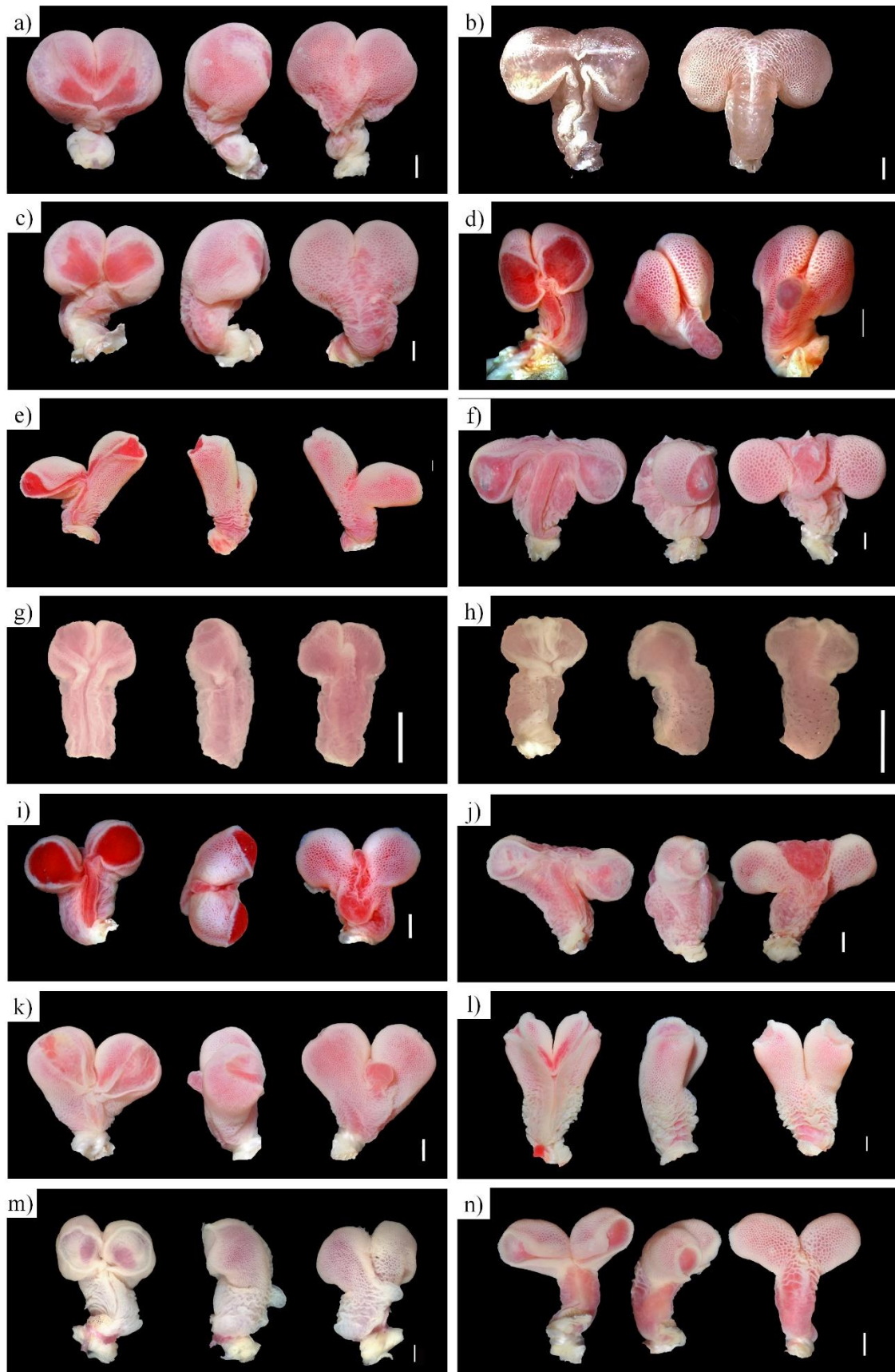
Figure 8: Hemipenes of *Norops* and *Dactyloa* species studied. a) *D. punctata*, b) *D. phyllorhina*, c) *D. transversalis*, d) *N. auratus*, e) *N. brasiliensis,* f) *N. chrysolepis,* g) *N.*

fuscoauratus, h) *N. fuscoauratus* with the pigmentation patterns, i) *N. meridionalis*, j) *N. tandai,* k) *N. ortonii,* l) *N. planiceps*, m) *N. scypheus*, n) *N. trachyderma*.

DACTYLOA SPECIES

Dactyloa punctata (Fig. 1.3a)

Hemipenis robust and bilobed, with globular lobes representing more than half of the hemipenis length. Sulcus spermaticus deep and bifurcated, with well-developed sulcal lips. It opens into a wide and elongate naked region extending laterally from the base of the lobes to the apex. Outside this naked area, lobes densely calyculate. A triangular flap, covered by enlarged and irregular folds, is present in the asulcate face, initiating midway on the lobes and pointing toward the base of the hemipenes. Hemipenis truncus short, wrinkled on both sulcate and assulcate faces. Base short and smooth.

Dactyloa phyllorhina (Fig. 1.3b)

Hemipenis robust and bilobed, with globular lobes representing about half of the hemipenis length. Sulcus spermaticus deep and bifurcated, with well-developed sulcal lips. It opens into a wide and elongate naked region extending laterally from the base of the lobes to the apex. Outside this naked area, lobes densely calyculate. A skin ridge present in asulcate face, initiating midway on the lobes where it is surrounded by enlarged calyces and reaching the median region of truncus where it is covered by enlarged and irregular transverse folds. Truncus wrinkled on both sulcate and assulcate faces.

Dactyloa transversalis (Fig. 1.3c)

Hemipenis robust and bilobed, with globular lobes representing at least half of the hemipenis length. Sulcus spermaticus deep and bifurcated, with well-developed sulcal lips. It opens into a wide and elongate naked region extending laterally from the base of the lobes to the apex. Outside this naked area, lobes densely calyculate. Asulcate face between lobes covered by enlarged and irregular calyces, truncus with a shallow medial skin ridge surrounded by transverse folds.

NOROPS SPECIES:

Norops auratus (Fig. 1.3d)

Hemipenis bilobed, with globular lobes representing about half of the hemipenis length. Sulcus spermaticus deep and bifurcated, with poorly-developed sulcal lips. It opens into a round naked disk extending laterally from base of lobes to almost the apex. Lobes

strongly calyculate outside the naked disk. A finger-shaped process projects from the crotch on the asulcate face, surrounded by enlarged calyces. Assulcate and lateral faces of truncus covered with well-delimited transverse folds; oblique or longitudinal wrinkles on the sulcate face.

Norops brasiliensis (Fig. 1.3e)
Hemipenis bilobed, with tubular lobes representing about half of the hemipenis length. Sulcus spermaticus deep and bifurcated, with well-developed sulcal lips. It opens into a flat and naked disk on terminal region of each lobe, separated from the surrounding calyculated area by a raised edge of tissue. Lobes strongly calyculate. A shallow medial skin ridge present on the asulcate face, from the crotch to halfway the truncus. Hemipenial truncus covered with calyces distally and flounces basally, both on sulcate and asulcate faces.

Norops chrysolepis (Fig. 1.3f)
Hemipenis bilobed, with globular lobes representing about half of the hemipenis length. Sulcus spermaticus deep and bifurcated, with well-developed sulcal lips becoming thicker at the lobes. It opens into a round naked disk that extends laterally from base of lobes to almost the apex. Outside the naked disk, lobes strongly calyculate. Lobes separated by a large, naked, triangular expansion that pushes the lobes to the sides, giving the hemipenis a 'T' shape. An extension of this expansion, with wrinkled surface, projects shortly towards the truncus and is followed by a medial and shallow skin ridge that extends towards the base of the hemipenis. A thin skin pleat extends from the basal region of the hemipenis to the base of the lobes laterally, demarcating the assulcate and sulcate faces. Hemipenis truncus covered with flounces on assulcate and sulcate faces.

Norops fuscoauratus (Fig. 1.3g and 1.3h)
Hemipenis bilobed, with globular lobes representing less than half of the hemipenis length. Sulcus spermaticus deep and bifurcated, with poorly-developed sulcal lips. It opens into a round naked disk that extends laterally from the base of the lobes to the apex. Lobes strongly calyculate outside the naked disk. A fleshy medial skin ridge on asulcate face, from the crotch towards the truncus. Truncus covered with flounces on assulcate and sulcate faces. Some of the hemipenes showed small pigmented spots on truncus (Fig. 3.9). Ammount of pigmentation varied among specimens and localities, and in a same

locality there were specimens with pigmented and specimens with non-pigmented hemipenis (e.g. Guyana: Potaro-Siparuni and Brazil: Pacoti-CE and Porto Velho-RO).

Norops meridionalis (Fig. 1.3i)

Hemipenis bilobed, with globular lobes representing about half of the hemipenis length. Sulcus spermaticus deep and bifurcated, with well-developed sulcal lips that become thicker at the lobes. It opens into a round naked disk that extends laterally from base of lobes to almost the apex. Lobes strongly calyculate outside the naked disk. A fleshy projection between the lobes on asulcate face, projecting only shortly beyond the crotch. The distal part of this projection is small expansion that becomes a triangular pleat toward the hemipenes truncus. A thin skin pleat extends from the hemipenial base to the base of the lobes laterally, demarcating the asulcate and sulcate faces. Truncus with a naked region right below the triangular pleat projection on asulcate face, and longitudinal wrinkles on sulcate face.

Norops tandai (Fig. 1.3j)

Hemipenis bilobed, with globular lobes representing about half of the hemipenis length. Sulcus spermaticus deep and bifurcated, with well-developed sulcal lips that become thicker at the lobes. It opens into a round naked disk that extends laterally from base of lobes to almost the apex. Lobes strongly calyculate outside the naked disk; separated by a large, naked, triangular expansion that pushes them to the sides, giving the hemipenes a 'T' shape. An extension of this expansion, with wrinkled surface, projects shortly towards the truncus and is followed by a medial and shallow skin ridge that extends towards the hemipenial base. A thin skin pleat extends from the basal region of the hemipenes to the base of the lobes laterally, demarcating the assulcate and sulcate faces. Truncus covered with flounces on assulcate and sulcate faces.

Norops ortonii (Fig. 1.3k)

Hemipenis bilobed, with globular lobes representing more than a half of the hemipenis length. Sulcus spermaticus deep and bifurcated with well-developed sulcal lips, which become shallow halfway the lobes. The sulcus opens into an elongate naked area, extending laterally from base of lobes to the apex. Lobes strongly calyculate outside of the disk. A finger-shaped process projects from the crotch on the asulcate face,

surrounded by enlarged calyces. Assulcate and lateral faces of hemipenial truncus covered with transverse folds.

Norops planiceps (Fig. 1.3l)

Hemipenis bilobed, with tubular lobes representing about half of the hemipenis length. Sulcus spermaticus deep and bifurcated, with well-developed sulcal lips. It opens into a flat and naked disk on terminal region of each lobe, separated from the surrounding calyculated area by a raised edge of tissue. Lobes strongly calyculate. A fleshy skin ridge present on the asulcate face, from the crotch to halfway the truncus. Hemipenial truncus covered with calyces distally and flounces basally, both on sulcate and asulcate faces.

Norops scypheus (Fig. 1.3m)

Hemipenis bilobed, with globular lobes representing about half of the hemipenis length. Sulcus spermaticus deep and bifurcated, with well-developed sulcal lips. It opens into a round naked disk that extends laterally from base of lobes to almost the apex. Lobes strongly calyculate outside the naked disk. Presence of a projection composed by a delicate soft skin lump situated medially on the truncus assulcate face. Truncus covered with flounces in the asulcate and sulcate surface.

Norops trachyderma (Fig. 1.3n)

Hemipenis bilobed, with tubular lobes representing about half of the hemipenis length. Sulcus spermaticus deep and bifurcated, with poorly-developed sulcal lips. It opens into a naked disk on the terminal region of each lobe, separated from the surrounding calyculated area by a raised edge of tissue. A fleshy medial skin ridge on asulcate face, from the crotch towards the truncus. Truncus distally with flounces on asulcate face, surrounding the skin ridge, and shallow wrinkles on sulcate face; naked towards the hemipenial base.

RELATION TO PHYLOGENY

In Fig. 2.3 the hemipenes are plotted in the graphical representation of compiled phylogenetic hypothesis. Some characteristics of hemipenial morphology seem to be linked to phylogeny, but in certain cases, similar structures appear in phylogenetically distant species in the same genus
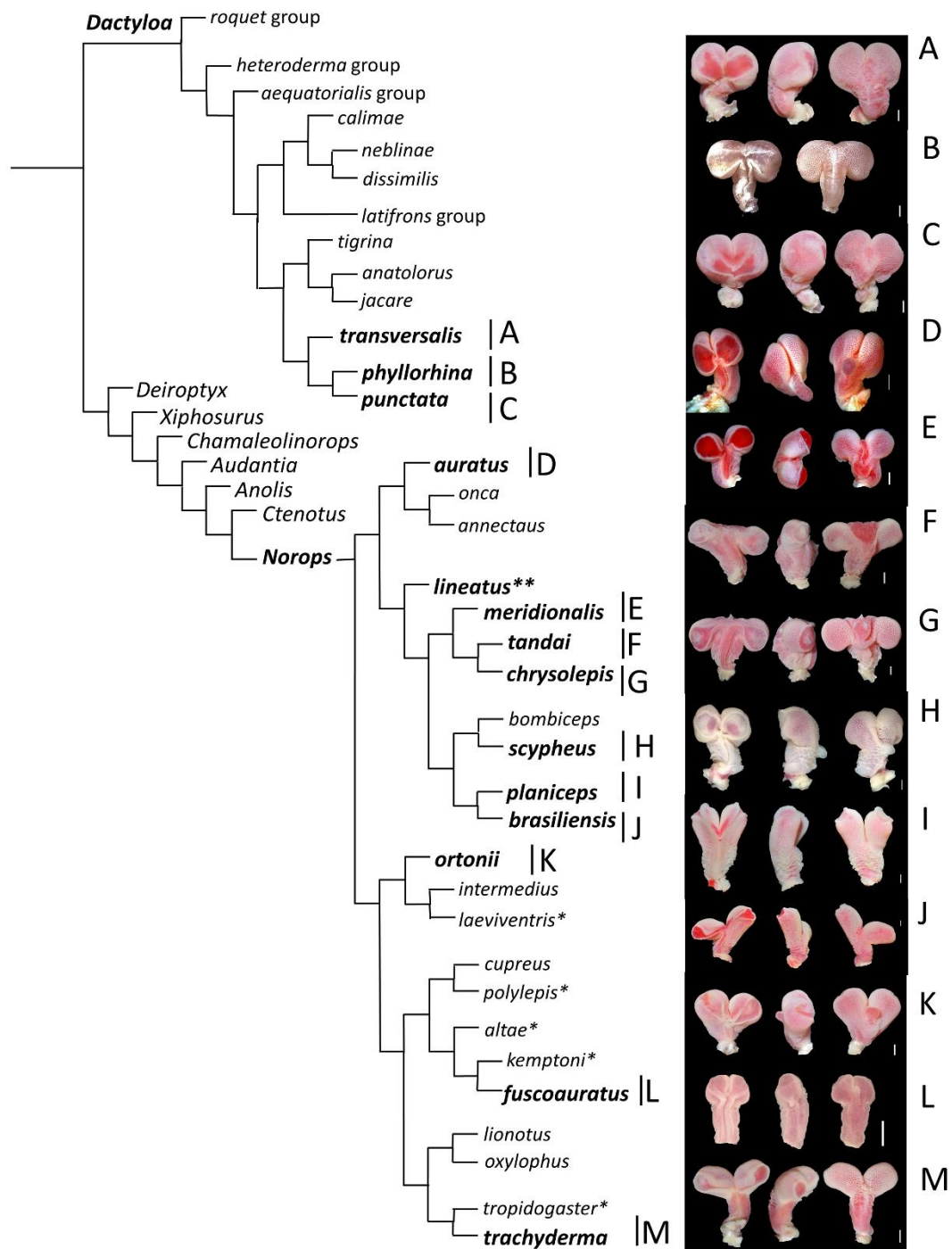
Figure 9 Graphical representation of the phylogenetic relationship for Brazilian Dactyloidae species based on Nicholson et al, (2012), D'Angiolella et al, (2011) and Prates et al, (2014). Names in bold represent species that had their hemipenes prepared; * represents hemipenes already described in the literature and names in bold with ** represent hemipenes that were prepared, but used here only for comparison purposes.

In *Dactyloa*, hemipenes of the three species examined present robust, globular lobes, with a wide and elongate naked area, in contrast with most *Norops* hemipenes, where lobes tend to be proportionally smaller and the naked area form a round disk (except in *N. ortoni*, whose hemipenis present an elongate naked area). Hemipenes of *D. transversalis* and *D. phyllorhina* are more similar to each other than to that of *D. punctata* in presenting a longer truncus, a skin ridge on the asulcate face, and no triangular flap covered by fold between lobes. Considering the phylogeny, these may represent plesiomorphic characters, while the triangular flap in *D. punctata* hemipenis could be an autapormorphy of this species.

Among the *Norops chrysolepis* species group, the hemipenes of *N. meridionalis*, *N. tandai*, and *N. chrysolepis* are similar for presenting thick sulcal lips, a wide and subdivided fleshy projection between the globular lobes, and a thin skin pleat demarcating the assulcate and sulcate faces on truncus.

In relation to *N. planiceps* and *N. brasiliensis,* both have in common lobes tubular-shaped; naked disk in terminal position on lobes, delimited by a raised edge of skin; and a medial skin ridge on the asulcate face of truncus. The hemipenis of *N. scypheus* is similar to those of *N. meridonalis*, *N. tandai* and *N. chrysolepis* in having globular lobes and naked disk on lobes that extends from base of lobes to almost the apex. However, it is also similar to the hemipenes of *N. brasiliensis* and *N. planiceps* for lacking a fleshy projection between lobes and presenting instead a small skin lump medially on asulcate face of truncus.

The other Brazilian species of *Norops* here studied are not each other's sister species*,* thus similarities are either plesiomorphic or represent paralelisms. The hemipenis of *N. trachyderma* is similar to those of *N. brasiliensis* and *N. planiceps* in having tubular lobes, a terminal naked disk, and a medial skin ridge on the asulcate face, extending from the crotch towards the truncus. This later characteristic is also present in *N. fuscoauratus*. Hemipenes of *N. ortonii* and *N. auratus* are similar for presenting globular lobes, a finger-shaped process projecting from the crotch on the asulcate face, and the hemipenial truncus covered by well-delimited transverse folds. Besides, *N. ortonii* presents the naked area on lobes elongate, not forming a definite disc, as in the other *Norops* examined, and to a certain extant reminding of those of *Dactyloa*.

4. DISCUSSION

The use of hemipenial characters in systematic studies of Dactyloid lizards has increased substantially in the past years (Köhler et al. 2012 and references therein). This sudden interest is due mostly to the discovery of a large number of potential informative characters, capable of providing valuable information concerning two or more morphologically similar species (Köhler et al. 2007; Köhler & Vesely, 2010). In a variety of studies, divergent hemipenial morphology was the starting point for systematic revisions and/or species description (Köhler 2009, 2010, 2011). In the present work, we report that hemipenes of Brazilian anole species share several similarities but present considerable differences from one another in shape and ornamentation.

Similarities between the hemipenes of *N. meridionalis* and the hemipenes of *N. tandai* and *N. chrysolepis* suggests the close relationship between them. The inclusion of *N. meridionalis* in the *N. chrysolepis* species group was not possible due to the poorly supported phylogenetic relationship of *N. meridionalis* with the rest of the group (D'Angiolella et al. 2011). Allthough, these three species share the thin skin pleat demarcating the assulcate and sulcate faces on truncus, a character that probably represents the sinapomorphy of this clade.

One of us (JK) had the opportunity to prepare hemipenes of *N. lineatus*, the species most closely related to the *N. chrysolepis* species group. The hemipenes of this species is similar to the species of the *N. chrysolepis* species group for being a bilobed organ and for having the sulcus spermaticus opening into a nude disk situated laterally at the lobes and extending to the apex. Although, it presents a median asulcal finger-like process situated at the lobes, resembling that of *N. auratus*.

N. trachyderma is the sister specie of *N. tropidogaster*, a species distributed in Colombia and in eastern Panama that posses a large, bulbuous and bilobed hemipenes (Köhler et al. 2012). The description and illustration of the hemipenis of *N. tropidogaster* provided by Köhler et al. (2012) indeed resemble that of *N. trachyderma*, both in form and structures.

N. fuscoauratus is phylogenetically related to *N. kemptoni*, *N. altae*, and *N. polylepis,* species occurring in Panama and Costa Rica in Central America (Nicholson et al. 2012). The hemipenes of *N. kemptoni* differs from *N. fuscoauratus* hemipenes for

being a unilobed organ with a median finger-like process at asulcal face of lobes (Köhler et al, 2007; Ponce & Köhler, 2008). In the past years, three new species related *to N. altae* and *N. polylepis* were described: *N. monteverde* (Köhler, 2009), *N. tenorioensis* (Köhler et al. 2010) and *N. osa* (Köhler, 2011). Among these species, *N. polylepis, N. tenorionsis* and *N. altae* have bilobed and robust hemipenes, while *N. monteverde* and *N. osa* have small and unilobate organs, all of them distinct in form and structures from *N. fuscoauratus* hemipenes. However, Köhler (2011) identified a possible hybrid between *N. osa* and *N. polylepis*, which exibits a very similar hemipenes both in form and structure to the hemipenis of *N. fuscoauratus*. All these species have similar or even undistinguishable (*N. osa* and *N. polylepis*) external morphology and there is no current phylogenetic hypothesis that have included all of them in the analysis.

N. ortonii is closely related to *N. laeviventris*, but no hemipenial description or illustration are provided in literature for this species. Except for the work of Lotzkart et al. (2010) that superficially mention the hemipenes of *N. laeviventris*, describing it possess a well-developed asulcal processus.

Our results confirm that hemipenial characters can be phylogenetically informative and a useful tool in lizard systematics. In addition, the species here analyzed have distribution ranges that surpasses the Brazilian territory, with the exception of the endemic *N. brasiliensis*, an inhabitant of gallery forests in the Cerrado Biome. So all the information here provided might be useful in further comparative studies in a continental scale.

REFERENCES

Arnold E.N. (1973). Relationships of the Palaearctic lizards assigned to the genera *Lacerta*, *Algyroides* and *Psammodromus* (Reptilia: Lacertidae). *Bulletin of the British Museum (Natural History). Zoology*. 25:289–366.

Arnold E.N. (1986). Why copulatory organs provide so many useful taxonomic characters: the origin and maintenance of hemipenial differences in lacertid lizards (Reptilia: Lacertidae). *Biological Journal of the Linnean Society 29*:263–281.

Böhme W. (1988). Zur genitalmorphologie der sauria: funktionelle und stammesgeschichtliche aspekte. *Bonn zoological Bulletin* 27:1–176.

Böhme, W. (1991). New findings on the hemipenial morphology of monitor lizards and their systematic implications. Pp. 42-49. In Böhme, W. & H.G. Horn (eds.), Advances in Monitor Research, Mertensiella 2. Deutsche Gesellschaft für Herpetologie und Terrarienkunde e.V., Rheinbach.

Böhme, W., & Ziegler, T. (2008). A review of iguanian and anguimorph lizard genitalia (Squamata: Chamaeleonidae; Varanoidea, Shinisauridae, Xenosauridae, Anguidae) and their phylogenetic significance: comparisons with molecular data sets. *Journal of Zoological Systematics and Evolutionary Research*, *47*(2), 189-202.

Bérnils, RS and HC Costa (org.). (2014). Brazilian reptiles: List of species. Version 2014.1. Available at http://www.sbherpetologia.org.br/. Sociedade Brasileira de Herpetologia.

Cope, E.D. (1896). On the hemipenes of the Sauria. *Proceedings of The Academy of Natural Sciences Philadelphia 48*: 461–467.

D'Angiolella, A. B., Gamble, T., Avila-Pires, T. C., Colli, G. R., Noonan, B. P., & Vitt, L. J. (2011). *Anolis chrysolepis* Duméril and Bibron, 1837 (Squamata: Iguanidae), revisited: molecular phylogeny and taxonomy of the *Anolis chrysolepis* species group. *Bulletin of the Museum of Comparative Zoology*, *160*(2), 35–63.

Dowling H.G., Savage J.M. (1960). A guide to the Snake hemipenis: a survey of basic structure and systematic characteristics. *Zoologica* 45:17–28.

Freitas, M.A., Machado, D.C., Venâncio N.M., França D.P.F., Veríssimo, D., (2013). First record for Brazil of the odd anole lizard, *Anolis dissimilis* Williams, 1965 (Squamata: Polychrotidae) with notes on coloration. *Herpetological Notes* 6, 383–385.

Hillis, D. M. (1987). Molecular versus morphological approaches to systematics. *Annual review of Ecology and Systematics*, 23-42.

Klaver, C., Bohme W. (1986). Phylogeny and classification of the Chamaleonidae (Sauria) with special reference to hemipenis morphology. *Bonn zoological Monograph* 22:1–64.

Keogh S. (1999). Evolutionary implications of hemipenial morphology in the terrestrial Australian elapid snakes. *Zoological Journal of the Linnean Society* 125: 239–278.

Köhler, G. (2009). New species of *Anolis* formerly referred to as *Anolis altae* from Monteverde, Costa Rica (Squamata: Polychrotidae). *Journal of Herpetology*, *43*(1), 11-20.

Köhler, G. (2010). A revision of the Central American species related to *Anolis pentaprion* with the resurrection of *A. beckeri* and the description of a new species (Squamata: Polychrotidae). *Zootaxa*, *2354*, 1-18.

Köhler, G. (2011). A new species of anole related to *Anolis altae* from Volcán Tenorio, Costa Rica (Reptilia, Squamata, Polychrotidae). *Zootaxa.*, (3120), 29-42.

Köhler, G., & Smith, E. N. (2008). A new species of anole of the *Norops schiedei* group from western Guatemala (Squamata: Polychrotidae). *Herpetologica*, *64*(2), 216-223.

Köhler, G., & Sunyer, J. (2008). Two new species of anoles formerly referred to as *Anolis limifrons* (Squamata: Polychrotidae). *Herpetologica*, *64*(1), 92-108.

Köhler, G., & Vesely, M. (2007). The hemipenis of *Opipeuter xestus* (Squamata: Gymnophthalmidae). *Salamandra Bonn*, *43*(1), 49.

Köhler, G., & Vesely, M. (2010). A revision of the *Anolis sericeus* complex with the resurrection of *A. wellbornae* and the description of a new species (Squamata: Polychrotidae). *Herpetologica*, *66*(2), 207-228.

Köhler, G., Ponce, M., Sunyer, J., & Batista, A. (2007). Four new species of anoles (genus *Anolis*) from the Serranía de Tabasará, west-central Panama (Squamata: Polychrotidae). *Herpetologica, 63*(3), 375-391.

Köhler, G., Dehling, D. M., & Koehler, J. (2010). Cryptic species and hybridization in the *Anolis polylepis* complex, with the description of a new species from the Osa Peninsula, Costa Rica (Squamata: Polychrotidae). *Zootaxa*, *2718*, 23-38.

Köhler, J., Hahn, M., & Köhler, G. (2012). Divergent evolution of hemipenial morphology in two cryptic species of mainland anoles related to *Anolis polylepis*. *Salamandra*, *48*(1), 1-11.

Köhler, G., Batista, A., Vesely, M., Ponce, M., Carrizo, A., & Lotzkat, S. (2012). Evidence for the recognition of two species of *Anolis* formerly referred to as *A. tropidogaster* (Squamata: Dactyloidae). *Zootaxa*, *3348*, 1-23.

Köhler, G., Pérez, R. G. T., Pareja, M. G., Petersen, C. B. P., & Mendez de la Cruz, F. R. (2013). A contribution to the knowledge of *Anolis macrinii* Smith, 1968 (Reptilia: Squamata: Dactyloidae). *Breviora*, 1-14.

Köhler, G., Pérez, R. G. T., Petersen, C. B. P., & de la Cruz, F. R. M. (2014). A revision of the Mexican *Anolis* (Reptilia, Squamata, Dactyloidae) from the Pacific versant west of the Isthmus de Tehuantepec in the states of Oaxaca, Guerrero, and Puebla, with the description of six new species. *Zootaxa*, *3862*(1), 1-210.

Lotzkat, S., Köhler, J. J., Hertz, A., & Köhler, G. (2010). Morphology and colouration of male *Anolis datzorum* (Squamata: Polychrotidae). *Salamandra*, *46*(1), 48-52.

Lüpold, S., McElligott, A. G., & Hosken, D. J. (2004). Bat genitalia: allometry, variation and good genes. *Biological Journal of the Linnean Society*, *83*(4), 497-507.

Miller, M. A., Pfeiffer, W., & Schwartz, T. (2010). Creating the CIPRES Science Gateway for inference of large phylogenetic trees. In *Gateway Computing Environments Workshop (GCE), 2010* (pp. 1-8). IEEE.

Maduwage, K., & Silva, A. (2012). Hemipeneal Morphology of Sri Lankan Dragon Lizards (Sauria: Agamidae). *Ceylon Journal of Science (Biological Sciences)*, *41*(2), 111-123.

Myers, C.W., & Cadle, J.E. (2003). Points of view. *Herpetological Review, 34*(4), 295-302.

Myers, C.W., & Trueb, L. (1967). The hemipenis of an anomalepidid snake. *Herpetologica,* 235-238.

Myers, C.W., Fuenmayor, G.R., & Jadin, R.C. (2009). New species of lizards from Auyantepui and La Escalera in the Venezuelan Guayana, with notes on "microteiid" hemipenes (Squamata: Gymnophthalmidae). *American Museum Novitates*, 1-31.

Nicholson, K.E., Crother, B.I., Guyer, C., & Savage, J.M. (2012). It is time for a new classification of anoles (Squamata: Dactyloidae). *Zootaxa,* 3477, 1-108.

Nicholson, K.E., Crother, B.I., Guyer, C., & Savage, J.M. (2014). Anole classification: A response to Poe. *Zootaxa,* 3814(1), 109-120.

Nunes, P.M.S., Fouquet, A., Curcio, F. F., Kok P., & Rodrigues, M.T. (2012). Cryptic species in *Iphisa elegans* Gray, 1851 (Squamata: Gymnophthalmidae) revealed by hemipenial morphology and molecular data. *Zoological Journal of the Linnean Society, 166*(2), 361-376.

Nunes, P.M.S., Curcio, F. F., Roscito, J. G., & Rodrigues, M. T. (2014). Are Hemipenial Spines Related to Limb Reduction? A Spiny Discussion Focused on Gymnophthalmid Lizards (Squamata: Gymnophthalmidae). *The Anatomical Record, 297*(3), 482-495.

Padial J.M., Miralles, A., de la Riva, I., Vences, M. (2010). The integrative future of taxonomy. *Frontiers in Zoology* 7: 1–14.

Pesantes O.S. 1994. A method for preparing the hemipenis of preserved snakes. *Journal of Herpetology 28*:93–95.

Ponce, M., & Köhler, G. (2008). Morphological variation in anoles related to *Anolis kemptoni* in Panama. *Salamandra*, *44*(2), 65-84.

Rivas, G.A., Nunes, P. M. S., Dixon, J. R., Schargel, W. E., Caicedo, J. R., Barros, T. R., & Barrio-Amoros, C. L. (2012). Taxonomy, hemipenial morphology, and natural history of two poorly known species of *Anadia* (Gymnophthalmidae) from northern South America. *Journal of Herpetology*, *46*(1), 33-40.

Rodrigues M.T., Camacho A, Nunes P.M.S., Recoder R.S., Teixeira-Jr. M, Valdujo P.H., Ghellere J.M.B., Mott T, Nogueira C. 2008. A new species of the lizard genus *Bachia* (Squamata: Gymnophthalmidae) from the Cerrados of Central Brazil. *Zootaxa 1875*:39–50.

Savage J.M. 1997. On terminology for the description of the hemipenes of Squamate reptiles. *Journal of Herpetology 7*:23–25.

Schneider, H., Smith, A.R., & Pryer, K.M. (2009). Is morphology really at odds with molecules in estimating fern phylogeny? *Systematic Botany*, *34*(3), 455-475.

Sunyer, J., Vesely, M., Kohler, G. (2008). Morphological variation in *Anolis wermuthi* (Kohler & Obermeier, 1998) a species endemic to the highlands of north-central Nicaragua. *Senckenbergiana Biologica* 88(2):335-343.

Wiens, J.J. (2004). The role of morphological data in phylogeny reconstruction. *Systematic Biology*, *53*(4), 653-661.

Yoshizawa, K., & Johnson, K.P. (2006). Morphology of male genitalia in lice and their relatives and phylogenetic implications. *Systematic Entomology*, *31*(2), 350-361.

Zaher H., Prudente A.L.C. (1999). Intraspecific variation of the hemipenes in *Siphlophis* and *Tripanurgos*. *Journal of Herpetology* 33:698.

Zaher, H., & Prudente, A.L.C. (2003). Hemipenes of *Siphlophis* (Serpentes, Xenodontinae) and techniques of hemipenial preparation in snakes: a response to Dowling. *Herpetological Review*, *34*(4), 302-306.

Ziegler, T., Vences, M., Glaw, F., & Böhme, W. (1997). Genital morphology and systematics of *Geodipsas* Boulenger, 1896 (Reptilia: Serpentes: Colubridae), with description of a new genus. *Revue Suisse de Zoologie*, *104*(1), 95-1.

APPENDIX

Table 3.1: Museum numbers and locality of *Norops* and *Dactyloa* hemipenes preprared for the present study.

Identification Number	Genus	Species	Locality	Country
MPEG28904	*Dactyloa*	*punctata*	Floresta Nacional de Caxiuana, PA	Brazil
MPEG16011	*Dactyloa*	*punctata*	29 km North of Rio Branco, AC	Brazil
MPEG28866	*Dactyloa*	*punctata*	Floresta Nacional de Caxiuana, PA	Brazil
MPEG21575	*Dactyloa*	*transversalis*	Floresta Nacional Serra da Cotia, RO	Brazil
MPEG21576	*Dactyloa*	*transversalis*	Floresta Nacional Serra da Cotia, RO	Brazil
MPEG4106	*Norops*	*auratus*	Boa Vista, RR	Brazil
MPEG4068	*Norops*	*auratus*	Boa Vista, RR	Brazil
MPEG18236	*Norops*	*brasiliensis*	Minacu, GO	Brazil
MPEG12383	*Norops*	*brasiliensis*	Arari, Maranhao	Brazil
MPEG24491	*Norops*	*brasiliensis*	Tanguro, MT	Brazil
MPEG29707	*Norops*	*chrysolepis*	Laranjal do Jari , AP	Brazil
MPEG27374	*Norops*	*chrysolepis*	Serra do Acari, PA	Brazil
MPEG22197	*Norops*	*chrysolepis*	Porto Trombetas, Oriximina, PA	Brazil
MPEG27367	*Norops*	*chrysolepis*	Urucara, PA	Brazil
MSH12316	*Norops*	*fuscoauratus*	Santa Isabel do Rio Negro, AM	Brazil
MPEGVXG14	*Norops*	*fuscoauratus*	Vitoria do Xingu, PA	Brazil
MPEGBP02	*Norops*	*fuscoauratus*	Bacia Rio Capim, Paragominas, PA	Brazil
MPEG29607	*Norops*	*fuscoauratus*	Afua, Ilha do Marajo, PA	Brazil
MPEG20590	*Norops*	*fuscoauratus*	P. Walter, Jurua, AC	Brazil
MPEG28863	*Norops*	*fuscoauratus*	Floresta Nacional Caxiuana, PA	Brazil
AMNHR-115871	*Norops*	*fuscoauratus*	Napo	Ecuador
AMNHR-133697	*Norops*	*fuscoauratus*	Amazonas	Venezuela
MZUSP27091	*Norops*	*fuscoauratus*	Napo, Limoncocha	Ecuador
MZUSP65666	*Norops*	*fuscoauratus*	Estação Ecológica de Saltinho, PE	Brazil
MZUSP81620	*Norops*	*fuscoauratus*	Apiacás, MT	Brazil
MZUSP16182	*Norops*	*fuscoauratus*	Canavieiras, BA	Brazil
AMNH151836	*Norops*	*fuscoauratus*	Guyana	Guyana
MBS024	*Norops*	*meridionalis*	Mina Guapore, MT	Brazil

MBS010	*Norops*	*meridionalis*	Mina Guapore, MT	Brazil
MPEG21781	*Norops*	*ortonii*	Floresta Nacional de Caxiuana, PA	Brazil
MPEG26941	*Norops*	*ortonii*	Porto Urucu, AM	Brazil
MPEG31113	*Norops*	*ortonii*	Taracaua, AC	Brazil
MPEG22225	*Norops*	*planiceps*	Sao Joao Lucas, RR	Brazil
MPEG15814	*Norops*	*planiceps*	Inpa, Manaus, AM	Brazil
MPEG3922	*Norops*	*planiceps*	Coronel Mota, RR	Brazil
MSH12327	*Norops*	*planiceps*	Santa Isabel do Rio Negro, AM	Brazil
MPEG16765	*Norops*	*planiceps*	Reserva Duke, Manaus, AM	Brazil
MPEG15277	*Norops*	*scypheus*	Maraa, AM	Brazil
MCZ110284	*Norops*	*scypheus*	Sarayacu: Pastaza	Ecuador
MPEG27674	*Norops*	*tandai*	Maues, AM	Brazil
MPEG26931	*Norops*	*tandai*	Porto Urucu, AM	Brazil
MPEG27082	*Norops*	*tandai*	Mutum, Juruti, PA	Brazil
MPEG27673	*Norops*	*tandai*	Maues, AM	Brazil
MPEG29414	*Norops*	*tandai*	Itaituba, PA	Brazil
MPEG 18924	*Norops*	*tandai*	Careiro da Varzea, AM	Brazil
MPEG30038	*Norops*	*trachyderma*	Itaituba, PA	Brazil
MPEG31114	*Norops*	*trachyderma*	Taracaua, AC	Brazil
MPEG30332	*Norops*	*trachyderma*	Rio Jurua, AC/AM	Brazil
MPEG20737	*Norops*	*trachyderma*	Porto Walter, Rio Jurua, AC	Brazil
MPEG17586	*Norops*	*trachyderma*	Santarem, PA	Brazil